Wyoming Water Research Program
Annual Technical Report
FY 2013

Introduction

The NIWR/State of Wyoming Water Research Program (WRP) coordinates participation in the NIWR program through the University of Wyoming's Office of Water Programs (OWP). The primary purposes of the WRP are to support and coordinate research relative to important water resources problems of the State and Region, support the training of scientists in relevant water resource fields, and promote the dissemination and application of the results of water-related research. In addition to administrating the WRP, the Director of the OWP serves as the University of Wyoming advisor to the Wyoming Water Development Commission (WWDC).

Primary participants in the WRP are the USGS, the WWDC, and the University of Wyoming. A Priority and Selection Committee (P&S Committee), consisting of representatives from State and Federal agencies, solicits and identifies research needs, selects projects, and reviews and monitors project progress. The Director of the OWP serves as a point of coordination for all activities and serves to encourage research by the University of Wyoming addressing the needs identified by the P&S Committee. State support for the WRP includes direct funding through the WWDC and active State participation in identifying research needs and project selection and oversight. The State provides direct WWDC funding for the OWP to identify water related research needs, coordinate research activities, coordinate the Wyoming WRP, and serve as the University advisor to the WWDC.

The WRP supports faculty and students in University of Wyoming academic departments. Faculty acquire their funding through competitive, peer reviewed grants, submitted to the WRP. Since its inception in the year 2000, the WRP has funded a wide array of water related projects across several academic departments.

Research Program Introduction

Since inception of the NIWR program in 1965, the Wyoming designated program participant has been the University of Wyoming. Until 1998, the Wyoming NIWR program was housed in the Wyoming Water Resources Center (WWRC). However, in 1998 the WWRC was closed. In late 1999, the Wyoming Water Research Program (WRP) was initiated to oversee the coordination of the Wyoming participation in the NIWR program. The primary purpose of the Wyoming Institute beginning with FY00 has been to identify and support water-related research and education. The WRP supports research and education by existing academic departments rather than performing research in-house. Faculty acquire funding through competitive, peer reviewed proposals. A goal of the program is to promote coordination between University, State, and Federal agency personnel.

In conjunction with the WRP, an Office of Water Programs (OWP) was established by State Legislative action beginning July 2002. The duties of the Office are specified by the legislation as: (1) to work directly with the Director of the Wyoming Water Development Office to identify research needs of State and Federal agencies regarding Wyoming water resources, including funding under the National Institutes of Water Resources (NIWR), (2) to serve as a point of coordination for and to encourage research activities by the University of Wyoming to address research needs, and (3) to submit a report annually prior to each legislative session to the Select Water Committee and the Wyoming Water Development Commission on the activities of the office.

The WRP, which is coordinated through the OWP, is a cooperative Federal, State, and University effort. Activities are supported by the NIWR, Wyoming Water Development Commission, and University of Wyoming. A State Advisory Committee serves to identify research priorities, select projects for funding, and monitor project progress. Reports for the following FY13 WRP research projects are given herein in the order listed below:

Project 2012WY79B Final Report: A Treatise on Wyoming Water Law, Lawrence J. MacDonnell, Professor of Law, UW, Mar 2012 thru Feb 2014.

Project 2012WY80B Final Report: Integrated Accelerated Precipitation Softening (APS) Microfiltration (MF) Assembly and Process Development to Maximize Water Recovery during Energy Production and CO2 Sequestration, Jonathan A. Brant, Assist. Prof., Dept. of Civil and Architectural Engineering, and Dongmei (Katie) Li, Assist. Prof., Dept. of Chemical and Petroleum Engineering, UW, Mar 2012 thru Feb 2014.

Project 2012WY81B Annual Report: Multi-Frequency Radar and Precipitation Probe Analysis of the Impact of Glaciogenic Cloud Seeding on Snow, Bart Geerts, Prof., Dept. of Atmospheric Science, UW, Mar 2012 thru Feb 2015.

Project 2012WY82B Annual Report: Decadal Scale Estimates of Forest Water Yield After Bark Beetle Epidemics in Southern Wyoming, Brent E. Ewers, Assoc. Prof., Dept. of Botany; Elise Pendall, Assoc. Prof., Dept. of Botany and Program in Ecology; Urszula Norton, Asst. Prof., Plant Sciences Dept.; and Ramesh Sivanpillai, Academic Professional Research Scientist, WyGISC/Dept. of Botany, UW, Mar 2012 thru Feb 2015.

Project 2013WY84B Final Report: Mapping Annual Surface Area Changes Since 1984 of Lakes and Reservoirs in Wyoming that are not Gauged Using Multi-Temporal Landsat Data, Ramesh Sivanpillai, Senior Research Scientist Extended Term, Dept.of Botany & Wyoming Geographic Info Science Center (WyGISC), UW, Mar 2013 Feb 2014.

Project 2013WY85B Annual Report: Micro-Patterned Membrane Surfaces with Switchable Hydrophobicity, Carl P. Frick, Assist. Prof., Dept. of Mechanical Engr., and Jonathan A. Brant, Assist. Prof., Dept. of Civil and Architectural Engr., UW, Mar 2013 Feb 2015.

Project 2013WY86B Annual Report: Use of Fe(VI) for the Improvement of Water Quality in Wyoming, Maohong Fan, SER Assoc. Prof., Dept. of Chemical & Petroleum Engr., and Lamia Goual Assist. Prof., Dept. of Chemical and Petroleum Engr., UW, Mar 2013 Feb 2016.

Project 2013WY87B Annual Report: Rumen Microbial Changes Associated with High Sulfur -- A Basis for Developing Treatments for Ruminant Livestock in High Sulfur Water Regions, Kristi M. Cammack, Assist. Prof. and Kathy J. Austin, Research Scientist, Animal Science, UW; Cody L. Wright, Ph.D., Prof. and Ken Olson, Assoc. Prof., Animal Science, S. D. State Univ.; and Gavin Conant, Assist. Prof. and William Lamberson, Prof., Animal Sciences, Univ. of Missouri, Mar 2013 Feb 2015.

A Treatise on Wyoming Water Law

Basic Information

Title:	A Treatise on Wyoming Water Law
Project Number:	2012WY79B
Start Date:	3/1/2012
End Date:	2/28/2014
Funding Source:	104B
Congressional District:	1
Research Category:	Social Sciences
Focus Category:	Law, Institutions, and Policy, None, None
Descriptors:	None
Principal Investigators:	Lawrence MacDonnell

Publication

1. MacDonnell, Lawrence, 2014. Treatise on Wyoming Water Law, Rocky Mountain Mineral Law Foundation, 9191 Sheridan Blvd., Suite 203, Westminster, CO 80031, 245 pp.

A Treatise on Wyoming Water Law

(Final Report: Year 2 of 2)

Lawrence J. MacDonnell, Principal Investigator

Abstract:

This project sought support for student research assistance associated with preparation of a treatise on Wyoming water law. Since the time of Elwood Mead, Wyoming has been a leader in the development of water law in the American West. Wyoming specifically adopted the prior appropriation doctrine in its 1890 Constitution and established a Board of Control and State Engineer to administer water use in the state. The legislature followed up the next year with new legislation putting in place the basic concepts adopted in the Constitution. Significant legislative changes have followed to produce the statutory system now in place in the State. In addition, the Wyoming Supreme Court has decided hundreds of cases involving issues of water law. The State Engineer and the Board of Control have adopted regulations and other guidance. Consequently, Wyoming today operates under a comprehensive set of laws, decisions, and administrative rules. Yet there is no single written source that provides a thorough summary and discussion of this legal system. This project was intended to fill this gap.

Progress

A book entitled "Treatise on Wyoming Water Law" by Lawrence J. MacDonnell has been published. The reference is: MacDonnell, Lawrence, Treatise on Wyoming Water Law, Rocky Mountain Mineral Law Foundation, 99191 Sheridan Blvd., Suite 203, Westminster, CO 80031, https://www. rmmlf.org, 245 pp.

The following is an abbreviated Table of Contents:

Chapter 1 provides a historical overview of the development of Wyoming water law, including discussion of important legislative enactments and related court cases. Chapter 2 represents the heart of the treatise as it provides a summary of all the relevant statutory provisions and their judicial interpretation. Chapter 3, concerns the determination and administration of water rights by the State Engineer and the Board of Control and the process for judicial review. The fourth chapter includes the law relating uses of interstate rivers and also relates to the Wind River reservation and the law governing uses of water on the reservation. Chapter 1 has also been published as an article in the Wyoming Law Review.

Several law students worked as project research assistants. In addition to funding one full-time student during the summer of 2012, five part-time research assistants were employed during the 2012-2013 school year. In addition, two students worked full-time during the summer of 2013.

The PI was able to draw from this research to prepare and present on March 7, 2013 "Elwood Mead's Vision for Wyoming Water: Then and Now," as the 2012 President's Speaker for the university. This presentation was recorded and is available on Wyocast.

Integrated Accelerated Precipitation Softening (APS) - Microfiltration (MF) Assembly and Process Development to Maximize Water Recovery During Energy Production and CO2 Sequestration

Basic Information

Title:	Integrated Accelerated Precipitation Softening (APS) - Microfiltration (MF) Assembly and Process Development to Maximize Water Recovery During Energy Production and CO2 Sequestration
Project Number:	2012WY80B
Start Date:	3/1/2012
End Date:	2/28/2014
Funding Source:	104B
Congressional District:	1
Research Category:	Water Quality
Focus Category:	Treatment, Water Supply, Water Use
Descriptors:	None
Principal Investigators:	Jonathan Brant, Dongmei Li

Publications

There are no publications.

Final Report

Integrated Accelerated Precipitation Softening (APS) – Microfiltration (MF) Assembly and Process Development to Maximize Water Recovery during Energy Production and CO_2 Sequestration

PI: Jonathan A. Brant, Assistant Professor, Department of Civil and Architectural Engineering, University of Wyoming,

Co-PI: Dongmei (Katie) Li, Assistant Professor, Department of Chemical and Petroleum Engineering, University of Wyoming

Project Duration: 03/01/2012 to 02/28/2014

Abstract: The development of Wyoming's energy resources (coal bed methane extraction [CBM], hydraulic fracturing) and carbon dioxide (CO_2) sequestration sites all invariably result in the production of brackish wastewaters. The treatability of these waters varies from relatively simple for CBM water (dissolved solids < 2,000 mg/L) to complex for the water that is displaced during geologic sequestration of CO_2 (dissolved solids > 20,000 mg/L). Reverse osmosis (RO) is a proven desalination process, which requires hydraulic pressures to transport water across semi-permeable membranes. Although RO has been extensively used to treat a variety of source waters, including energy development produced water, managing the concentrate that is produced as a byproduct during RO has persisted as an environmental and economic challenge in maximizing water recovery rate. Here we propose to develop an integrated accelerated precipitation softening (APS)-microfiltration (MF) assembly for reducing the volume of concentrate that must be disposed of when using RO to treat high-salinity, energy activity related waters in Wyoming. The ability of chemical precipitation processes, including APS, to remove scale-forming elements from source waters is established. Conventional softening processes are hindered by the production of fine suspensions of mineral precipitates that require relatively long sedimentation times (1.5-3 hrs) and a residual sludge having a low solids content (2-30%). These issues generate concerns related to the size of softening facilities, solids carry over to downstream membrane processes, and sludge disposal. These concerns hinder the use of APS as a management strategy for RO concentrate. APS processes use calcite crystals to provide a preferential surface area for nucleation and growth to occur, thus accelerating the kinetics of mineral precipitation. As such, the accelerated APS process will allow the removal of $CaCO_3$ as well as other scale forming elements that will be incorporated in the $CaCO_3$ crystals and removed. Built upon the previous findings in the field of treating challenging source waters, the unique contribution of the proposed work lies in the three folds: 1) incorporating MF as a polishing step following precipitation softening and prior to secondary RO process; 2) application of calcite seeds to accelerate the softening process and to improve the treatability of the feed water for the secondary RO system; 3) application of an integrated rather than singular approach for maximizing the recovery/reuse potential of highly saline produced waters. The integrated APS-MF assembly for RO concentrate treatment will provide a superior feed water quality to secondary RO systems that will allow for water recovery ratios to approach, or exceed, 90%.

INTRODUCTION

The development of energy resources and CO_2 sequestration sites results in production of a large amount of brackish wastewater. Fourteen to eighteen billion barrels of wastewater is produced per year in the United States from oil and gas drilling [1]. A high total dissolved solids (TDS) concentration is one of the aspects that make produced water difficult to manage. TDS concentrations range between 1,000 mg/L and 300,000 mg/L [2]. To put this in perspective, the Colorado River has a TDS concentration of 600-800 mg/L and seawater has a TDS concentration of 30,000 mg/L[3]. Water with a high TDS concentration will harm the environment if it is discharged to the soil surface, therefore it must be treated for re-use by desalination, or disposed of by re-injection or evaporation[4-6]. A conceptual decision tree for managing produced waters is given in **Figure 1**.

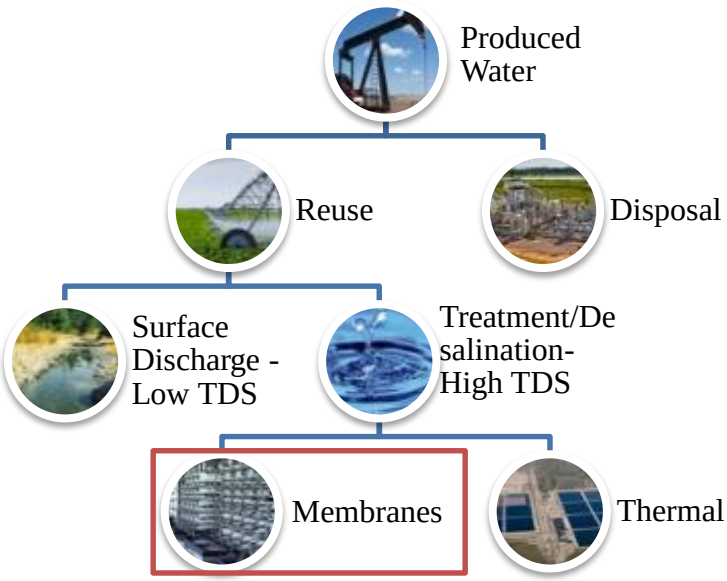

Figure 1: Schematic depicting current produced water disposal options. The red box indicates the category that this research falls within.

In **Figure 1,** the two common treatment strategies for desalination of produced water are membrane processes and thermal processes or distillation [7,8]. The advantages of membrane processes over thermal ones are that they typically require less energy to achieve separation [9]. However, membrane processes are characterized by lower overall water recoveries, or the amount of water that is converted into a product stream, compared to thermal processes. This is particularly evident for highly saline produced waters. For membrane processes the achievable water recovery is limited by many factors including membrane fouling, mineral precipitation (scale formation on the membrane), and the osmotic pressure that must be overcome to initiate water transport across the membrane. Low water recoveries are problematic for any number of reasons. Of most concern in this project was minimizing the volume of the concentrated reject stream that results from membrane desalination [4].

Beneficial reuse of produced waters is of interest to the energy industry and other stakeholders because of the anticipated economic impacts for producers and reduction in the industry's water footprint [1,10]. This latter area is of particular importance to arid regions like Wyoming. Because

the TDS concentration found in produced water is in most cases higher than acceptable levels for potable and non-potable reuse applications some form of treatment is required. The development of a treatment protocol is essential to the success of on-shore oil and gas production due to economic and environmental concerns. Currently, reinjection of produced waters into subsurface formations range in cost from $0.40 to $1.75/bbl and installation of an injection well can cost up to $3 million [12]. For comparison, seawater (TDS ~ 36,000 mg/L) reverse osmosis (RO) desalination systems are characterized by operating costs of approximately $0.16/bbl and capital costs of $125 to $295/bpd [12]. It is difficult to compare the two options in general terms, however, it is clear that both options are economically burdensome to the producer. As population expands and access to fresh water is further limited, the economic viability of reverse osmosis as a reuse technology will increase[1]. A U.S. Department of Energy (DOE) report on hydraulic fracturing flow back water treatment identified a price target of ≤ $2/bbl [13]. Withstanding practical limitations RO was found meet this cost criteria; however, the presence of sparingly soluble metals and minerals presented a challenge to the application of RO because of fouling concerns[13].

RO is a proven desalination technology that has been used for managing oil and gas produced waters [13]. Without proper pretreatment, RO systems treating produced waters have failed or performed poorly [6,15,16], due to severe membrane fouling. In these application the most problematic type of membrane fouling has been mineral scaling in most cases. Common mineral scale forming elements include calcium, barium, magnesium, iron and strontium [17-20]. These elements precipitate onto the RO membrane once their supersaturation concentration is exceeded. Increasing the feasibility of RO treatment of produced waters requires that effective technologies be developed and implemented for removing scale forming elements so as to increase the water recovery during desalination [4,21,22].

This overall goal of this work was to evaluate the effectiveness of accelerated precipitation softening (APS) combined with ceramic microfiltration (MF) membranes for removing scale forming elements from produced water. APS has been shown to reduce the concentration of scale forming elements, particularly calcium [17,25-27], in complex source waters. Additionally, ceramic MF has been shown to effectively remove suspended solids from produced waters [1,28,29] while operating under high solids loading rates. A DOE report on cost, performance and mobility challenges for these two pretreatment steps found that lime softening meets the cost requirements but has performance challenges when silica is present and the treatment has low mobility [13]. Lime softening can be used for suspended solids, calcium, silica, and oil removal [13]. It was also reported here that MF is effective at removing suspended solids and oil at low cost with good mobility, but small particles create a performance challenge [13]. Integration of the two technologies, particularly while using ceramic rather than polymeric membranes, is expected to mitigate the inherent drawbacks associated with the individual processes

The overall objective of this project is to build and evaluate the performance of an integrated APS-MF process in order to dramatically improve the treatability of concentrate streams, thus increasing the overall water recovery rate for RO desalination systems. The specific tasks that were pursued in this work were as follows:

1. To what extent does calcium carbonate seeding improve reaction kinetics in precipitation softening of produced water?

2. What role does microfiltration play in the removal of dissolved and particulate forms of calcium following accelerated precipitation softening?

3. How does APS-MF treatment change the mineral fouling and the specific water flux for secondary RO treating produced water?

EXPERIMENTAL

Produced Water. A synthetic water was created by dissolving dry inorganic salts, at the concentrations listed in **Table 1**, in doubly deionized water (DDW). The composition of the water was set to represent an average primary RO (PRO) concentrate, based on a survey of produced water chemistries in Wyoming

Table 1: Composition of synthetic PRO concentrate based on the average produced water quality found in Wyoming.

Salt	Concentration	
	mol/L	**g/L**
$CaCl_2$	0.02	2.93
Na_2SO_4	0.04	5.05
$NaHCO_3$	0.02	1.72
NaCl	0.10	5.90

The dry salts purchased from Fisher Scientific (Waltham, MA) were sodium bicarbonate (powder, certified ACS) and sodium chloride (crystalline, certified ACS). calcium chloride dehydrate (ACS reagent), sodium sulfate anhydrous, while calcium carbonate powder (precipitated, heavy) were purchased from ACROS Organics (New Jersey, USA). Confocal microscopy of the calcium carbonate particles revealed an average particle size of 7.8 microns. Other research groups have shown this particle size of calcium carbonate to have a specific surface area of 0.8 m^2/g [56]. Sodium hydroxide (10N, Fisher Scientific, Waltham, MA) was used for pH adjustment. Sulfuric acid (1N, VWR Scientific, Tualatin, OR) was used for acidification of reverse osmosis feed solutions.

Optimization of Calcium Removal using APS. A jar tester (Model 7790-711, Phipps & Bird, Richmond, VA) consisting of six three-liter plastic rectangular vessels with stir rods in each was used for initial precipitation experiments. The precipitation reaction was initiated by slowly adding sodium hydroxide to the synthetic PRO concentrate until the desired pH was achieved. Calcium carbonate particles were dispersed in the solution prior to pH adjustment in seeded experiments. The solutions were mixed at a speed of 45 RPM. Grab samples were taken from the jar tester using a 10 ml syringe, filtered using a 0.45-micron PVDF syringe filter (Millipore Corp., San Jose, CA), and analyzed to determine the dissolved calcium concentration. A range of pH values were explored, specifically 7.9, 9.5, 10.5, and 11.6. These values were chosen because they cover a range of saturation indices for calcium carbonate. These pH values correspond with Stiff and Davis Index values of 1.32, 3.06, 3.65, and 4.43, respectively. A dead-end filtration test cell apparatus (**Figure 2)** was used for both initial calcium removal studies via MF and preliminary RO membrane performance testing. Both MF and RO membranes used in the dead-end experiments were purchased from Sterlitech Corporation (Kent, WA).

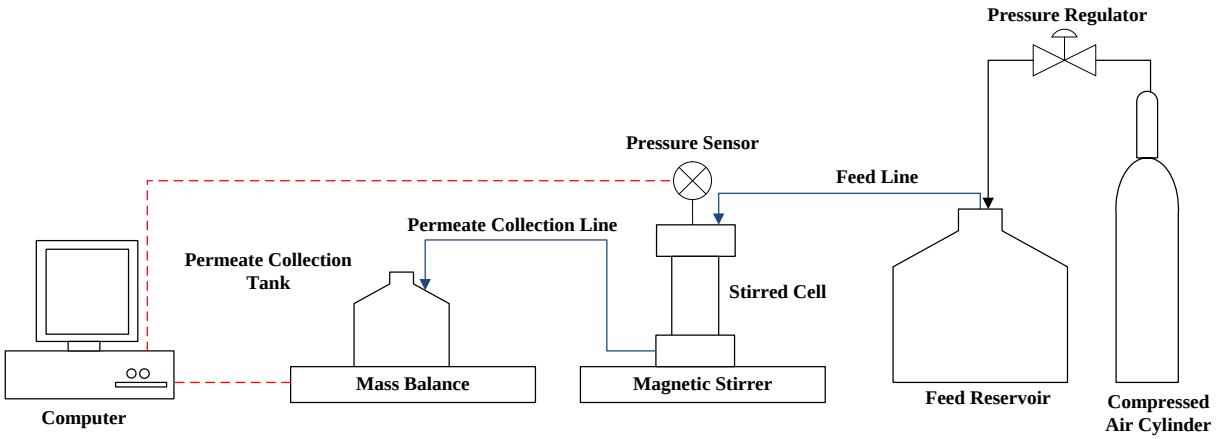

Figure 2: Process flow diagram of the dead-end membrane filtration/desalination test unit.

The feed solution was added to the 300 ml stirred cell assembly and the membrane disc was placed at the bottom of the cell. The active filter area for all dead-end filtration or permeation experiments was 0.0015 m^2. Air pressure was applied to the top of the cell until the desired operating pressure within the cell was reached. The microfiltration tests were performed at low pressure (2.0 bar) and run until all the feed solution was filtered through the membrane. The reverse osmosis tests were performed at high pressure (53 bar) and run for 12 hours. Filtrate was collected and weighed every 10 seconds (Model XS6035, Mettler Toledo, Columbus, OH). The experimental conditions and physical properties of the MF and RO membranes are listed in **Table 2**.

Table 2: Dead-end Experimental Conditions and Membrane Properties.

Membrane	Material	Pore Size	Pure Water Specific Flux L/m^2 hr bar 20 °C	pH Range	Operating Pressure (bar)	Stirring Speed (RPM)
PES MF	PES	0.45 micron	647	2-12	2.0	150
DOW SW RO	PA	MWCO 100 D	0.04	2-11	53	300

Calcium removal by, and fouling of the, MF were assessed using three types of feed water, *i.e.*, untreated, no-seeds, and APS. The untreated feed refers to the synthetic PRO concentrate with no treatment or pH adjustment. To initiate precipitation, the no-seeds feed sample was created by adjusting the pH of the synthetic PRO concentrate to 10.5 using sodium hydroxide (NaOH) and constantly stirring at 45 RPM for 10 minutes. Subsequently, the entire reaction content was poured into the stirred cell. For samples referred to as APS, 7 g/L of calcium carbonate seeds were added to the synthetic PRO concentrate, in addition to adjusting their pH to 10.5. The seeded APS water sample with pH 10.5 was then stirred continuously at 45 RPM for 10 minutes and poured into the stirred cell. Grab samples were taken, using a 10 ml syringe, from the starting feed water, as well as the filtrate, for water quality analysis, including turbidity and calcium concentration. Fouling of the RO membranes was assessed using two different feed solutions. The first solution is the untreated discussed above, while the second being the above APS solution followed by

microfiltration treatment, which is thereby referred to as 'APS+MF' sample. In order to minimize the occurrence of calcium carbonate membrane fouling, the pH of both feed solutions was reduced to pH 5.5 using sulfuric acid to dissolve remaining calcium carbonate precipitate.

Integrated APS-MF System Performance Analysis. APS experiments were done in a 5 L jacketed glass reactor (Prism Research, Raleigh, NC) with a conical bottom. A constant temperature of 20 ^{o}C was maintained using a recirculating digital temperature bath (Model Isotemp 3028P, Fisher Scientific, Waltham, MA). A constant mixing speed of 45 RPM was maintained using a three-blade mixer. First, 7 g/L of calcium carbonate seeds were added to the synthetic PRO concentrate (**Table 1**). After adding the seeds, the APS reaction was initiated by slow addition of sodium hydroxide until pH 10.5 was achieved. The reaction was allowed to proceed until a stable calcium concentration was achieved. Following the APS treatment, the contents of the reactor were pumped from the bottom of the reactor to the cross-flow microfiltration module. Mixing continued in the feed reactor at 45 RPM throughout the microfiltration treatment.

Ceramic MF membranes were selected for this phase of the APS-MF study because of their high chemical stability, durability, and water flux and, most importantly, wide pH tolerance (2-13). Specifically, a titanium dioxide membrane with a nominal pore size of 0.45 µm was purchased from Sterlitech Corporation (Kent, WA), which was constructed as a 250 mm long tube with 7 tubular channels, each having the diameter of 2 mm. The module was operated in an inside-out flow configuration, where feed solution was introduced to the inside of the channels. The membrane was housed in a stainless steel tube from Sterlitech Corporation (Kent, WA) that allowed for continuous cross-flow operation. The pure water specific flux for the membrane at 20°C was determined to be 37 L/m^2 hr bar.

The feed solution was pumped into the cross-flow ceramic microfiltration module (Sterlitech Corporation, Kent, WA) through a flow meter (Model 104FloSen, McMillian CO, Georgetown, Texas) by the feed pump (Model 7523-80, Cole Parmer, Vernon Hills, IL), following the blue line. Backpressure was applied to the module by restricting flow of concentrate returning to the feed reactor. The concentrate flow was controlled using a diaphragm liquid backpressure valve (Model EB2NL2, Equilibar, Fletcher, NC), which was opened and closed using regulated air pressure on the diaphragm. Pressure increase across the microfiltration module resulted in an increase of filtrate across the microfiltration membrane. The filtrate then passed through a flow meter (Model L-50CCMD, Cole Parmer, Vernon Hills, IL) before being collected. Pressure transducers (Setra, Boxborough, MA) were mounted on both the filtrate and concentrate lines exiting the module. The APS-MF system was operated in two different modes: filtrate withdraw and filtrate recycle. In the filtrate withdraw mode the filtrate was collected in a storage vessel. In this mode, the concentration of those materials in the feed solution that were rejected by the MF membrane increased over time. In the filtrate recycle mode the system was operated as a closed loop system. Therefore, the concentrations of materials in the feed solution remained relatively constant over time.

Grab samples for water quality analysis of the starting PRO concentrate, APS effluent, and filtrate after MF treatment were collected. The calcium concentration, turbidity, and total suspended and dissolved solids of each solution were determined for each sample. Decline in TMP or filtrate flux during filtration is often used indicators for membrane fouling. For the APS-MF system, the filtrate flux was set as a constant, while the TMP was measured to monitor changes in membrane resistance, which is proportional to membrane fouling.

RESULTS AND DISCUSSION

Optimization of Calcium Removal in APS. The solution chemistry and reaction conditions for removing calcium through precipitation and APS are well-established in the literature [25-27,30,39,48]. Maximizing calcium removal, while mitigating fouling of downstream MF membranes in the APS treatment scheme, remains however less understood, especially when the untreated water has high TDS concentrations, such as produced waters. The fouling propensity of the untreated PRO concentrate (**Table 1**) and APS treated produced water samples with TDS of 14,000 mg/L were therefore assessed for the MF membranes, while measuring calcium removal. Specific process variables that were optimized during these tests included solution pH, calcium carbonate seed concentration, and reaction time within the softening reactor. Optimal reaction conditions were defined as those that resulted in the most rapid reaction (precipitation) kinetics and the greatest amount of calcium removal. Calcium removal as a function of solution pH is reported in **Figure 3** for the produced water sample represented in **Table 1**. As demonstrated in **Figure 3a** calcium removal increased as the solution pH became more basic in accordance with established calcium solubility relationships.

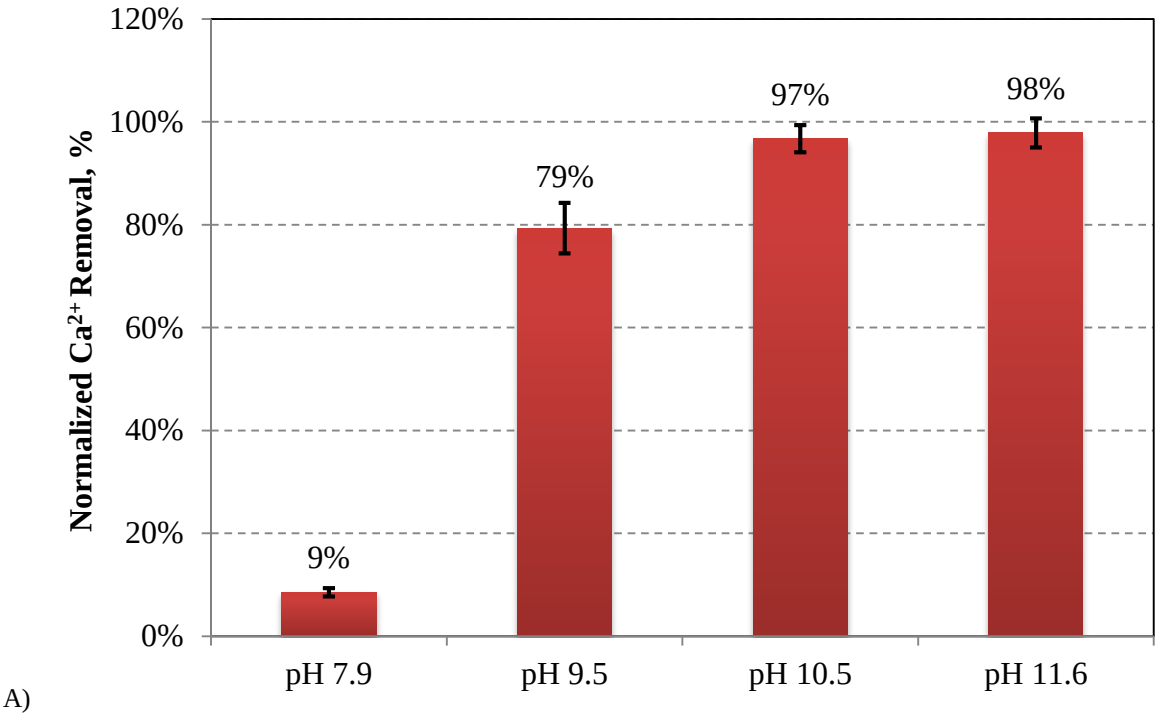

A)

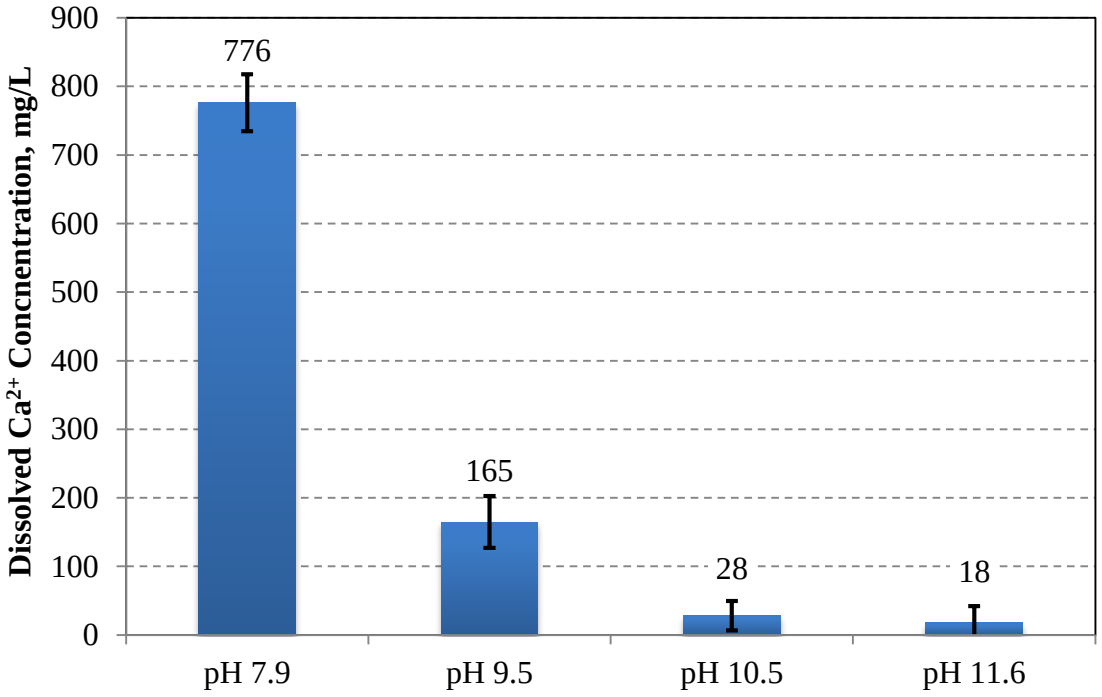

B)

Figure 3: Calcium reduction via jar precipitation softening for various pH conditions after 1 hour of reaction and 45 RPM stirring speed. (A) Percent reduction in calcium reduction (B) Final dissolved calcium concentration after softening (*# of samples per pH (n)* = 3, T = 25°C).

The improvement in calcium removal is most dramatic as the pH increased from approximately 8 to 9.5 (P value > 0.001, making these values statistically different, given p = 0.05 significance scale) and less dramatic as it was increased from 9.5 to 10.5 (P value = 0.0067). There was no

statistical difference (P value = 0.57) in the calcium removal at solution pH ≥ 10.5, which approached 97%. Our data agree well with published values in the literature regarding removing calcium via pH adjustment only [25,26]. Calcium precipitation increased as the concentration of carbonate ions (CO_3^{2-}) increased with increasing pH [3]. The ratio of HCO_3^-/CO_3^{2-} is greater than 1 at pH 7.9, approximately equal to 1 at 9.5, less than 1 at pH 10.5, and close to zero at pH 11.6. In other words CO_3^{2-} is the predominant carbonate species at pH ≥ 10.5, which, therefore, is the typical pH used for calcium removal. The increasing concentration of CO_3^{2-} with increasing solution pH results in an increase in the saturation level of calcium carbonate. The Stiff and Davis index (SDI), which is a quantitative indicator of the saturation level and used to express the precipitating potential of $CaCO_3$, is 1.13, 2.73, 3.73, and 4.83 for pH 7.9, 9.5, 10.5, and 11.6, respectively. In addition to higher saturation, the equilibrium calcium concentration is lower for higher pH values; both impact the lower final dissolved calcium concentration at high pH seen in water softening.

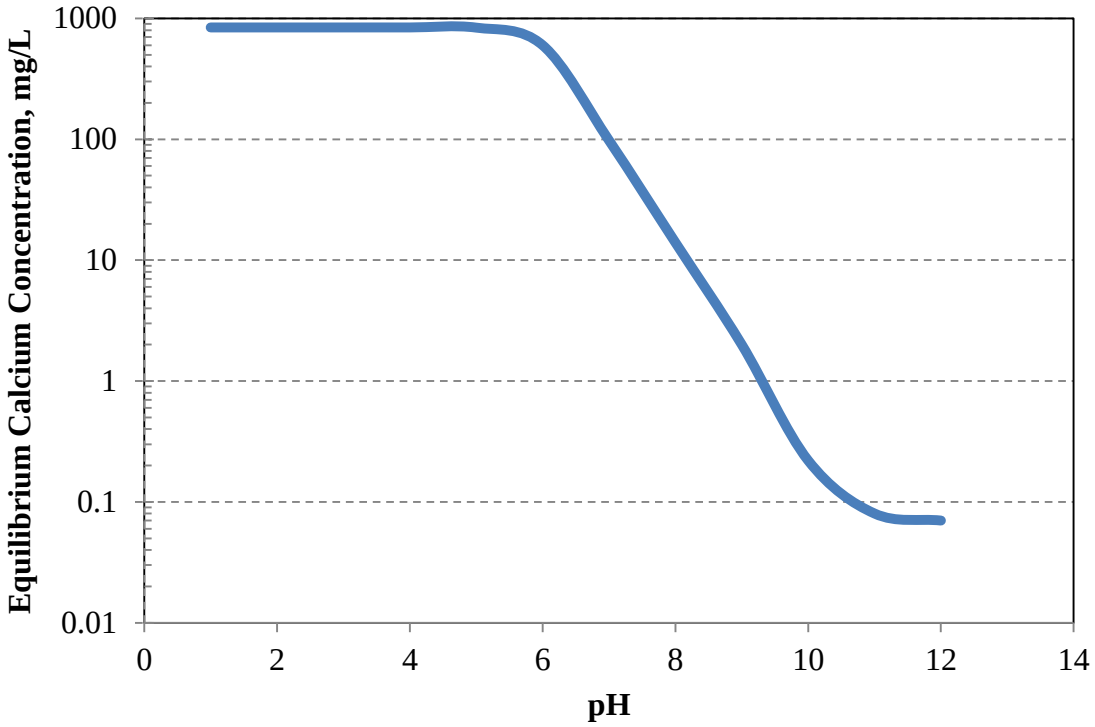

Figure 4: Theoretical equilibrium solubility for calcium for the synthetic water used in this experiment at various pH values. Ionic strength of fresh water was used for predictions. (T = 25 ºC)

The theoretical equilibrium calcium concentration that occurs as a function of solution pH is reported in **Figure 4**. From **Figure 4** the equilibrium calcium concentration is reduced from 100 mg/L at pH 7 to < 1 mg/L at pH 10.5. A previous study on precipitation softening has however demonstrated that the practical minimum solubility limit for calcium at pH 10.5 is 10 mg/L [31]. The difference between the theoretical and practical solubility for calcium is likely due to kinetics, competing ion effects and impacts of solution ionic strength on water activity and calcium

solubility [59]. Because the calcium concentrations at pH 10.5 and 11.6 were not statistically different (P = 0.57), a solution pH of 10.5 was used in the subsequent APS experiments.

To determine the concentration of calcium carbonate seeds that provides sufficient surface area for calcium precipitation at pH 10.5, the kinetics of calcium precipitation was investigated at various seed concentrations. The change in dissolved calcium concentration as a function of reaction time for different $CaCO_3$ seed concentrations at pH 10.5 given in **Figure 5**. The corresponding precipitation rates, *i.e.*, milligrams of precipitated calcium per minute, were determined from **Figure 5**.

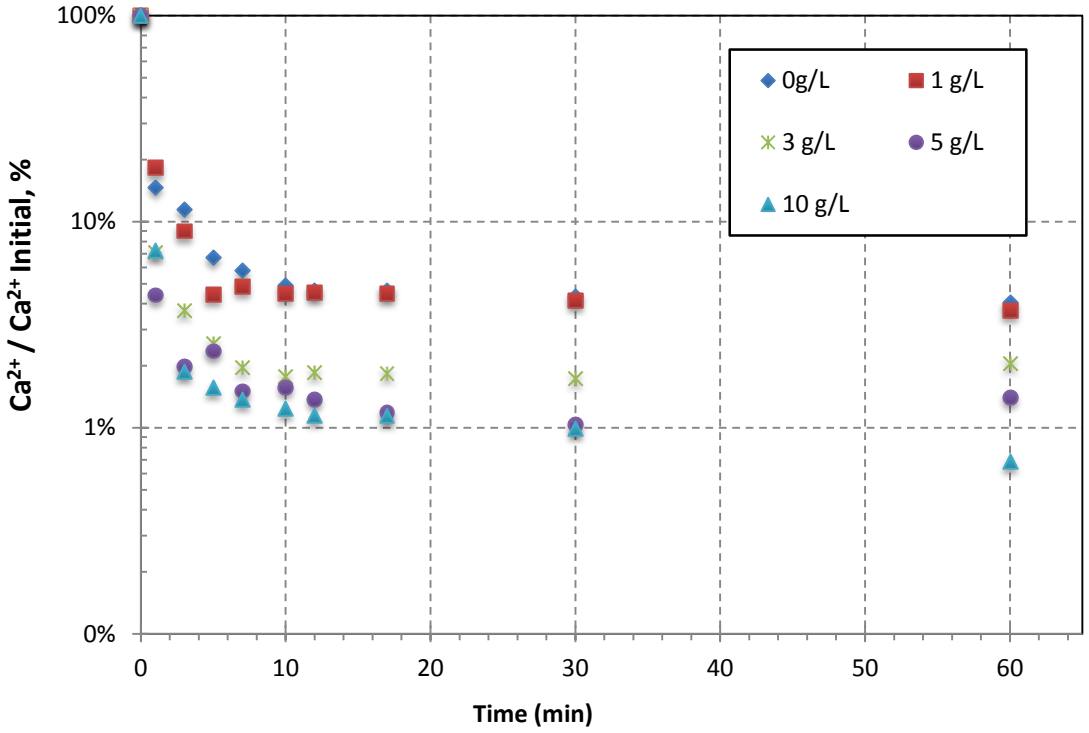

Figure 5: Calcium reduction for different seed concentrations using jar testing at pH = 10.5 and temperature = 25°C. Error bars are not shown for clarity. (n = 3, T = 25°C)

Precipitation kinetics were explored for seeded concentrations of 0, 1, 3, 5, and 10 g/L. The rate of calcium removal for each of the different seed concentrations was calculated for the following three time intervals: 0 to 3 mins, 3 to 10 mins, and 10 to 60 mins (**Figure 5**). The removal rate from 0 to 3 minutes differed greatly for different seeding concentrations, which leveled off after 3 minutes. Although the differences in calcium removal rates for seeded concentrations ranging from 0 g/L to 10 g/L were not quite statistically significant (p-value = 0.097), **Figure 5** shows noticeable variations. Similar dissolved calcium reduction rates less than 250 mg Ca^{2+}/min are observed for 0, 1, and 3 g/L seeding doses. A 15% increase in rate was monitored with 5 and 10 g/L seeding doses, with calcium reduction rate up to 280 mg Ca^{2+}/min. However, higher seeding doses than 5 g/L did not result in significant additional improvement in calcium reduction rate. This suggests that 5 g/L seeding concentration generated the required surface area for nucleation, determined to be 4 m^2/L of solution or 0.005 m^2/ g Ca^{2+}, further testing is required to understand

how the required surface area changes with starting dissolved calcium concentration [56]. The final calcium concentration measurement showed 96% removal (Ca^{2+} = 32 mg/L) for > 5 g/L seeding and 99% removal (Ca^{2+} = 15 mg/L) for >5 g/L seeding. While the difference in calcium removal is not statistically significant (P = 0.19), the trend shows a closer approach to the practical equilibrium calcium concentration of 10 mg/L using seeding than without seeding. A seeding concentration of 7 g/L was chosen in the following experiments to insure adequate surface area for precipitation, in addition to a reasonable reaction time. 10 minutes of reaction was chosen for further APS reaction, because less than 1% increase in calcium removal was noted after 10 minutes of reaction. Finally, it is worth pointing out that our kinetic results are consistent with literature data [25,26]. For example, Rahardianto et al. found that equilibrium calcium concentration was reduced to 52 mg Ca^{2+}/L after 15 minutes of reaction with seeding for PRO concentrate with a starting calcium concentration of 740 mg/L and TDS of 7,000 mg/L [3].

For the following MF study, the water softening kinetics as well as optimized pH via jar testing were used. The conditions utilized were pH adjustment to 10.5, 7 g/L of calcium carbonate seed dosing, and 10 mins of softening reaction before filtration. Initially, optimization of MF conditions were carried out in dead-end filtration experiments on three different feed solutions. The untreated PRO concentrate test was used to evaluate the ability of the MF to remove calcium without softening pretreatment ('Untreated+MF'). The 'No-seeds+MF' and the 'APS+MF' tests were used to evaluate MF performance after softening without and with seeds. APS followed by 20 mins of settling without filtration was also considered ('APS+settling'). From **Figure 6** the calcium removal ranged from 0% to 99% across the different treatment types. In the absence of precipitation through either pH adjustment or APS no calcium was removed from the untreated solution by the MF ('Untreated+MF'). Recall that MF particulates and not dissolved solutes. In contrast, 'APS+MF' was the most effective treatment for removing dissolved calcium from the feed water, followed closely by 'APS+settling' and 'No-seeds+MF'. Initiating precipitation before MF as in the 'No-seeds+MF' and 'APS+MF' treatment scenarios, resulted in greater than 90% calcium removal. The 3% additional removal achieved in the 'APS+MF' treatment scheme could be attributed to the larger particles found in the APS solution compared to the 'No-seeds+MF' treatment.

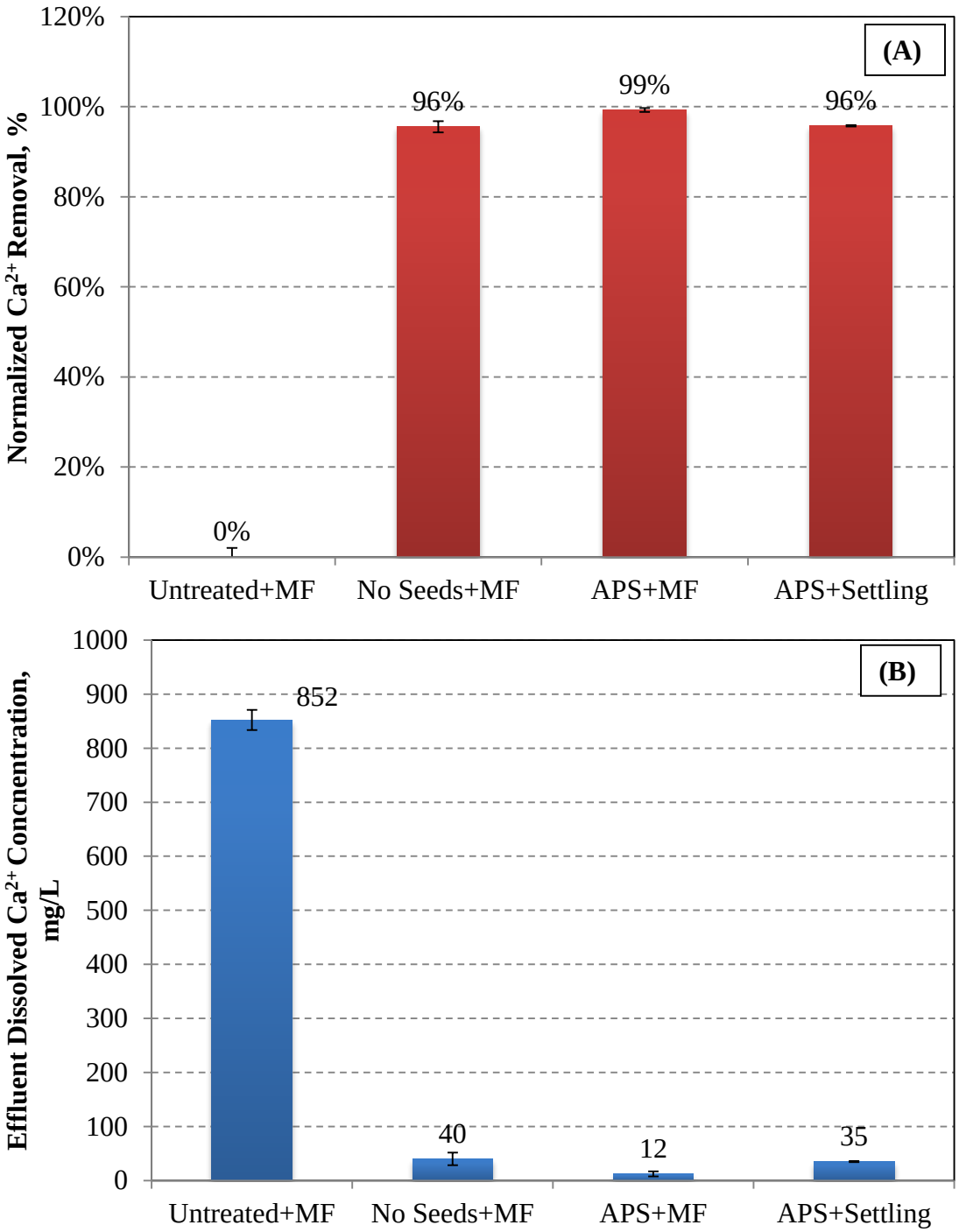

Figure 6: (A) Normalized calcium reduction after different levels of treatment. (B) Final dissolved calcium concentration after treatment (n = 3, T = 25°C).

The small particles in the 'No-seeds+MF' feed may be passing through the MF membrane, resulting in a higher calcium concentration in the 'No-seeds+MF' effluent than in the 'APS+MF' effluent. This was confirmed in **Figure 7**, where the turbidity of the 'No-seeds+MF' effluent is much higher than the 'APS+MF' effluent indicating increased particulate passage.

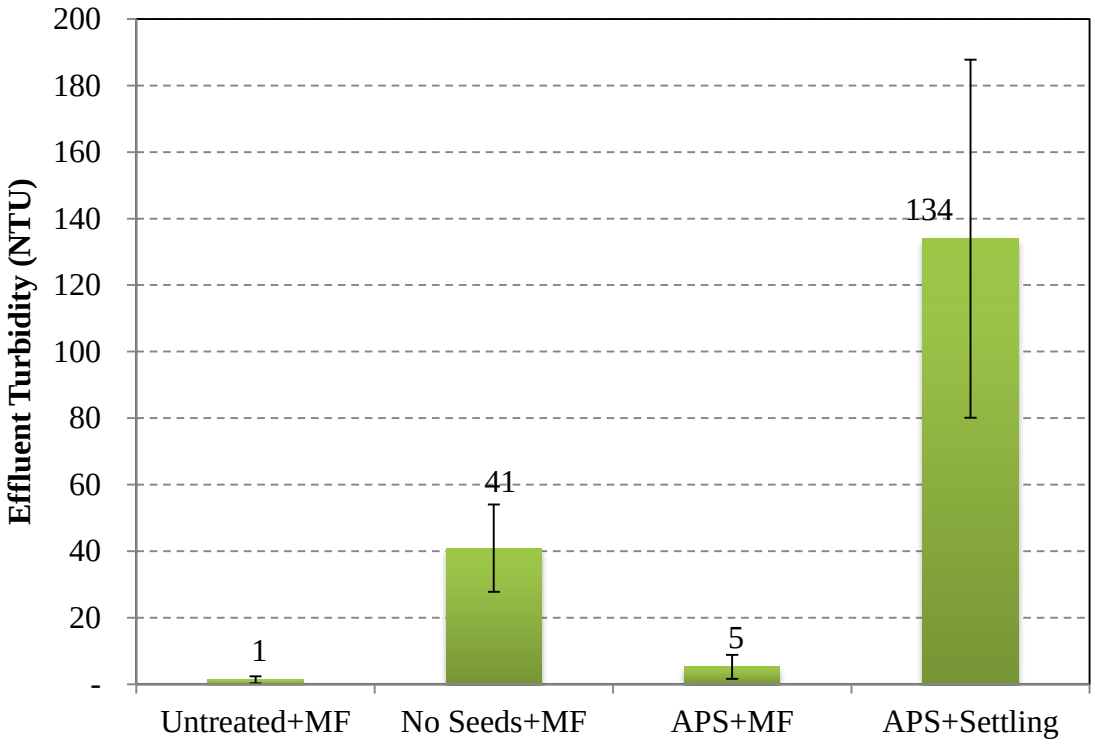

Figure 7: Turbidity of the effluent from different levels of treatment. The initial turbidity values for the different treatment stages were as follows: 'Untreated+MF' = 2.35 NTU, 'No-seeds+MF' = 317 NTU, and for the 'APS+MF' the turbidity was above the detection limit for the turbidimeter (> 800 NTU). The turbidity of the APS solution before settling was also above the detection limit the instrument (n = 3, T = 25°C).

Among all the treatment scenarios, the 'APS+MF' treatment produced the lowest turbidity stream, generating higher quality effluent than the traditional 'APS+settling' treatment protocol. The 'APS+settling' effluent had 26× the turbidity in the 'APS+MF' effluent, in addition to 3% less calcium removal. To further shed light on possible particulate passage, particle size distribution in the feed was explored (**Figure 8)**.

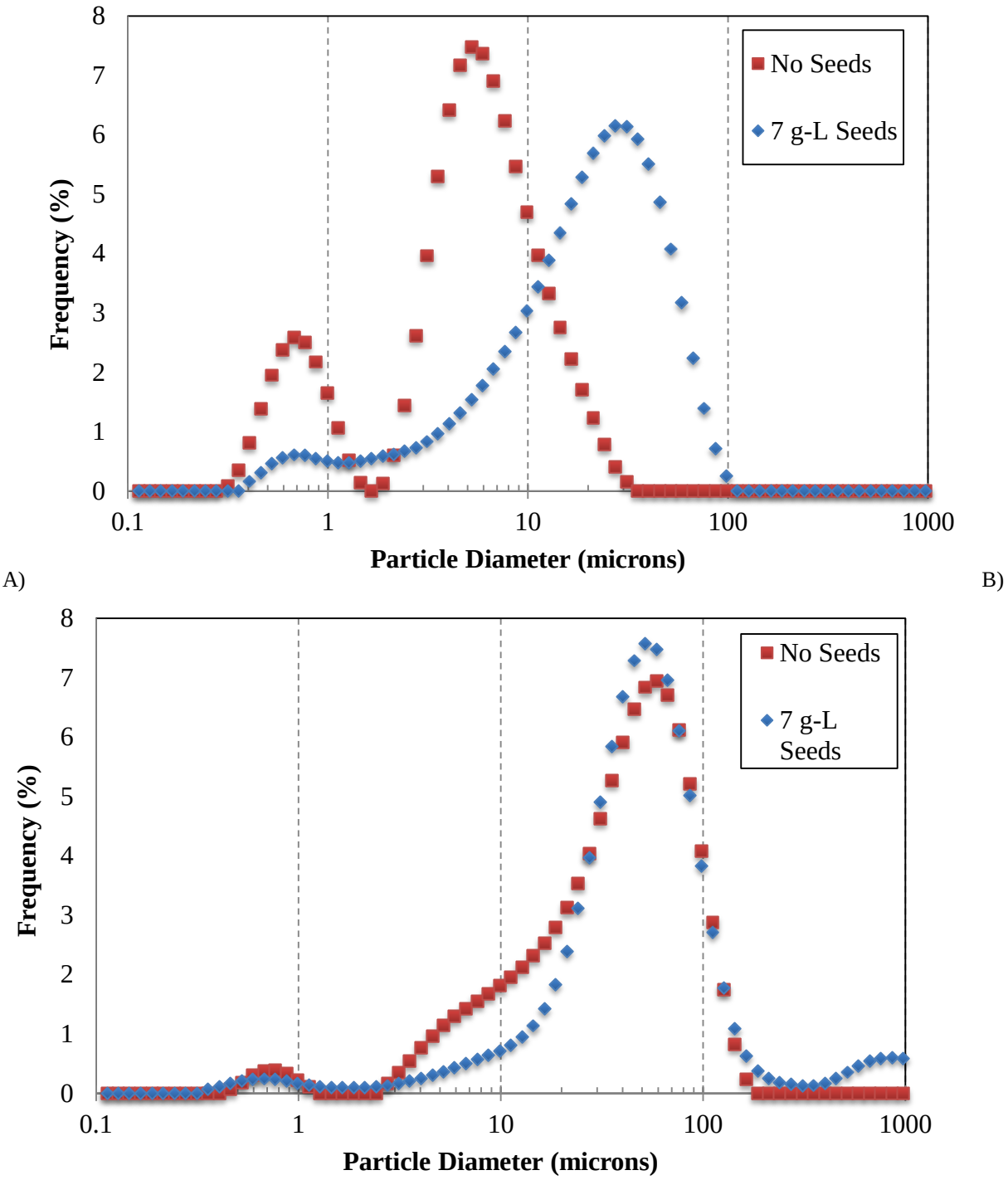

Figure 8: Particle size distribution measured by the granulometer after 5 (A) and 15 (B) minutes of reaction at pH 10.5

Comparing the particle size distribution among no-seeding and seeding, after 5 mins (**Figure 8a**) and 15 mins (**Figure 8b**) of the reaction, the seeded feed has its primary particle peak at 30 µm early in the reaction and 60 µm as the reaction proceeds. The unseeded reaction solution has peaks

at 0.67 and 6 µm at the beginning of the reaction but they appear to grow as the reaction proceeds, with the peak shifting to 60 µm. This indicates that the unseeded solution has particles less than 1 micron in size early in the reaction while the seeded solution has particles greater than 10 microns, this could be due to precipitate growth on the seeds in the seeded solutions rather than formation and growth of precipitates overtime in the unseeded solution. As the reaction proceeds the unseeded and seeded solutions look similar in particle size distribution, as the precipitates grow overtime in both solutions.

In addition to larger particles found in the APS feed to the MF, consequently less particle passing through the MF membrane, the formation of a cake layer may have contributed to the improved turbidity and calcium removal in the MF step, compared to the 'no seeded+MF' treatment. Cake layer formation with filtration of APS feed was further evidenced by the normalized water flux for the different feed conditions used for the MF membrane (**Figure 9).**

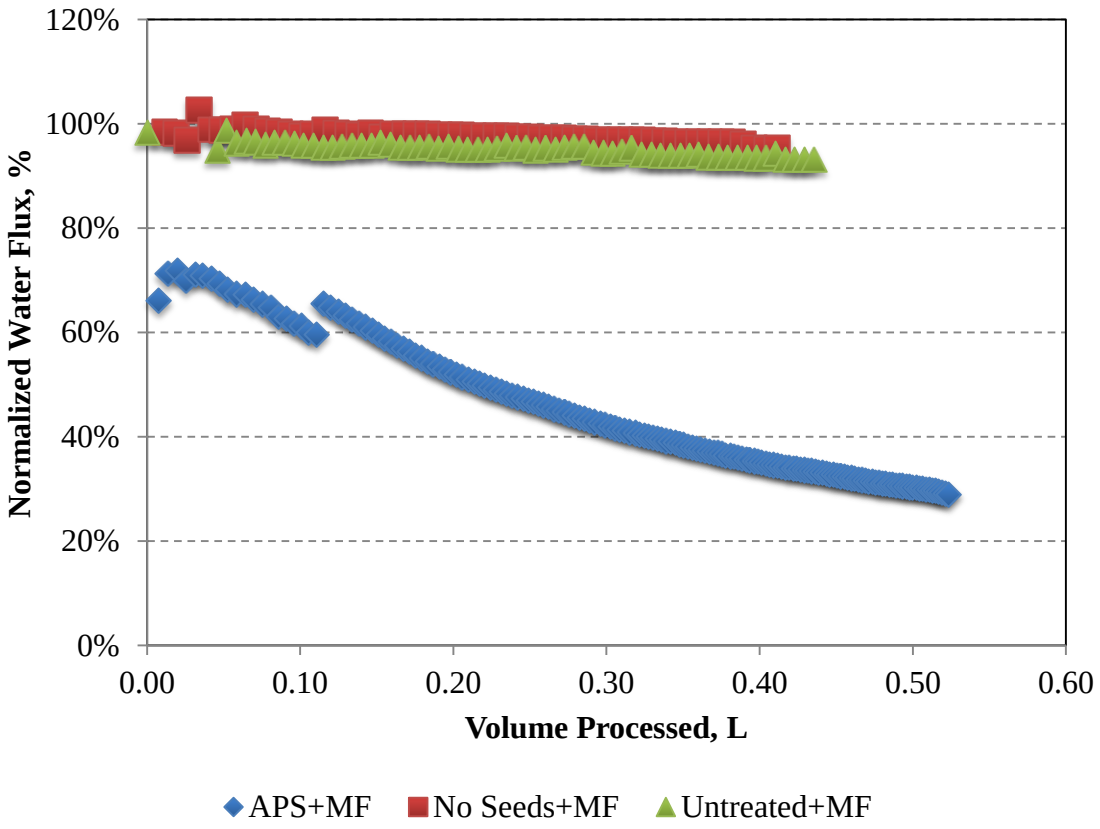

Figure 9: Normalized water flux as a function of the filtered water volume for the PES MF membrane with a nominal pore size of 0.45 µm (P = 2 bar, *n* = 3, T = 25°C).

Flux decreased by 60% from starting flux for the seeded APS treated feed water, which was possibly due to the buildup of a calcium carbonate particulate cake, from the high concentration of suspended precipitates in the feed water. Decreased flux with increasing amount of filtered water generally indicates an increase in cake thickness [31]. On the other hand, there was no significant flux decline for the untreated or no-seeds feed for the 500 ml of water filtered. The presence of a cake layer was confirmed by an evaluation of weight of solids remaining on the

membranes. **Table 3** shows the mass of solids loaded onto the membrane in each treatment scheme. The mass of solids was greatest for the APS feed because of the high concentration of suspended solids after the APS reaction.

Table 3: Mass of solids retained on the MF membrane after filtration of each feed water.

Feed Water	'Untreated+MF'	'No-seeds+MF'	'APS+MF'
Mass of Solids on Membrane [g]	0.0015	0.005	0.11

The data reported in **Table 3** is consistent with the flux profiles reported in in **Figure 9**, where the 'APS+MF' treatment generated 20x more solids loaded on the membrane than the 'no-seeds +MF' treatment, since cake build-up on the surface would cause a steady flux decline for 'APS+MF'. The mass of solids loaded on the membrane was used to calculate the resulting cake resistance coefficient, with the cake resistance coefficient for the 'APS+MF' treatment shown in **Figure 10**. The cake resistance coefficient shows a steady increase in resistance to water flux due to cake build up from the calcium carbonate particulates. This is consistent with the hypothesis that cake formation was a contributor to the flux decline noted in **Figure 9**.

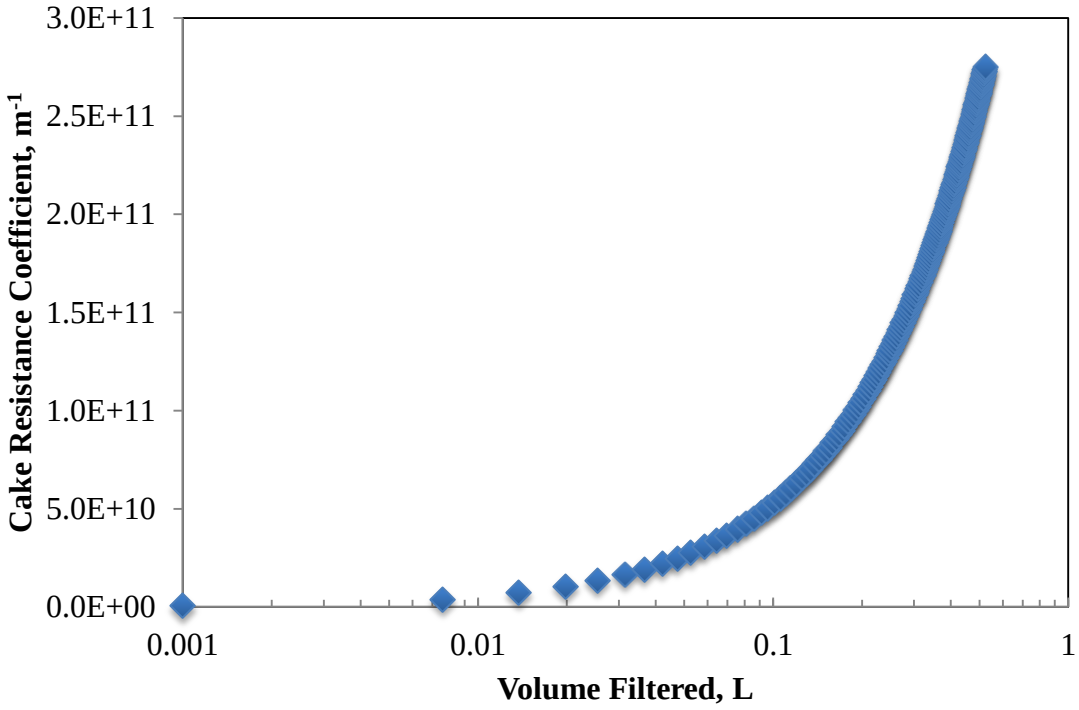

Figure 10: Cake resistance coefficient as a function of filtered water volume for the PES MF membrane filtering APS treated feed water. The virgin hydraulic resistance for the MF membrane was 3.6×10^{10} m^{-1}.

SEM/EDS analysis was done for the surface of each membrane, which showed no particles on the surface of the 'Untreated+MF' membrane, small groups of particles on the surface of the 'No-

seeds+MF' membrane, and a cake layer covering the surface of the 'APS+MF' membrane. EDS analysis revealed that the particles on the surface of the membrane are primarily composed of calcium carbonate, as expected with chemical water softening. To further quantify the water quality improvement using the 'APS+MF' treatment scheme, dead-end RO testing was performed on the treated and untreated water. The fouling propensity of these water samples was evaluated by evaluating possible water recovery and SEM/EDS analysis of the surface of the membrane to explore possible fouling. The pH of both the untreated and treated RO feed solution was reduced to 5.5 using sulfuric acid to eliminate any remaining precipitates and to reduce calcium carbonate fouling tendency. The feed conditions to the dead-end RO are summarized in **Table 4**.

Table 4: Summary of RO feed conditions

Feed	**Calcium Concentration (mg/L)**	**Turbidity (NTU)**	**TDS (mg/L)**	**pH**
Untreated	852	0.85	14,000	5.5
'APS+MF' Treated	12	0.1	14,000	5.5

The fouling propensity of the two solutions was evaluated using two RO fouling indices, *i.e.*, % saturation of calcium sulfate and the Stiff and Davis Index. If the percent saturation value of calcium sulfate reaches above 100%, it indicates fouling from calcium sulfate precipitation may occur. A Stiff and Davis Index above 1 indicates that fouling from calcium carbonate may occur. **Figure 11** shows the calcium fouling propensity for the untreated and 'APS+MF' treated feed water. With untreated feed water, both calcium carbonate and calcium sulfate fouling could occur in an RO system. While calcium carbonate fouling would not occur until 80% recovery (**Figure 11a**), calcium sulfate fouling could occur independent of recovery (**Figure 11b**). However, if the feed water was properly pretreated with the 'APS+MF' system, calcium carbonate fouling can be prevented in an RO system, as shown by **Figure 11a** ('APS+MF', pH 5.5). Additionally, calcium sulfate fouling can also be avoided, unless the water recovery rate requirement is higher than 97%.

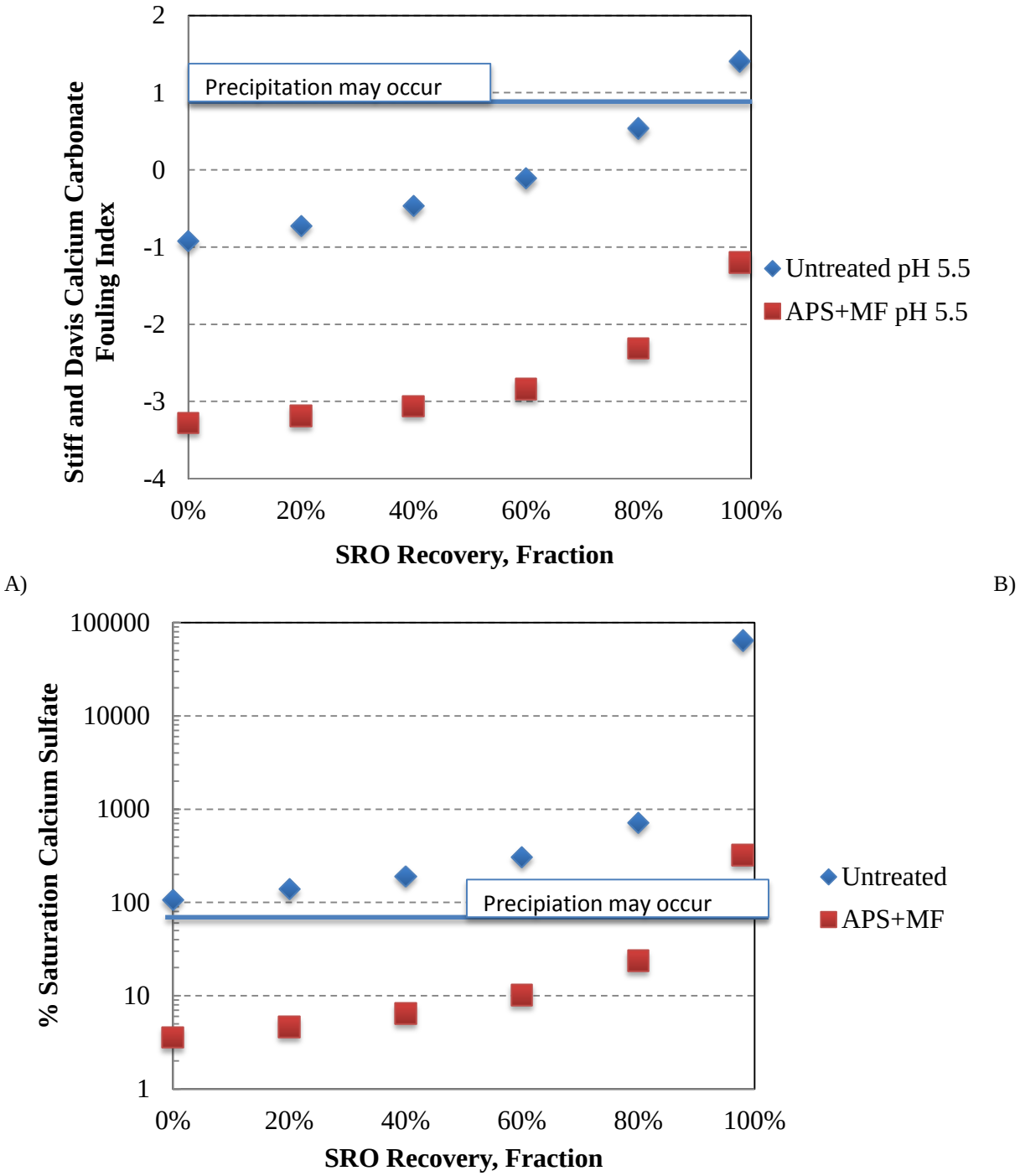

Figure 11: Precipitation potential during RO treatment for untreated and pretreated feed water defined by calcium fouling indices, (A) the Stiff and Davis Index and (B) % Saturation of Calcium Sulfate.

The normalized water flux as a function of the feed water recovery for the RO membrane treating the raw and APS-MF treated source water is given in **Figure 12.** For both source waters the flux declined as the recovery increased (i.e., the feed solution became more concentrated. The gradual

loss in flux can be attributed to an increase in osmotic pressure with increasing recovery. The applied pressure to the dead-end cell was not changed throughout the test, therefore as osmotic pressure increased with increasing water recovery, the water flux declined for both the treated and untreated RO tests. The theoretical change in osmotic pressure with SRO recovery is plotted in **Figure 13**.

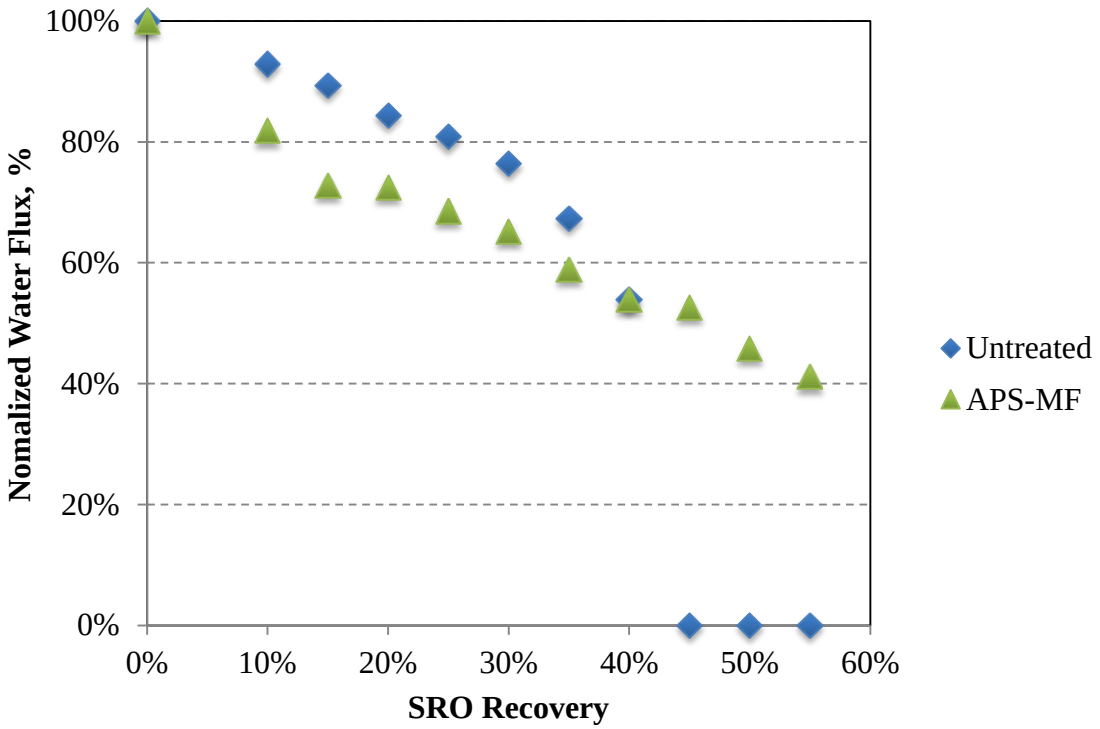

Figure 12: Normalized water flux vs. amount of water recovered from the system for the untreated and 'APS+MF' treated feed conditions. Assuming a TDS concentration of 14,000 mg/L comprised of sodium chloride and 100% RO membrane rejection (n = 3, T = 25°C)

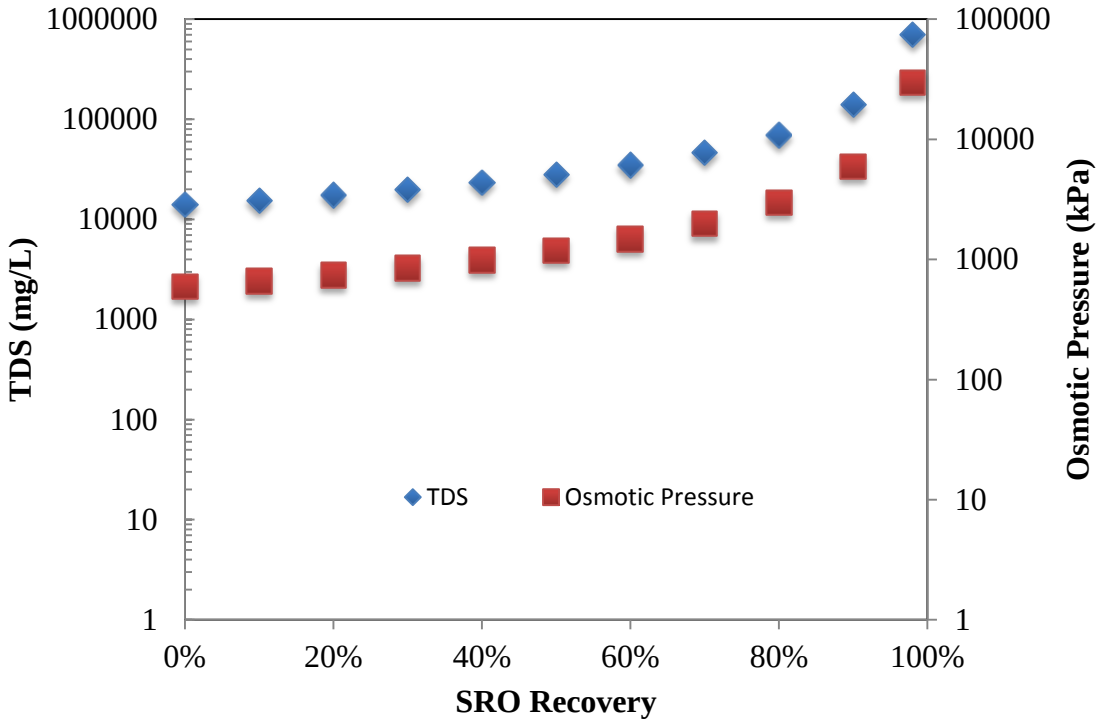

Figure 13: Relationship between the TDS concentration and osmotic pressure with the feed water recovery for the RO process. The initial TDS concentration was 14,000 mg/L.

Figure 12 shows that the untreated RO test has a complete loss in flux at 40% recovery, which cannot be explained by the increase in osmotic pressure through 40% recovery seen in **Figure 13**. This could be explained using **Figure 11**, the deviation of the untreated flux from the treated flux begins at 35% SRO recovery, which corresponds with 150% calcium sulfate saturation and untreated flux stops at 40% SRO recovery, which corresponds to 200% calcium sulfate saturation. This indicates calcium sulfate scaling may have occurred on the RO membrane for the untreated feed water. FESEM analysis of the virgin and fouled RO membranes (**Figure 14**) verified the presence of mineral scale on the membrane receiving raw influent (i.e., having not been treated with the APS-MF).

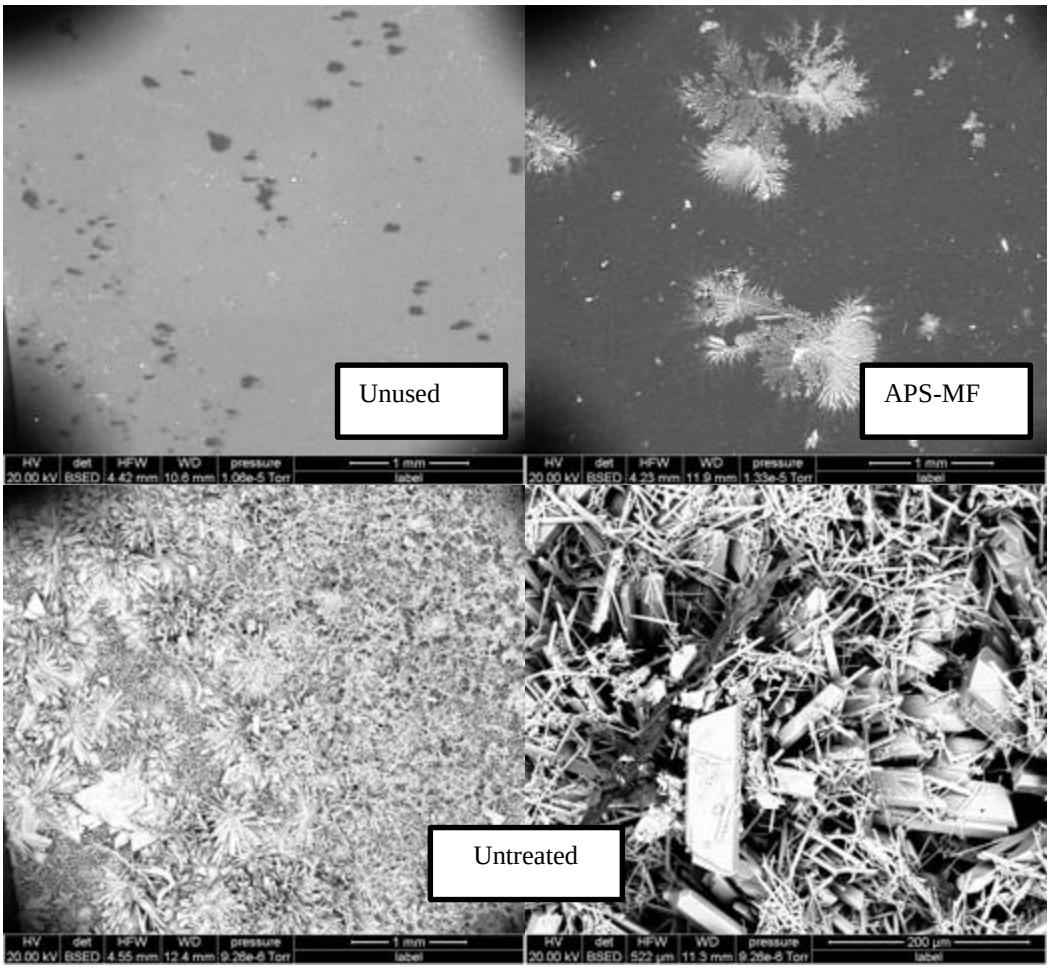

Figure 14: SEM images and elemental analysis of RO membranes for various feed water conditions. Surface element analysis from EDS showed 50% Calcium and 50% Sulfate for Untreated, 3% Sodium, 5% Chloride, 6% Sulfate, and >1% Calcium and Iron for APS-MF treated

From **Figure 14** the entire surface of the RO membrane for the untreated feed is covered in mineral scale crystals, consistent with the flux stoppage observed in **Figure 12**. The elemental analysis of the surface revealed that the crystals were primarily made up of calcium and sulfate, which confirmed the predictions made with data from **Figure 11**. The APS-MF treated RO test did not have any calcium scaling on the surface. Some sodium chloride crystals were observed on the surface; however, this was most likely a result of drying the membrane that had been in contact with the produced water. Therefore, the integrated APS-MF pretreatment system greatly improves the all RO system performance by treating PRO concentrate, reducing fouling in secondary RO and increasing overall water recovery.

Integrated APS-MF System Performance. The jar testing results from the calcium optimization studies were used to define the operating parameters for the bench scale integrated APS-MF treatment system, where both quality of the filtrate and microfiltration membrane fouling were evaluated for extended period of operation. **Figure 15** shows the visual difference in turbidity

between the feed water treated with APS and the resulting filtrate after microfiltration. It is observed that the clarity of the water is dramatically improved after the microfiltration process.

Figure 15: Images of the raw MF feed and its filtrate. The raw MF feed had a turbidity of >800 NTU, while that for the filtrate was = 0.15NTU.

The high turbidity of the feed water (>800 NTU) is due to the addition of seeds as sites for nucleation and growth of precipitates during the APS reaction, in addition to the precipitation of dissolved calcium during the APS reaction. No settling was allowed after APS, which resulted in a highly turbid feed to the MF. Total solids (TS), total suspended solids (TSS), and TDS were used to quantify the difference in water quality at different points in the process, *i.e.*, PRO concentrate as a feed, APS effluent, and filtrate after both APS and MF treatment (**Figure 16**).

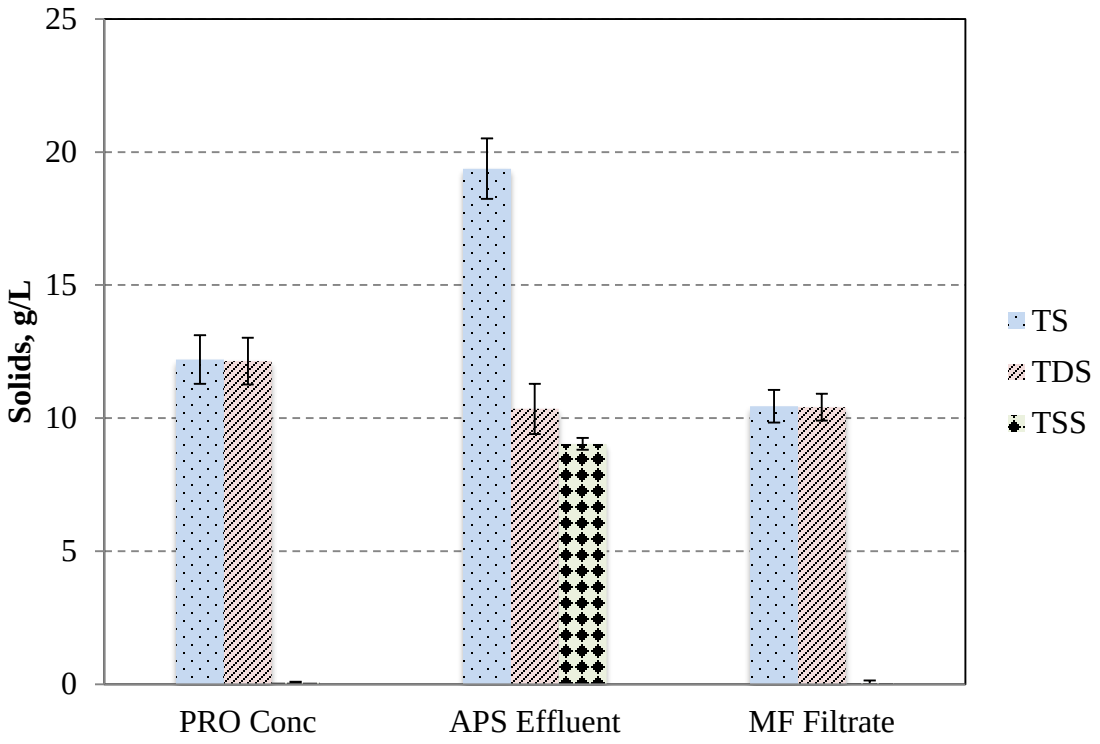

Figure 16: Concentrations of solids fractions in the APS effluent and MF filtrate at the beginning of the filtrate return tests. (n = 3, T = 25°C)

As shown in **Figure 16**, the PRO concentrate had no suspended solids, because it was a fully dissolved supersaturated solution. The APS effluent had a high concentration of suspended solids due to the introduction of seeds and the calcium precipitate totaling 9.0 ± 0.22 g/L of suspended solids. There was a 1.79 ± 1.0 g/L decrease in dissolved solids for the APS effluent and MF filtrate compared to the PRO concentrate, due to precipitation of dissolved calcium. At the beginning of filtrate return tests, the MF filtrate had no suspended solids, indicating that the 0.45-micron titanium dioxide (TiO_2) MF membrane removed the majority of the suspended calcium carbonate particulates. In filtrate withdraw tests, the TSS concentration in the feed tank increased as filtrate was removed from the system (**Figure 17).** The TSS concentration remained constant throughout the operation in the filtrate return mode.

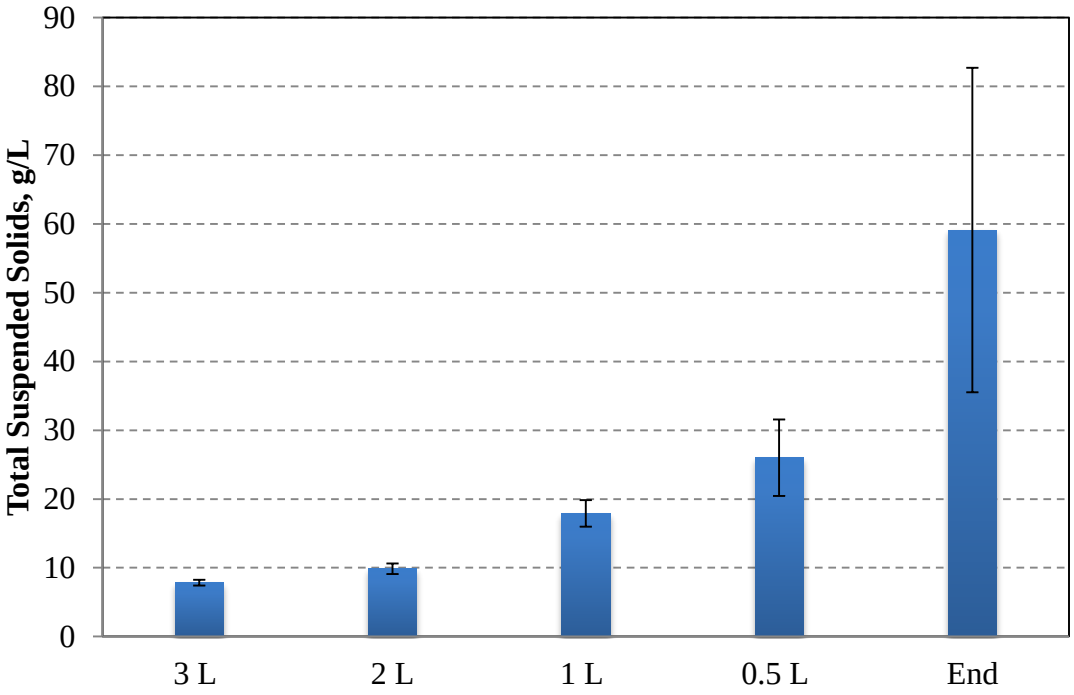

Figure 17: Total suspended solids during filtrate withdraw mode; feed tank is concentrated 8x the original total suspended solids by removing filtrate over time. The test was concluded when the feed tank contents could no longer be pumped through the system. (n = 3, T = 25°C)

With the filtrate being withdrawn from the system, the water content was lowered to 25% of the total final mass at the end of the test. Using turbidity and calcium concentration of the filtrate as indicators, the quality of the filtrate was analyzed continuously for both the filtrate return and filtrate withdraw modes to explore the possible impacts of cake filtration on water quality (**Figure 18**).

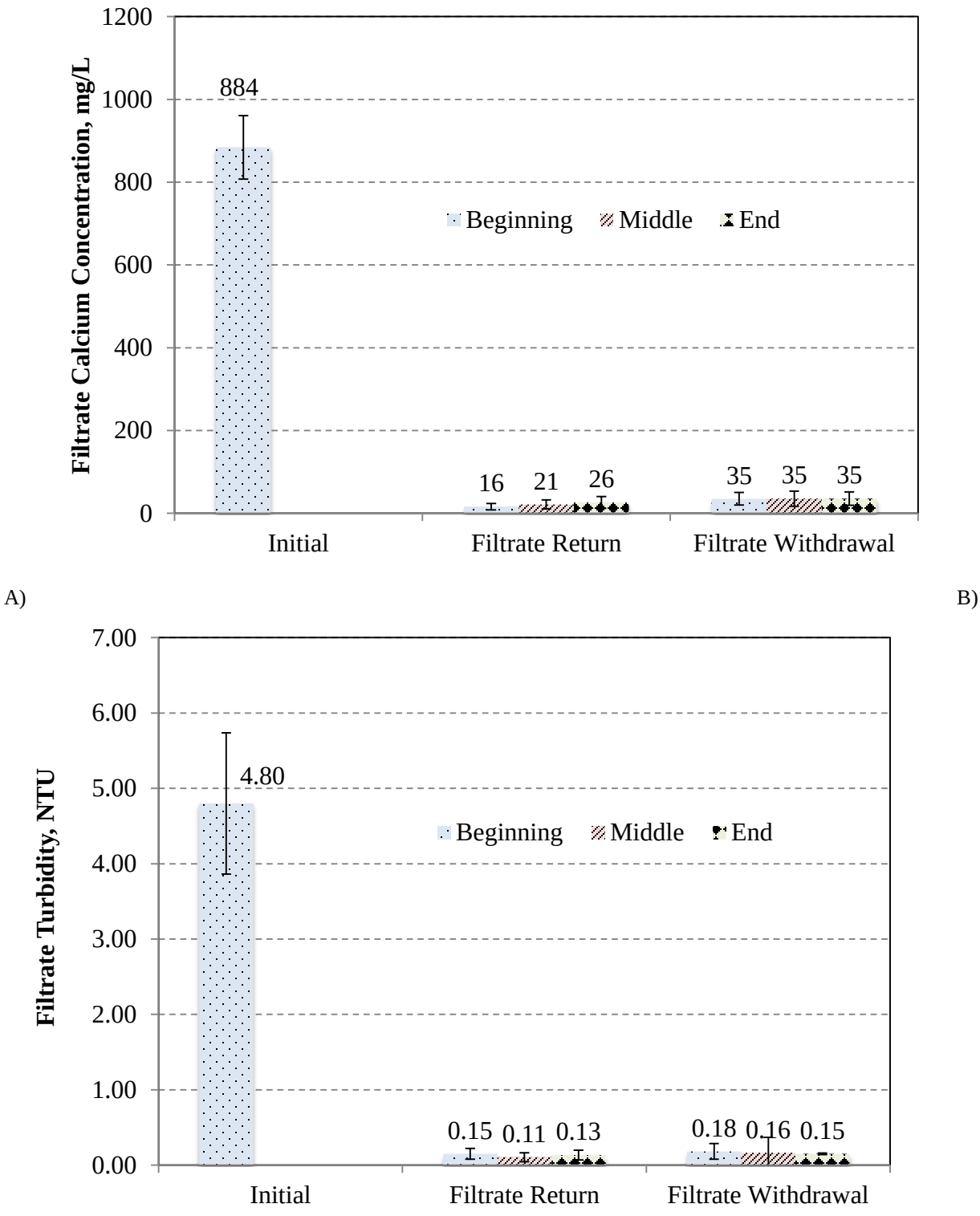

Figure 18: Filtrate quality for filtrate return and filtrate withdraw modes of operation. The beginning, middle, and end label refers to the averages of the water quality evaluated at the beginning, middle, and final point of overall test duration (n = 3, T = 25°C).

Compared to the dead-end experimental results, where 99% reduction in dissolved calcium was achieved, the integrated APS-MF achieved a calcium reduction of 96-98%. This slightly lower calcium removal might result from the lack of cake formation on the cross-flow microfiltration membrane surface, which has been claimed to be potentially beneficial for calcium removal in some cases[23,30,61]. No significant decrease in calcium concentration or decrease in turbidity was observed overtime in the filtrate for either filtrate return or filtrate withdrawal mode, further indicating that cake build up did not increase over time. If a filter cake was forming or increasing overtime, filtration efficiency may improve and cause an improvement in filtrate quality (i.e., decreased calcium and turbidity). After the MF process, the turbidity was reduced below 0.5 NTU, indicating the microfiltration membrane effectively removed the suspended calcium carbonate solids. The increase in filtrate calcium concentration for the filtrate withdraw mode (96% removal, 35 mg/L Ca^{2+}) compared to the filtrate return mode (98% removal, 21 mg/L Ca^{2+}), could be attributed to increased calcium carbonate particulate passage, as seen by an increase in turbidity from withdraw (0.16 NTU) to return (0.13 NTU) modes. The increased particulate passage could be attributed to a higher suspended solids concentration in the filtrate withdraw feed.

Membrane fouling was explored by keeping the filtrate flux constant while monitoring TMP throughout the tests in each mode, shown in **Figure 19**. When operating the system in constant flux mode, the TMP was increased in order to maintain a constant water flux.

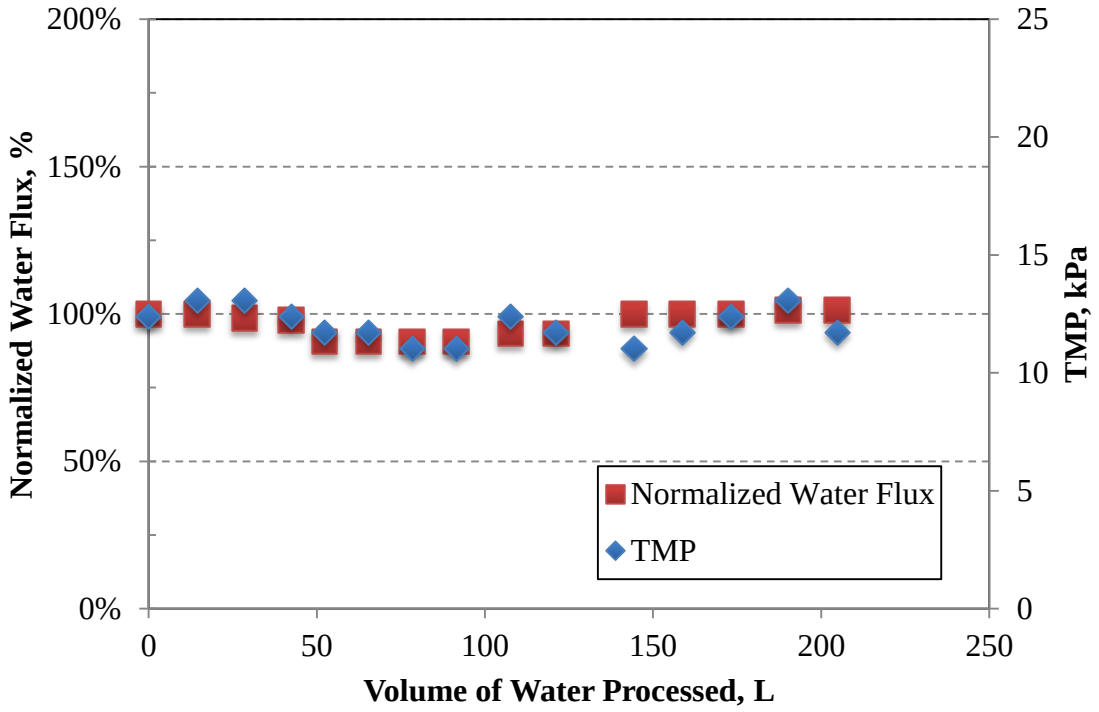

A)

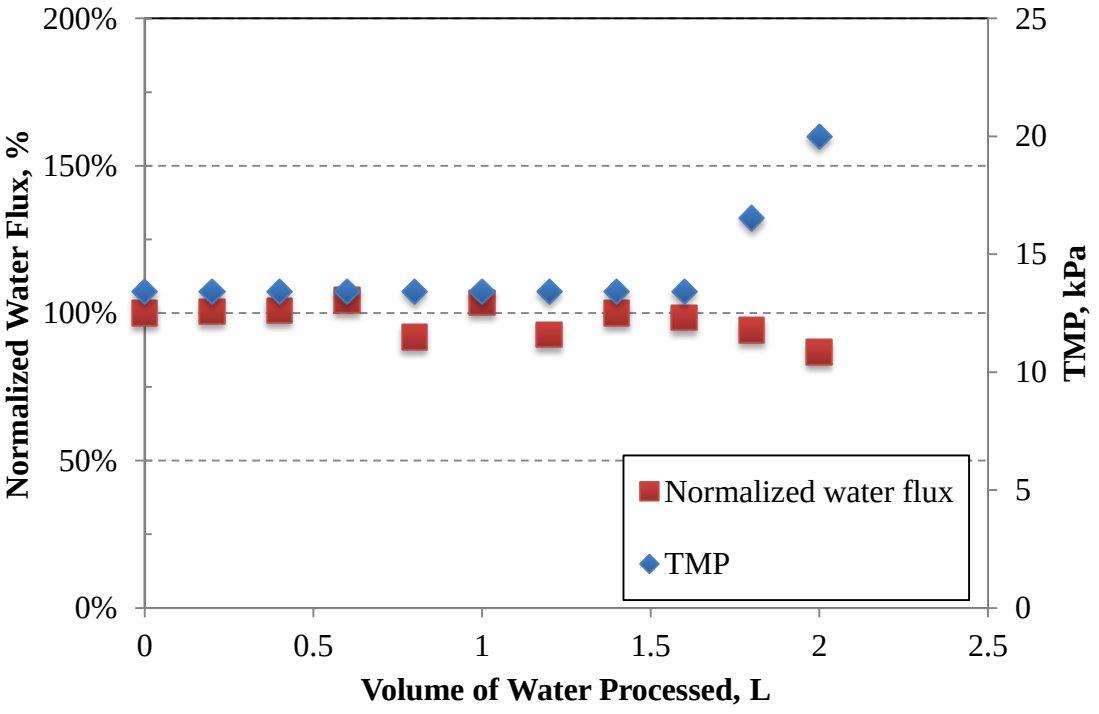

B)

Figure 19: Normalized water flux and TMP for the ceramic MF membrane operated in either filtrate recycle (A) or filtrate withdraw mode (B). No backwashing was used. (n = 3, T = 25°C)

From **Figure 19a** there was no observed increase in TMP during operation of the cross-flow MF for filtrate return mode without the use of backwashing for 200 L of filtrate. This occurred because the ceramic MF and calcium carbonate particles are both hydrophilic therefore no "sticking" occurs between the membrane and particle. Also, cross-flow operation reduces physical build-up of particles on the MF and the use of seeded softening creates large particles that likely did not clog the membrane pores. In filtrate withdraw mode (**Figure 19b**), the TMP rose and water flux fell towards the end of the operation, most likely due to the dramatic increase in TSS observed in **Figure 17** and the significant increase in viscosity.

To confirm the successful elimination of scaling elements from the PRO concentrate, a dead-end RO experiment was performed using the cross-flow APS-MF effluent. From **Figure 20** there was a decline in flux for both the untreated and treated feed water. The gradual loss in flux can be attributed to the gradual increase in osmotic pressure with increasing recovery, while maintaining a constant applied pressure**.** The RO membrane used for the APS-MF treated feed was able to recover 55% of the water fed over the 12-hrs of operation. The measured 55% recovery was not the limiting recovery, it was the recovery reached during the 12-hr test. The untreated feed water completely stopped flux after only 40% water recovery.

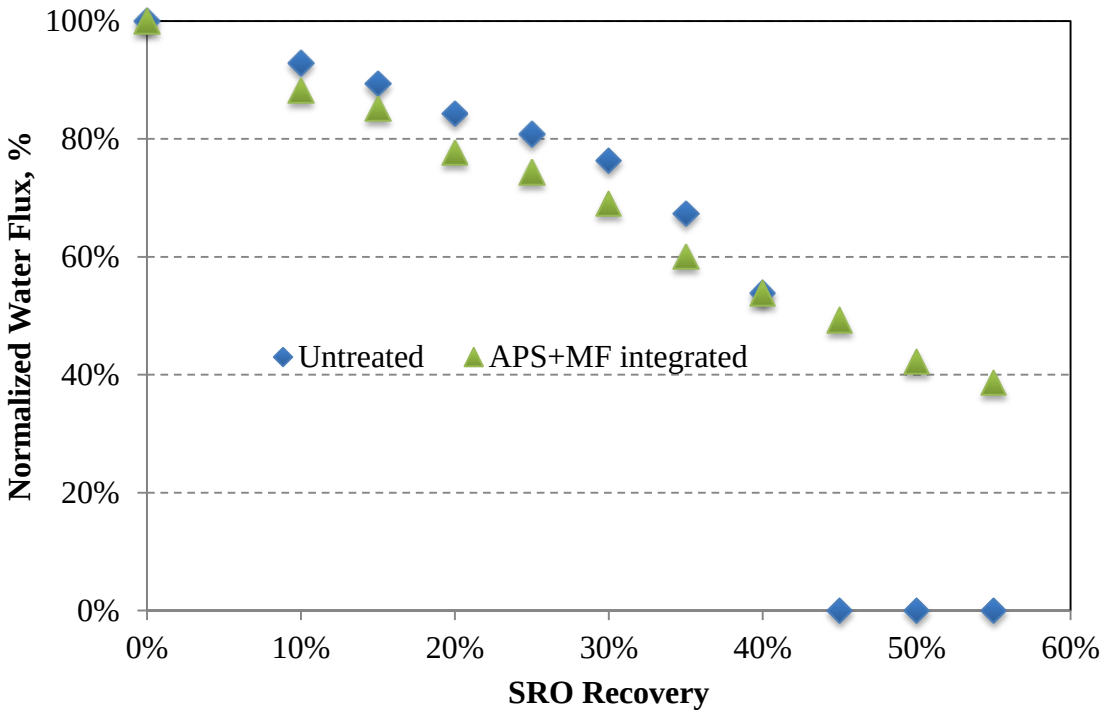

Figure 20: Normalized water flux as a function of the feed water recovery ratio for the RO system treating either raw or APS+MF treated feed waters.

CONCLUSIONS

A review of produced water in Wyoming revealed that water quality varies significantly throughout Wyoming. The majority of produced waters have a high TDS concentration above

6,000 mg/L, predominately made up of sodium chloride. Produced water typically has moderate to high levels of calcium, carbonate, and sulfate. The concentration of calcium, carbonate and sulfate vary based on the location of the well. Desalination technologies must be employed to treat the produced water for reuse because of the high TDS concentration. When membrane desalination is used mineral scaling from calcium should always be considered as a possible limitation on the desalination system's water recovery. Calcium sulfate is the primary problematic mineral scalant in RO systems; because calcium carbonate scaling can be mitigated using acidification. The proposed APS-MF pretreatment scheme targets the removal of calcium to reduce calcium sulfate scaling in membrane desalination.

Our calcium removal optimization studies, for the synthetic water tested, showed that pH 10.5 and 7 g/L of seeding is the optimal pH for calcium carbonate precipitation. Dead-end MF tests in our group demonstrated that the microfiltration step effectively removed calcium carbonate precipitates produced in the softening reaction. Filtration of APS feed water produced filtrate with a 3% lower dissolved calcium concentration and 8x lower turbidity than filtrate from water softened without seeds. The improved filtrate quality is likely due to cake filtration seen in APS-MF treatment, where small precipitate particles are removed in the cake. Dead-end RO testing revealed that the untreated PRO concentrate produced mineral scaling on the RO membrane, completely stopping water flux after only 40% SRO recovery. The APS-MF treated feed water eliminated mineral scaling over the recovery range tested (up to 55% SRO recovery). SEM results confirmed that calcium sulfate scale formed on the RO membranes with untreated PRO water sample, while no calcium scaling was observed on the RO membranes with treated PRO water samples. Integrated APS-MF system performance testing data showed that APS combined with cross-flow ceramic MF system could be operated long term without significant TMP increase. In addition, it could be operated without settling the water after the APS reaction, while maintaining a reasonable operating filtrate flux and TMP. The calcium and turbidity removal seen in the integrated cross-flow APS-MF system was consistent with the dead-end tests, which also enable subsequent RO operation without noticeable calcium scaling.

Student Support and Involvement: We successfully graduated one Master of Science (MS) graduate student (Jennifer Hegarty) with a degree in Chemical Engineering. Two undergraduate students (Kyle Meyers, Freshman in Chemical Engineering; Weikang Li, Senior in Petroleum Engineering) were mentored by the Co-PI for 2-yrs over the project duration. All students were trained on the water chemistry and jar testing procedures for produced water analysis.

Products: Jennifer presented results from her research at the 2013 North American Membrane Society (NAMS) conference in Boise, ID. Her poster presentation covered her results on the characteristics of CBM produced waters, accelerated precipitation softening (optimum seed concentration for calcium removal), and RO membrane fouling in the presence/absence of the accelerated softening pretreatment. The project team has also prepared a draft manuscript on calcium removal during APS-MF treatment, with an emphasis on oil and gas produced waters. The manuscript will be submitted to the journal *Desalination* in May 2014 for publication. Finally, Jennifer successfully defended thesis in February 2014 to obtain her MS in Chemical Engineering.

WORK CITED

1. Ebrahimi, M. *et al.* Multistage filtration process for efficient treatment of oil-field produced water using ceramic membranes. *Desalination and Water Treatment* **42,** 17–23 (2012).

2. Benko, K. L. & Drewes, J. E. Produced Water in the Western United States: Geographical Distribution, Occurrence, and Composition. *Environmental Engineering Science* **25,** 239–246 (2008).

3. Rahardianto, A., Gao, J., Gabelich, C. J., Williams, M. D. & Cohen, Y. High recovery membrane desalting of low-salinity brackish water: Integration of accelerated precipitation softening with membrane RO. *Journal of Membrane Science* **289,** 123–137 (2007).

4. Igunnu, E. T. & Chen, G. Z. Produced water treatment technologies. *International Journal of Low-Carbon Technologies* (2012). doi:10.1093/ijlct/cts049

5. Xu, P. Technical Assessment of Produced Water Treatment Technologies. *RPSEA Project* 1–158 (2009).

6. Doran, G. Developing a cost effective environmental solution for produced water and creating a new water resource. *ARCO Western Energy* 1–9 (1997).

7. Greenlee, L. F., Lawler, D. F., Freeman, B. D., Marrot, B. & Moulin, P. Reverse osmosis desalination: Water sources, technology, and today's challenges. *Water Research* **43,** 2317–2348 (2009).

8. Fakhru'l-Razi, A. *et al.* Review of technologies for oil and gas produced water treatment. *Journal of Hazardous Materials* **170,** 530–551 (2009).

9. Mondal, S. & Wickramasinghe, S. R. Produced water treatment by nanofiltration and reverse osmosis membranes. *Journal of Membrane Science* **322,** 162–170 (2008).

10. Gillespie, P. Oil and Gas Produced Water Management and Beneficial Use in the Western United States. *Science and Technology Program* **157,** 1–129 (2011).

11. Kemp, C. Bear River Basin Water Plan. *Wyoming Water Development Commission* 1–102 (2001).

12. Xu, P., Ruetten, J. & Dolnicar, S. Critical Assessment for Implmenting Desalination Technology. *Water Research Foundation and Drinking Water Inspectorate* 1–230 (2009).

13. Acharya, H. Cost Effective Recovery of Low-TDS Frac Flowback Water for Re-use. *Department of Energy: DE-FE0000784* 1–100 (2011).

14. Xu, P. & Drewes, J. E. Viability of nanofiltration and ultra-low pressure reverse osmosis membranes for multi-beneficial use of methane produced water. *Separation and*

Purification Technology **52,** 67–76 (2006).

15. Doran, G., Williams, K. & Drago, J. Pilot Study Results to Convert Oil Field Produced Water to Drinking Water or Reuse. *Society of Petroleum Engineers* 403–417 (1998).

16. Lawrence, A., Miller, J., Miller, D. & Hayes, T. Regional Assessment of Produced Water Treatment and Disposal Practices and Research Needs. *Society of Petroleum Engineers* 373–392 (1995).

17. Antony, A. *et al.* Scale formation and control in high pressure membrane water treatment systems: A review. *Journal of Membrane Science* **383,** 1–16 (2011).

18. Sheikholeslami, R. Composite scale formation and assessment by the theoretical Scaling Potential Index (SPI) proposed previously for a single salt. *Des* **278,** 259–267 (2011).

19. Ferguson, R. & ferguson, B. The Chemistry of Strontium and Barium Scales. *Asssociation of Water Technologies* 1–17 (2010).

20. Huang, Q. & Ma, W. A model of estimating scaling potential in reverse osmosis and nanofiltration systems. *Des* **288,** 40–46 (2012).

21. Van der Bruggen, B., Vandecasteele, C., Van Gestel, T., Doyen, W. & Leysen, R. Review of Pressure-DrivenMembrane Processes. *Environmental Progress* **22,** 43–56 (2004).

22. Huang, H., Schwab, K. & Jacangelo, J. G. Pretreatment for Low Pressure Membranes in Water Treatment: A Review. *Environ. Sci. Technol.* **43,** 3011–3019 (2009).

23. Oren, Y., Katz, V. & Daltrophe, N. C. Compact Accelerated Precipitation Softening (CAPS) with Submerged Filtration: Role of the CaCO 3'Cake' and the Slurry. *Ind. Eng. Chem. Res.* **41,** 5308–5315 (2002).

24. Gilron, J., Daltrophe, N., Waissman, M. & Oren, Y. Comparison between Compact Accelerated Precipitation Softening (CAPS) and Conventional Pretreatment in Operation of Brackish Water Reverse Osmosis (BWRO). *Ind. Eng. Chem. Res.* **44,** 5465–5471 (2005).

25. Qu, D. *et al.* Integration of accelerated precipitation softening with membrane distillation for high-recovery desalination of primary reverse osmosis concentrate. *Separation and Purification Technology* **67,** 21–25 (2009).

26. Rahardianto, A., McCool, B. C. & Cohen, Y. Accelerated desupersaturation of reverse osmosis concentrate by chemically-enhanced seeded precipitation. *Des* **264,** 256–267 (2010).

27. Rahardianto, A., Gao, J., Gabelich, C. J., Williams, M. D. & Cohen, Y. High recovery membrane desalting of low-salinity brackish water: Integration of accelerated precipitation softening with membrane RO. *Journal of Membrane Science* **289,** 123–137

(2007).

28. Zhong, J., Sun, X. & Wang, C. Treatment of oily wastewater produced from refinery processes using flocculation and ceramic membrane filtration. *Separation and Purification Technology* **32,** 93–98 (2003).

29. Rajagopalan, N. Field Evaluation of Ceramic Microfiltration Membranes in Drinking Water Treatment. *Monatana University System Water Center* 1–4 (2001).

30. Kedem, O. & Zalmon, G. Compact accelerated precipitation softening (CAPS) as a pretreatment for membrane desalinationI. Softening by NaOH. *Desalination* **113,** 65–71 (1997).

31. Crittenden, J. C., Trussell, R. R., Hand, D. H., Howe, K. J. & Tchobanoglous, G. *Water Treatment: Principles and Design*. (John Wiley Sons, INC, 2005).

32. International Energy Outlook 2013 - Energy Information Administration. *eia.gov* (2014). at <http://www.eia.gov/forecasts/ieo/index.cfm>

33. Azetsu-Scott, K. *et al.* Precipitation of heavy metals in produced water: Influence on contaminant transport and toxicity. *Marine Environmental Research* **63,** 146–167 (2007).

34. Survey, U. S. G. USGS Produced Water Database. (2006). at <http://energy.cr.usgs.gov/prov/prodwat/data.htm>

35. Benko, K. L. & Drewes, J. E. Produced Water in the Western United States: Geographical Distribution, Occurrence, and Composition. *Environmental Engineering Science* **25,** 239–246 (2008).

36. Koutsoukos, P. Common Foulants in Desalination: Inorganic Salts. *Encyclopedia of Desalination and Water Resource* 1–17 (2012).

37. Shirazi, S., Lin, C.-J. & Chen, D. Inorganic fouling of pressure-driven membrane processes — A critical review. *Des* **250,** 236–248 (2010).

38. Guo, W., Ngo, H.-H. & Li, J. A mini-review on membrane fouling. *Bioresource Technology* **122,** 27–34 (2012).

39. McCool, B. C., Rahardianto, A. & Cohen, Y. Antiscalant removal in accelerated desupersaturation of RO concentrate via chemically-enhanced seeded precipitation (CESP). *Water Research* **46,** 4261–4271 (2012).

40. Ferguson, R., ferguson, B. & Stancavage, R. Modeling Scale Formation and Optimizing Scale Inhibitor Dosages in Membrane Systems. *AWWA Membrane Technology Conference* 1–19 (2011).

41. Chesters, S. & Armstrong, M. Cost saving case study using a calcium sulphate specific antiscalant. *IDA Wolrd Congress* 1–10 (2009).

42. Ferguson, R. Mineral Scale Prediction and Control at Extreme TDS. 1–12 (2011).

43. Huang, H., Cho, H.-H., Schwab, K. J. & Jacangelo, J. G. Effects of magnetic ion exchange pretreatment on low pressure membrane filtration of natural surface water. *Water Research* **46,** 5483–5490 (2012).

44. Xu, P. & Drewes, J. E. Viability of nanofiltration and ultra-low pressure reverse osmosis membranes for multi-beneficial use of methane produced water. *Separation and Purification Technology* **52,** 67–76 (2006).

45. Waly, T., Kennedy, M. D., Witkamp, G.-J., Amy, G. & Schippers, J. C. The role of inorganic ions in the calcium carbonate scaling of seawater reverse osmosis systems. *Des* **284,** 279–287 (2012).

46. Waly, T., Kennedy, M. D., Witkamp, G.-J., Amy, G. & Schippers, J. C. Will calcium carbonate really scale in seawater reverse osmosis? *Desalination and Water Treatment* **5,** 146–152 (2009).

47. Lower, S. Carbonate equilibria in natural waters. *Environmental Chemistry* **Chem1,** 1–26 (1999).

48. Nason, J. A. & Lawler, D. F. Particle size distribution dynamics during precipitative softening: Constant solution composition. *Water Research* **42,** 3667–3676 (2008).

49. Szwarc, M. 'Living' Polymers. *Nature* **178,** 1168–1169 (1956).

50. CUI, Z., PENG, W., FAN, Y., XING, W. & XU, N. Effect of Cross-flow Velocity on the Critical Flux of Ceramic Membrane Filtration as a Pre-treatment for Seawater Desalination. *Chinese Journal of Chemical Engineering* **21,** 341–347 (2013).

51. Ould-Dris, A., Jaffrin, M. Y., Si-Hassen, D. & Neggaz, Y. Analysis of cake build-up and removal in cross-flow microfiltration of CaCO. *Jounal of Membrane Science* **175,** 267–283 (2000).

52. Yildiz, E., Nuhoglu, A., Keskinler, B., Akay, G. & Farizoglu, B. Water softening in a crossflow membrane reactor. *Desalination* **159,** 139–152 (2003).

53. Kweon, J. H. & Lawler, D. F. Fouling mechanisms in the integrated system with softening and ultrafiltration. *Water Research* **38,** 4164–4172 (2004).

54. Afonso, M., Alves, A. & Mohsen, M. Crossflow microfiltration of marble processing wastewaters. *Desalination* **149,** 153–162 (2002).

55. Ould-Dris, A., Jaffrin, M. Y., Si-Hassen, D. & Neggaz, Y. Effect of cake thickness and particle polydispersity on prediction of permeate flux in microfiltration of particulate suspensions by a hydrodynamic diffusion model. *Jounal of Membrane Science* **164,** 211–227 (2000).

56. Sukhorukov, G. B. *et al.* Porous calcium carbonate microparticles as templates for encapsulation of bioactive compounds. *J. Mater. Chem.* **14,** 2073 (2004).

57. Doll, J. M. & Foster, J. C. The Effect of Calcium Carbonate Particle Size and Shape on the Properties and Performance of Calcium Carbonate Granulations. *Specialty Minerals Inc* 1–21 (2009).

58. Khean, T. Studies in Filter Cake Characterization and Modelling. *University of Malaya* 1–194 (2003).

59. Coto, B., Martos, C., Peña, J. L., Rodríguez, R. & Pastor, G. Effects in the solubility of CaCO3: Experimental study and model description. *Fluid Phase Equilibria* **324,** 1–7 (2012).

60. Gilron, J., Chaikin, D. & Daltrophe, N. Demonstration of CAPS pretreatment of surface water for RO. *Desalination* **127,** 271–282 (2000).

61. Oren, Y., Katz, V. & Daltrophe, N. Improved Compact Accelerated Precipitation Softening (CAPS). *Desalination* **139,** 155–159 (2001).

Multi-frequency Radar and Precipitation Probe Analysis of the Impact of Glaciogenic Cloud Seeding on Snow

Basic Information

Title:	Multi-frequency Radar and Precipitation Probe Analysis of the Impact of Glaciogenic Cloud Seeding on Snow
Project Number:	2012WY81B
Start Date:	3/1/2012
End Date:	2/28/2015
Funding Source:	104B
Congressional District:	1
Research Category:	Climate and Hydrologic Processes
Focus Category:	Water Quantity, Climatological Processes, Hydrology
Descriptors:	None
Principal Investigators:	Bart Geerts

Publications

1. Yang, Yang, 2013. Snow transport patterns in orographic storms as estimated from airborne vertical-plane dual-Doppler radar data, MS Thesis, Atmospheric Science, UW, Dec, 47 pgs.
2. Chu, Xia, 2013. Cloud-resolving Large Eddy Simulations of the silver idodide dispersion from ground and its impact on orographic clouds and precipitation, MS Thesis, Atmospheric Science, UW, August, 97 pgs.
3. Miao, Q., and B. Geerts, 2013: Airborne measurements of the impact of ground-based glaciogenic cloud seeding on orographic precipitation. Advances in Atmospheric Science, 30, 1025-1038. doi: 10.1007/s00376-012-2128-2.
4. Geerts, B. and co-authors, 2013: The AgI Seeding Cloud Impact Investigation (ASCII) campaign 2012: overview and preliminary results. J. Wea. Mod., 45, 24-43.
5. Xue, L., X. Chu, R. Rasmussen, D. Breed, B. Boe, B. Geerts, 2014: The dispersion of silver iodide particles from ground-based. Part II: WRF Large-Eddy Simulations v.s. observations. J. Appl. Meteor. Climatol., 53, 940-958.
6. Pokharel, B., B. Geerts, and X. Jing, 2014a: The impact of ground-based glaciogenic seeding on orographic clouds and precipitation: a multi-sensor case study. J. Appl. Meteor. Climat., 53, 890-909. (21 Feb 2012 case study).

Multi-frequency radar and precipitation probe analysis of the impact of glaciogenic cloud seeding on snow

Year 2 Report
for a three-year (Mar 2012 – Feb 2015)
UW Office of Water Programs
U. S. Geological Survey and the Wyoming Water Development Commission grant
Dr. Bart Geerts, PI
5/1/2014

1. Abstract

This proposal (referred to as Cloud Seeding III) called for the analysis of radar, aircraft, and ground-based datasets collected as part of the ASCII (AgI Seeding Cloud Impact Investigation) campaign over the Medicine Bow mountains (aka the Snowy Range) and the Sierra Madre in Wyoming during the time of glaciogenic cloud seeding conducted as part of the multi-year Wyoming Weather Modification Pilot Project (WWMPP). This pilot project, administered by WWDC and contracted to the National Center for Atmospheric research (NCAR) and Weather Modification Inc (WMI), involves seeding from a series of silver iodide (AgI) generators located in the Snowy Range. Two previous UW Office of Water Programs grants (referred to as Cloud Seeding I and Cloud Seeding II) supported seven research flights over the Snowy Range. Analysis of these data led to a remarkable paper in the *J. Atmos. Sci.* (Geerts et al. 2010), and apparently national recognition in the form of a National Institutes of Water Resources (NIWR) "IMPACT" Award.

2. Objectives and methodology

The key objective is to examine the impact of cloud seeding on radar reflectivity between the AgI generators and the slopes of the target mountain. To do this, we use two radars: the Wyoming Cloud Radar aboard the UW King Air Research Aircraft (UWKA), and two profiling micro-rain radars (MRRs). A composite of reflectivity for seed and no-seed conditions for all downstream flight legs along the wind has been built, using both radars, both upstream of the AgI seed generators ("control") and downwind of the generators ("target"). The next step will be to ascertain that the observed differences in composites are both statistically significant and not attributable to differences in vertical air velocity.

3. Summary of the field work and principal findings

Our ongoing study provides experimental evidence from vertically-pointing airborne radar data, collected on seven flights, that ground-based AgI seeding can significantly increase radar reflectivity within the PBL in shallow orographic snow storms. As reported in Geerts et al. (2010), theory and a comparison between flight-level snow rate and near-flight-level radar reflectivity indicate a ~25% increase in surface snow rate during seeding, notwithstanding slightly stronger updrafts found on average during no-seeding periods. The partitioning of the dataset based on atmospheric stability and proximity to the generators yields physically meaningful patterns and

strengthens the evidence. Firstly, the AgI seeding signature is stronger and occurs over a greater depth on the less stable days than on the three more stable days. Secondly, it is stronger for the two legs close to the generators than for the two distant legs (Geerts et al. 2010). This work was supported by a previous UW Office of Water Programs grant, referred to as Cloud Seeding II.

These results have limitations, mainly because just seven storms were sampled and these storms represent a rather narrow region in the spectrum of precipitation systems in terms of stability, wind speed, storm depth and cloud base temperature. While the analysis yields strong evidence for an increase in reflectivity near the surface, the quoted change in snowfall rate (25%) is unlikely to be broadly representative. It appears that PBL turbulence over elevated terrain is important in precipitation growth, both in natural and in seeded conditions, and thus the same results may not be obtained if the precipitation growth primarily occurs in the free troposphere. This work needs to be followed up with a longer field campaign under similar as well as more diverse weather conditions. Such campaign should include ground-based instruments, such as vertically pointing or scanning radars and particle sizing and imaging probes.

Following the review of the *J. Atmos Sci.* paper (Geerts et al. 2010), we wrote a paper dealing with the importance of PBL turbulence on orographic precipitation (Geerts et al. 2011), and another paper further exploring seeded cloud properties with flight-level data (Miao et al. 2012).

The seven flights and follow-up publications, esp. Geerts et al. (2010), have served as a pilot effort for a much larger research project, known as ASCII, funded by the National Science Foundation. This grant is a collaboration between Dr. Geerts' team and several NCAR scientists (Rasmussen, Breed, Xue). The USGS/WWDC-funded field work and data analysis (esp. Geerts et al. 2010, in *J. Atmos. Sci.*) were instrumental in the success of this $569,097 grant entitled "The cloud microphysical effects of ground-based glaciogenic seeding of orographic clouds: new observational and modeling tools to study an old problem" (Aug 2011 – Jul 2014; reference: AGS-1058426). The emphasis of ASCII is on the cloud microphysical effects of glaciogenic seeding in cold orographic clouds, but ASCII examines glaciogenic seeding in the context of natural snow growth processes. The ASCII research grant is the first time in nearly three decades that NSF (or any federal agency) has supported weather modification research.

The first ASCII field phase was conducted in the Sierra Madre between 4 Jan and 4 March 2012, and it deployed the UWKA, a MGAUS sounding system, an automated weather station, and a Doppler on Wheels (DOW) radar, all funded directly by NSF at an additional cost of about $500K. The DOW was positioned on Battle Pass, and often encountered hostile conditions during ASCII. Hidden in the trees about 600 m downwind of the pass, a scaffold was erected to make measurements with an array of instruments characterizing snow at the surface and overhead (Fig. 4b). ASCII-phase 1 involved 17 intensive observation periods, and is regarded a success, notwithstanding several technical challenges and a relatively warm, dry winter.

The second ASCII field phase was conducted in Jan-Feb 2013, and again focused on the Medicine Bow Range. The NSF funding supported 10 UWKA successful research flights. We also deployed a series of snow probes at GLEES (MRR, disdrometer). Both ASCII campaigns are conducted in the context of the WWMPP, which conducts the ground-based glaciogenic seeding. WWMPP alos released soundings for us from Saratoga, funded by this grant.

4. Significance

Our findings are believed to be significant. This project was selected along with the Wyoming Institute, for the 2012 National Institutes of Water Resources (NIWR) "IMPACT" Award. This NIWR Impact Award was officially awarded at the NIWR meeting at Lake Tahoe in June 2013. Three equally-weighted criteria are used to select the winner of this award, i.e. magnitude, timing, and confidence. The award is national, following a regional selection process, and then a selection amongst the 8 NIWR regions nationwide.

5. Peer-reviewed publications

The following peer-reviewed papers were at least partly supported by this grant (note significant overlap between this grant and the NSF ASCII grant, hence the statement "partly supported"). Research for these papers was conducted in Years 1 and/or Year 2 of the grant.

Miao, Q., and B. Geerts, 2013: Airborne measurements of the impact of ground-based glaciogenic cloud seeding on orographic precipitation. *Advances in Atmospheric Science*, **30**, 1025-1038. doi: 10.1007/s00376-012-2128-2. (link).

Geerts, B. and co-authors, 2013: The AgI Seeding Cloud Impact Investigation (ASCII) campaign 2012: overview and preliminary results. *J. Wea. Mod.*, **45**, 24-43.

Xue, L., X. Chu, R. Rasmussen, D. Breed, B. Boe, B. Geerts, 2014: The dispersion of silver iodide particles from ground-based. Part II: WRF Large-Eddy Simulations v.s. observations. *J. Appl. Meteor. Climatol.*, **53**, 940-958.

Pokharel, B., B. Geerts, and X. Jing, 2014a: The impact of ground-based glaciogenic seeding on orographic clouds and precipitation: a multi-sensor case study. *J. Appl. Meteor. Climat.*, **53**, 890-909. (21 Feb 2012 case study)

Pokharel, B., and B. Geerts, 2014: The impact of glaciogenic seeding on snowfall from shallow orographic clouds over the Medicine Bow Mountains in Wyoming. *J. Wea. Mod.* , accepted.

Chu, X., B. Geerts, L. Xue, and R. Rasmussen, 2014: Radar observations and WRF LES simulations of the impact of ground-based glaciogenic seeding effect on orographic clouds and precipitation: Part I: Observations and model validations. *J. Appl. Meteor. Climat.*, accepted.

Pokharel, B., B. Geerts, K. Friedrich, Xiaoqin Jing, Roy Rasmussen, and D. Breed, 2014b: The impact of ground-based glaciogenic seeding on clouds and precipitation over mountains: a multi-sensor case study of shallow precipitating orographic cumuli. *Atmos. Res.*, in review. (13 Feb 2012 case study)

Yang, Y. B. Geerts, R. Rasmussen, and S. Haimov, 2014: Snow transport patterns in orographic storms as estimated from airborne vertical-plane dual-Doppler radar data. *Mon. Wea. Rev.*, in review.

6. Presentations supported by the Grant

Dr. Geerts and his research group gave oral presentations at a series of meetings in Year 2. These were partly funded by the NSF ASCII grant, partly by the UW Office of Water programs grant.

a. <u>Weather Modification Association meetings</u>

Binod Pokharel presented an ASCII overview oral paper at the 45th Annual Meeting of the American Weather Modification Association, in San Antonio TX, 10-12 April 2013. Binod's trip was paid through an award he received (see below).

Bart Geerts presented an ASCII overview oral paper at the 46th Annual Meeting of the American Weather Modification Association, in Reno NV, 23-25 April 2014. At this meeting, Binod Pokharel presented two posters (based on the papers Pokharel 2014a, and Pokharel et al. 2014b, listed above), and Xia Chu presented a poster based on Chu et al. (2014).

b. Wyoming Weather Modification Pilot Project Technical Advisory Team meetings

Bart Geerts presented an ASCII research update at the WWMPP Technical Advisory Team meetings in July 2013, and Binod gave an updated at the WWMPP TAT meeting in Cheyenne in January 2014.

c. Seminars

Bart Geerts gave the following invited seminars in Year 2:

- 2013/5/6: Dept. of Atmospheric and Environmental Sci., University at Albany ("Glaciogenic seeding of orographic clouds revisited")
- 2013/6/4: invited talk at NCAR, Boulder CO: "ASCII overview, key findings, and lessons learned" (this was a planning meeting to prepare for a new, larger NSF proposal following up on ASCII)
- 2013/6/13: invited presentation at the National Institutes for Water Resources (NIWR) annual meeting, South Tahoe CA: "Impact of glaciogenic cloud seeding on mountain snowfall: an old question revisited."
- 2013/11/6: Cocorahs webinar on glaciogenic cloud seeding , total full-time attendees: 87 (available at http://youtu.be/Br8W0sf3bdM)
- 2014/4/16: Enhanced water recovery from clouds: is it possible? University of Wyoming Spring 2014 Faculty Senate Award Speech, in Laramie
- 2014/4/22: Enhanced water recovery from clouds: is it possible? University of Wyoming Spring 2014 Faculty Senate Award Speech, in Casper

7. Media coverage

In Year 2 Geerts' research was covered in the Laramie Boomerang, the Casper Star Tribune, the Wyoming Business Chronicle, and the University of Wyoming News (http://www.uwyo.edu/uw/news/). The Associated Press had an article on 5/1/2014, and several news outlets carried the article, upon which Geerts was interviewed by ClimateWire in Washington, D.C. We were also part of the Weather Channel's "Hacking the Planet" series in early April 2013. The episode in which we are featured can be viewed at http://youtu.be/rVl_pjEOi9w (this is one of several episodes in the Hacking the Planet series). Note that this is an unlisted and unlinked video, i.e. it is *not* public – the only way to access it is through this link. The reason, of course, is copyright issues.

8. Dissertations/theses

Two MSc students partly or entirely funded by this grant have graduated in Year 2:

- Ms. Yang Yang (MSc) has been partly supported by the current and a previous UW Office of Water programs grant she defend her thesis "Snow transport patterns in orographic storms as estimated from airborne vertical-plane dual-Doppler radar data" on 23 May 2013, and officially graduated in Fall 2013.
- Ms. Xia Chu (MSc) is partly supported by this grant. She defended her thesis "Cloud-resolving Large Eddy Simulations of the impact of AgI nuclei dispersed from the ground on orographic clouds and precipitation: model validation" on 6 June 2013, and officially graduated in Summer 2013.

Other students

- Mr. Binod Pokharel (PhD) is supported by the NSF "ASCII" grant. He passed his Qualifying Exam in Jan 2014, and plans to complete his PhD by May 2015.
- Ms. Xiaoqin Jing (MSc) started in summer 2012, and is funded by this grant from the UW Office of Water Programs. Her work focuses on DOW observations during ASCII_12. She hopes to defend her thesis in June 2014.
- Ms. Xia Chu (PhD) now is pursuing a PhD, on the same topic as her MSc work. Her work is partly supported by this grant.

9. Awards

Graduate student Binod Pokharel, who has been partly funded by this grant, received the 2012 North American Interstate Weather Modification Council Student Award. This is a $1000 fellowship plus all travel expenses to the WMA annual meeting, in 2013 in San Antonio TX, where Binod gave a presentation.

Bart Geerts received the Spring 2014 UW Faculty Senate Award. He gave presentations on weather modification at the UW campuses in Laramie and Casper WY, and received a $1000 honorarium.

Decadal Scale Estimates of Forest Water Yield After Bark Beetle Epidemics in Southern Wyoming

Basic Information

Title:	Decadal Scale Estimates of Forest Water Yield After Bark Beetle Epidemics in Southern Wyoming
Project Number:	2012WY82B
Start Date:	3/1/2012
End Date:	2/28/2015
Funding Source:	104B
Congressional District:	1
Research Category:	Climate and Hydrologic Processes
Focus Category:	Hydrology, Surface Water, Water Quantity
Descriptors:	None
Principal Investigators:	Brent E. Ewers, Urszula Norton, Elise Pendall, Ramesh Sivanpillai

Publications

1. Ewers, BE., 2013. Understanding Stomatal Conductance Responses to Long-Term Environmental Changes: A Bayesian Framework that Combines Patterns and Processes. Tree Physiology. 33:119-122.
2. Schlaepfer, DR, BE Ewers, BN Shuman, DG Williams, JM Frank, WJ Massman, WK Lauenroth., 2014. Terrestrial water fluxes dominated by transpiration: Comment Arising from S. Jasechko et al. Nature 496:357-351 (2013).

Annual Report to Wyoming Water Development Commission for the Project:

Decadal Scale Estimates of Forest Water Yield After Bark Beetle Epidemics in Southern Wyoming

(Year 2 of 3)

PIs Brent E Ewers, Elise Pendall, Urszula Norton, Ramesh Sivanpillai

Abstract

The forests in Wyoming are undergoing profound changes in their hydrologic partitioning of precipitation due to an ongoing epidemic of bark beetles. These forests are key components of major river watersheds and could magnify any impacts on downstream users of water. Recent research at the forest stand scale has shown that while the trees die over the first several years of an outbreak, evapotranspiration declines, soil moisture increases, soil nitrogen increases and snowpack increases and melts faster. These changes in forest hydrology strongly suggest that streamflow should increase. However, ongoing streamflow measurements show no increase. This conundrum between stand processes and watershed processes will be directly addressed by this project. Further, the length of time in which hydrological changes at the stand scale will persist is unknown because of lack of knowledge about how these stands will experience succession after bark beetle epidemics. To address these issues we will 1) quantify tree, seedling, sapling and other understory species composition in forest stands to characterize succession and 2) utilize multiple remote sensing tools to improve scaling between well-instrumented forest stands and watersheds. In addition to these two objectives we will synthesize a large amount of prior and ongoing data collection into an explicit data informatics framework. This framework will serve two purposes 1) novel data syntheses can occur in near real-time, enabling model-data fusion to improve predictions of streamflow and 2) rapidly serve data and model results for public and land manager use. This project builds on previous work that quantified and predicted water yield from bark beetle infested stands in the first five years of an outbreak and extends the time frame of predictions out to multi-decades. This work will enable both State and Federal water managers to make crucial predictions of streamflow from infested mountain ranges on time-frames that are relevant to land management decisions.

Objectives

1) Establish a web service for public and water management use that will provide direct access to data and model predictions

2) Predict the impact of forest succession from lodgepole and spruce-fir forests after bark beetle mortality on forest water yield and nitrogen loss from stands

3) Use ongoing stand and catchment scale measurements with remote sensing tools and mechanistic models to estimate bark beetle impacts on water yield at the mountain range scale

Methodology

We have adopted the Terrestrial Regional Ecosystem Exchange Simulator-Cavitation (TREESCav) model for all the simulations for this project. The TREESCav model has the appropriate tree hydraulic and photosynthesis mechanisms to simulate bark beetle attacks. The model also has a full water budget including snow melt, sublimation, interception, soil moisture, drainage, tree transpiration and evaporation. The model includes Bayesian model-data fusion so that parameterization rigorously uses data. The

hydrology community has begun to recognize that simulation of water budgets from vegetated watersheds must include carbon and nitrogen cycles for mechanistic and thus predictive understanding. Such an approach is necessary when projecting forest changes after a disturbance because carbon and nitrogen cycling co-limit forest production along with water. Thus, we have implemented new algorithms of soil carbon and nitrogen processing that can be compared to soil measurements of both processes from a recently finished NSF grant. This project will supply some ongoing measurements of soil carbon and nitrogen pools and fluxes to constrain TREESCav as succession continues.

Our remote sensing approach utilizes Landsat data as an appropriate compromise between spatial and temporal resolution based on preliminary analyses comparing the data to MODIS and Aerocam.

The testing of both the TREESCav model and remote sensing data sets requires multiple data sets interacting at various temporal and spatial scales. To facilitate these comparisons and prepare the data for public sharing, we have adopted Structured Query Language (SQL) approaches. We have implemented SQL databases for all of the vegetation data from the Chimney Park and GLEES research sites which was funded by a grant from this agency that ended in Feb. 2013 (see final report for details). The database for the stand level fluxes, water budgets and vegetation are now completed. We have also finished the work with UW IT to allow serving of data. The spatial interface for querying data will be under beta-testing in May 2014 and will be available for public use on July 1, 2014.

Principal Findings (Cited Papers are in Publications Section)

We have built a quantified response of water budgets to bark beetles over the first five years of the mortality event. We have found clear patterns in changes in live basal area which sets up the other responses. Soil moisture, litterfall, and vegetation cover all show that the forest is recovering from the mortality event within about five years which is less than half the time we predicted prior to collecting the data. As a consequence of the extra litterfall (Figure 1) that is being decomposed while soil moisture is higher in the initial years, soil gas fluxes of CH4 (values closer to zero indicate less update and more water-saturated soils) and N2O (higher values indicate greater N cycle stimulation) are both significantly impacted (Figure 2). These change reflect differences in the water and soil N cycle which lead to increases in new plant cover (Figure 1). The very strong increase in vegetation cover uses more water and likely contributes to the over compensation of water vapor flux as mortality increases (Figure 3). Surprisingly, our results show that streamflow, when normalized by annual precipitation, actually decreases as mortality increases in contrast to hypotheses and some other watershed data. Our explanation for this difference includes the following components 1) forest succession is happening faster than expected, 2) the morality of 80% is not consistent within the flux tower footprint or watersheds, some patches are higher or lower, 3) the timing of each patch of mortality is not synchronized so that when one patch is at peak mortality impacts on stand properties (3-4 years, Figure 1), other patches that were attacked earlier are already recovering. In fact, studies of bark beetle infestation rates in watersheds show an average of 5-7 years to reach maximum mortality supporting our contention.

All three of our objectives require successful testing of the TREESCav models against the bark beetle mortality datasets from the Chimney Park and GLEES research sites.

The Bayesian approach to model parameterization via fusion with data is superior for processes that have uncertainty in both the processes and data (Ewers et al 2013). With this conceptual framework in place, we have tested the model against tree transpiration, evapotranspiration, tree hydraulic and tree nonstructural carbohydrates and total net ecosystem exchange of CO2. The model has been very successful in simultaneously simulating all of these processes except for one (see next paragraph). Our Bayesian model-data fusion analyses now show that the model is simulating the data as best as possible given the uncertainties in the data itself. We were only able to simulate these fluxes successfully when appropriate root and microbial response to soil moisture and nitrogen were included showing the link to stand water budgets and water quality. The resulting posterior distribution of major parameters after testing the model against data is shown in Figure 4. The effort required to obtain these results has been significant in both coding and processing time. With the help of Jared Baker from UW-ARCC, TREESCAv is now running on Mt Moran HPC reducing the time to run a full Bayesian simulation of one year from 10 days to 8 hours. This dramatic decrease in simulation time now allows spatial scaling of TREESCav simulation to whole watersheds and mountain ranges which will be implemented this summer and early fall.

An unexpected finding from our work is the enormous amount of water vapor fluxes that occur during the winter (Figure 5). If we run TREESCav using incoming snow fall, the model is only able to simulate about 10% of this winter water vapor flux from snow. Other models that rely on a basic snow energy balance perform just as poorly. We now have a new water vapor isotope laser purchased using NSF EPSCOR funds (a project that was funded partially due to previous funding from this agency). This laser will allow partitioning of water vapor fluxes every half hour during the entire year. Thus, we can determine when water vapor flux is occurring from snow in either the pack or the canopy with little liquid water present (sublimation). We will formulate a mechanistic snow sublimation submodel in TREESCav to appropriately simulate these enormous winter water vapor fluxes.

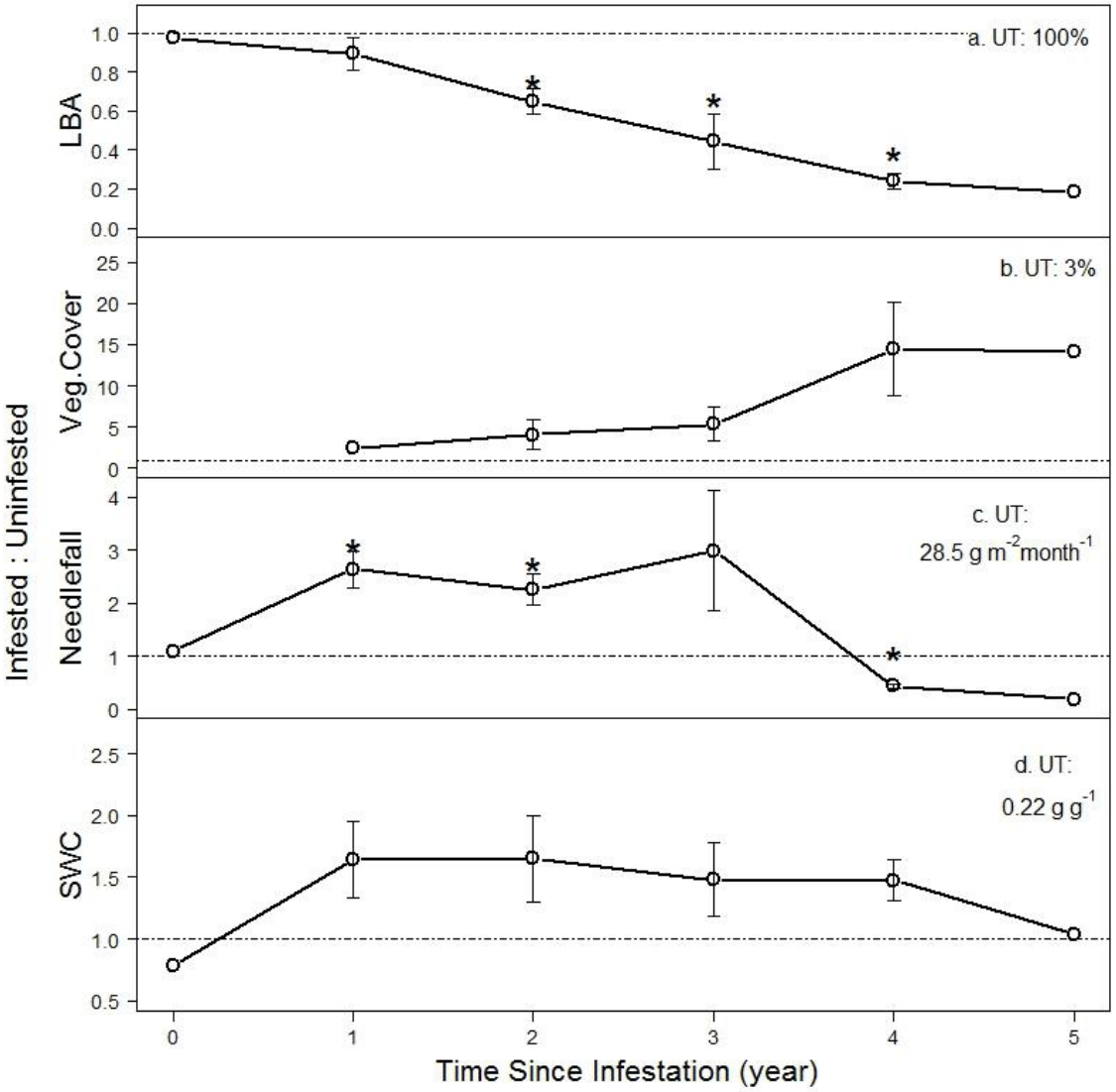

Figure 1. Effects of the beetle infestation on (a) Live Basal Area LBA, (b) understory vegetation cover (c) needle fall rate, (d) soil moisture (SWC), as a function of time since infestation (year) in lodgepole pine forest, southeastern Wyoming. Values for the y-axis represent ratios of variable from MPB effects stand to unifested stand. Horizontal dashed line represents the mean value associated with uninfested stand (UT). From Borkhuu et al In Review.

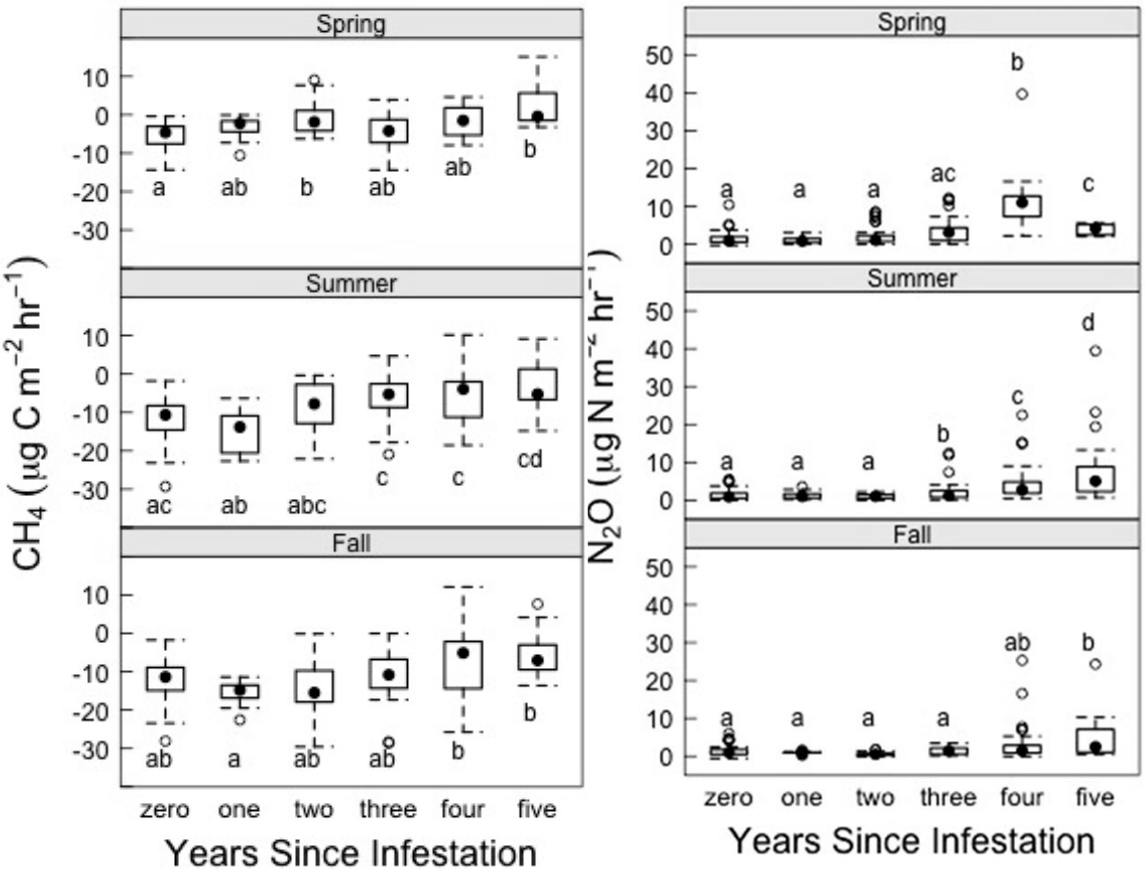

Figure 2. Seasonal (a) CH_4 and (b) N_2O fluxes (ug m^{-2} hr^{-1}) in different years following MPB infestation of the lodgepole forests. From Norton et al In Revew.

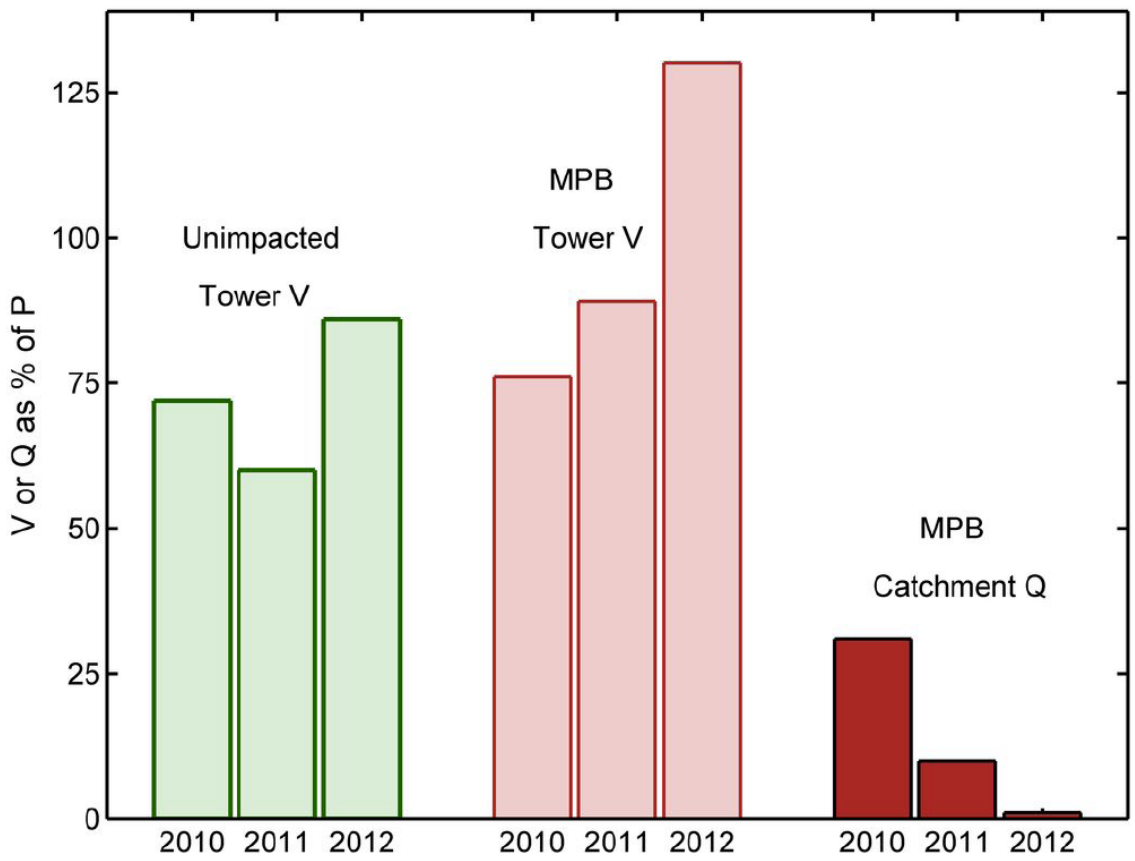

Figure 3. Annual observation of hydrologic paritionin to vapor loss V and streamflow Q expressed as a percentable of precipitation P (i.e. V: P = vapor loss coefficient and Q: P = runoff coefficient). Partitionin was less variable at the Unimpacted site and followed the pattern of interannual climate, with V: P inversely related to annual P (Table 3). The MPB site showed greater partitioning and less to Q in 2011 as compared to 2010 in spite of larger P. In 2012, which was very dry at the MPB site, tower V exceeded P, in part due to a release of stored water, and very little Q was observed. From Biederman et al In Review.

a)

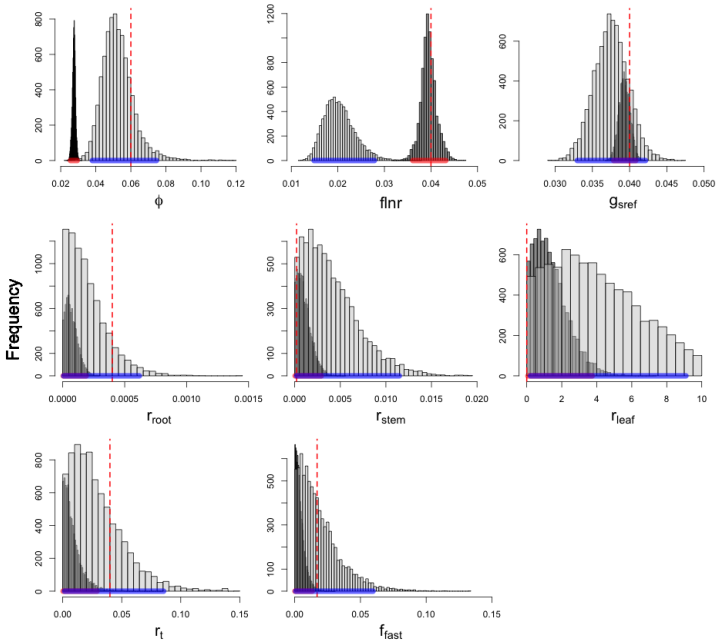

b)

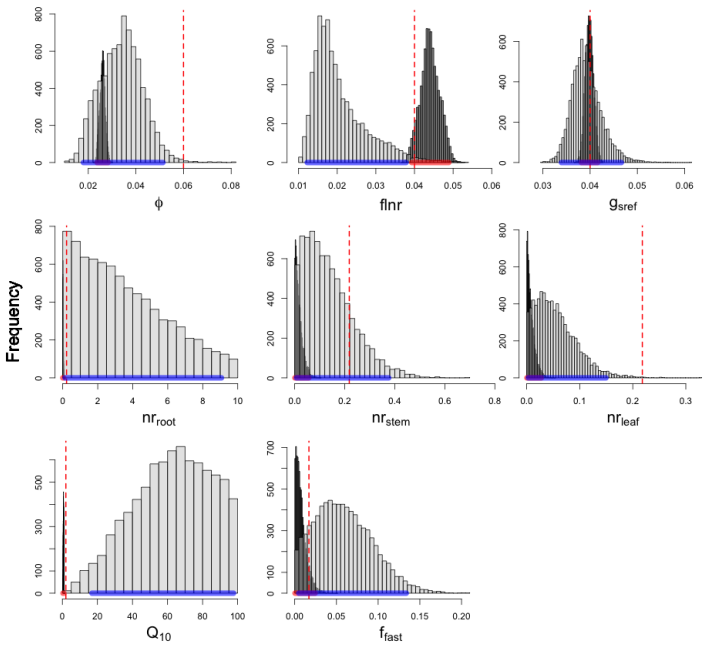

Figure 4. Posterior distributions for TREESCav. The two sets of parameters in (a) and (b) are from a parsimony analysis that supports the parameterization in (a) more. Parameter distributions from hourly aggregation are shown in darker grey with 95% credible intervals highlighted in red, while distributions from daily aggregation are shown in lighter grey with 95% credible intervals highlighted in blue. Overlap in 95% credible intervals is displayed in purple. Parameter values taken from literature or measured are shown with a red dashed vertical line. The parameters include the major carbon, water and nitrogen cycling components in the TREES model. Gsref is most relevant to evapotranspiration because it is the total canopy conductance that is responding to the mortality event. From Peckham et al In Prep.

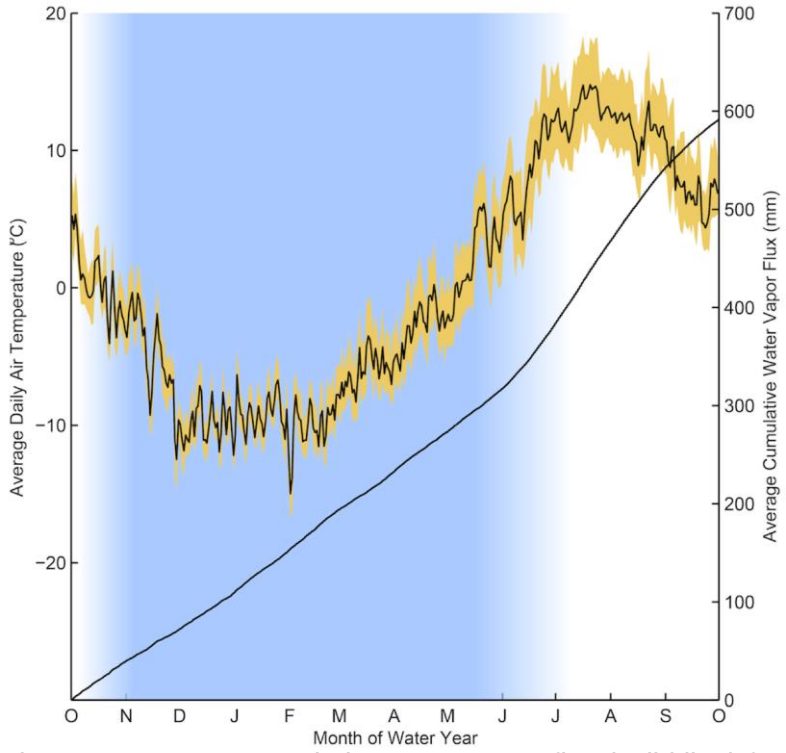

Figure 5. Average cumulative water vapor flux (solid line) for the past eight years at GLEES. The snowpack persists for an average of eight months per year (blue shading) while the climate is below freezing a majority of that time (lines with yellow shading: average daily minimum, mean, and maximum air temperatures). Sublimation accounts on average for 50 +/- 10% (SD among years) of the total annual water vapor flux. From Schaepfer et al 2014.

Once the stand scale analyses are complete, we will run the model at the watershed and mountain range scale using Landsat data sets tested against ground data. The Landsat analyses are funded by the Wyoming Weather Modification Project. Ongoing analyses of this data have shown that dead trees are well correlated to several individual spectral bands and indices. However, no spectral analyses have been able to distinguish between spruce/fir and lodgepole pine dead trees so we are adding ancillary data on slope, aspect and elevation to produce final maps. The stand-scale version of TREESCav will then be run at the watershed and landscape/mountain range scale using these final maps.

Simulating the impact of tree mortality at decadal scales will require continued refinement of the soil carbon and nitrogen processes and the implementation of a canopy completion algorithm in TREESCav. We know have data from 3-4 years of recovery in some stands which shows a dramatic increase in understory vegetation including tree saplings and seedlings as well as increased nitrogen and loss in soils. (FIGURE XXXX). Our preliminary analyses show that TREESCav misses these vegetation and thus hydrology dynamics unless soil nitrogen processes and light competition are appropriately captured (FIGURE XXXX). We aim to be running these analyses with presentable results by Summer 2014.

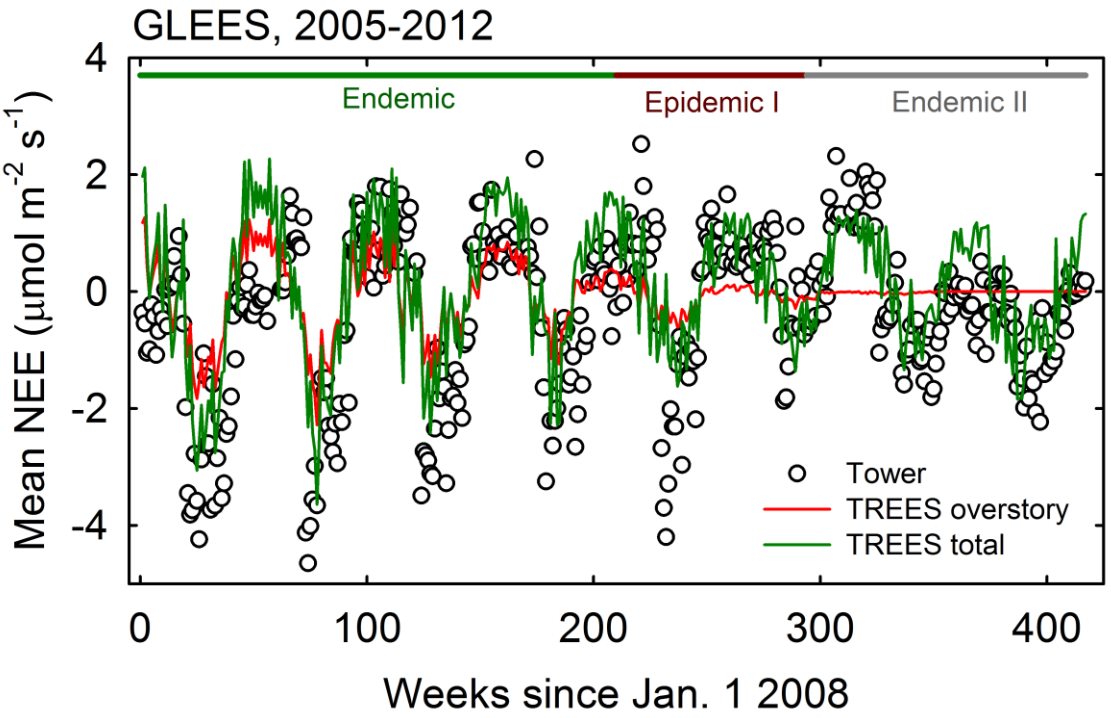

Figure 6. TREESCav simulations of net ecosystem exchange of CO2 using a preliminary algorithm of canopy competition. Notice that during the prior to the beetle mortality (Endemic) the fluxes are similar for overstory and total because the large trees outcompete the understory. When the overstory dies in Epidemic I and the understory begins to recover in Epidemic II, the competition shifts more to non-trees (see flat red line) but TREEScav still capture the overall CO2 fluxes. CO2 fluxes are an appropriate first testing phase of this algorithm because total ecosystem photosynthesis must be appropriately simulated with respect to competition before we can expect to successfully simulate ET and waterbudgets.

Significance

Many studies over the past 5 years have documented increased mortality of forests globally. However, none of these studies have truly mechanistic connections between tree mortality and larger scale consequences such as water yield and quality. Our study is making these connections by rigorously testing a simulation model with stand data from two different forests in Wyoming experiencing mortality from bark beetles. By starting with the stand-scale of data and incorporating carbon and nitrogen cycling, we have much more confidence when we infer changes at larger spatial scales in watersheds and landscapes/mountain ranges and longer temporal scales as the forests recover from the disturbance

Surprisingly, we find relatively little impact of the mortality event on watershed responses due to the spatial patchiness of the mortality and the overall timing to maximum mortality which is opposed by the fast recovery of the individual patches. These spatial and temporal scalings provides an explanation for why our results are different from many other studies that focus on forested watersheds that have more uniform mortality or simulate mortality as uniform. At the very least, our results suggests extreme caution

should be taken when simulation models assume that bark beetle remove tree transpiration in the same manner as clearcutting or fires.

We also found that winter water vapor fluxes (nominally snow sublimation) were an enormous component of total annual water vapor fluxes. These large winter water vapor fluxes can not be simulated by any model, so we will develop a new snow sublimation model for TREESCAv. These large winter water vapor fluxes also suggest that water managers can not just use incoming snow to predict streamflow in any mechanistic manner. These results also have implications for the Wyoming Weather Modification Project because the small potential increases in snowfall predicted by that project may be offset by sublimation.

When our publically accessible, spatially queriable server goes public on July 1 after beta-testing in May, our serving of data from this project will enable policy implications to occur faster. We are using leveraged funds from the WyCEHG (see leveraged funding below) to support this distribution of data with links in the coming year to other relevant water projects around southern Wyoming.

Students/Post-Docs Supported
Bujidma Borkhuu-ongoing PhD student, main responsibilities are soil measurements and assistance with atmospheric measurements. Receives partial funding from this project.

Andrew King-ongoing MS student, main responsibilities are remote sensing image analysis and comparison to vegetation databases established through this project. Receives partial funding from this project.

Nick Brown-ongoing MS student, main responsibilies are soil measurements of nitrogen and carbon cycles. Receives partial funding from this project.

John Frank- ongoing PhD student, main responsibilities are all of the flux measurements from the spruce and fir bark beetle site (note: John Frank is a full time employee of the USFS RM Exp St in Ft. Collins, and does not receive any salary support from this project). Support from this project is used for field visits and site maintenance through a USFS subcontract.

David Reed-ongoing PhD Student, main responsibilities are the atmospheric and streamflow measurements. Receives partial funding from this project.

Scott Peckham-ongoing post-doctoral scientist, main responsibilities are coding modifications to the TREES model and model-data fusion analyses as well as supervision of the Chimney Park lodgeople pine site. Receives full support from this project.

Publications (*Students and Post-Docs are italicized*)
Biederman, J, A Harpold, D Gochis, *BE Ewers*, **D Reed**, S Papuga, P Brooks. Compensatory vapor flux reduces water for streamflow following severe bark beetle-induced forest mortality. Water Resources Research.

Ewers, BE. 2013. Understanding stomatal conductance responses to long-term environmental changes: A Bayesian framework that combines patterns and processes. Tree Physiology. 33:119-122

Norton, N, BE Ewers, **B Borkhuu**, E Pendall. In Review. Five years of mountain pine beetle infestation in lodgepole pine (Pinus contorta) forests increases soil N2O and CH4 fluxes. Biogeochemistry.

Peckham, SD, BE Ewers, DS Mackay, E Pendall, **JM Frank**, WJ Massman. Are simple models better? Bayesian analysis of a carbon cycle model and its respiration components. In preparation for Global Change Biology.

Schlaepfer, DR, BE Ewers, BN Shuman, DG Williams, **JM Frank**, WJ Massman, WK Lauenroth. 2014. Terrestrial water fluxes dominated by transpiration: Comment Arising from S. Jasechko et al. Nature 496:357-351 (2013). Ecosphere. In press.

Presentations (*Students and Post-Docs are bolded*)

(Invited) Ewers BE. Hydraulic Limitations Help Explain the Behavior of Plants: from clocks to mortality to ghosts. Department of Biology, University of Northern Colorado. January, 2014.

Massman, WJ, **Frank, JM**, Swiatek, E, Zimmerman, H, Ewers, BE. Which are more accurate, orthogonal or non-orthogonal sonic anemometers? American Geophysical Union Meeting, San Francisco, CA. Dec, 2013.

Bowling, DR, Ewers, BE, et al. Land-atmosphere carbon cycle research in the southern Rocky Mountains. American Geophysical Union Meeting, San Francisco, CA. Dec, 2013.

Kipnis, E, Chapple, WD, Traver, E, **Frank, JM,** Ewers, BE, Miller, SN, Williams, DG. Spatial variability of snow water isotopes in montane southeastern Wyoming. American Geophysical Union Meeting, San Francisco, CA. Dec, 2013.

Brooks PD, Harpold, AA, Biederman JA, Gochis DJ, Litvak, ME, Ewers, BE, Broxton, PD, **Reed, DE**. Non-linear feedbacks between forest mortality and climate change: implications for snow cover, water resources, and ecosystem recovery in western North America. American Geophysical Union Meeting, San Francisco, CA. Dec, 2013.

Ewers BE, et al. Bark beetle impacts on ecosystem processes are over quickly and muted spatially. American Geophysical Union Meeting, San Francisco, CA. Dec, 2013.

Mackay, DS, Ewers, BE, Peckham, SD, Savoy, P, Reed, DE, Frank, JM. Towards scaling interannual ecohydrological responses of conifer forests to bark beetle infestations from individuals to landscapes. American Geophysical Union Meeting, San Francisco, CA. Dec, 2013.

Biederman, Ewers, BE, Reed, D, et al. Compensatory vapor loss and biogeochemical attenuation along flowpaths mute the water resources impacts of insect-induced forest mortality. American Geophysical Union Meeting, San Francisco, CA. Dec, 2013.

Peckham, SD, Ewers, BE, Mackay, DS, Pendall, E, Frank, JM, Massman, WJ. Simulating stand-level water and carbon fluxes in beetle-attacked conifer forests in the Western US. American Geophysical Union Meeting, San Francisco, CA. Dec, 2013.

(Invited) Ewers BE. Quantifying how bark beetles impact forest hydrology. Presentation to American Association for the Advancement of Science External Advisory Committee to UW EPSCOR.

(Invited) Ewers BE. Causes and consequence of bark beetle-induce mortality on water, carbon, and nitrogen cycling. Ecological Society of America Annual Meeting. Minneapolis Minnesota. August, 2013.

Peckham, SD, BE Ewers, DS Mackay, E Pendall, HN Scott, JM Frank, MG Ryan and WJ Massman. Bayesian analysis of a carbon cycle model: Implications for parameter estimation, model selection, and simulation of beetle-caused forest mortality. Ecological Society of America Annual Meeting. Minneapolis Minnesota. August, 2013.

Mackay, DS, BE Ewers, **SD Peckham**, PR Savoy, **D Reed**, **JM Frank**, NG McDowell. Plant hydraulic controls over the susceptibility of trees to mortality following climate-enhance disturbances. Ecological Society of America Annual Meeting. Minneapolis Minnesota. August, 2013.

(Invited) Ewers BE. Impacts of bark beetle outbreaks from stands to watersheds. Public Lecture Sponsored by UW Ruckelhaus Institute. Laramie, WY May 2013.

(Invited) Ewers BE. Impacts of bark beetle outbreaks from stands to watersheds. Public Lecture Sponsored by UW Ruckelhaus Institute. Steamboat Springs, CO May 2013.

(Invited) Ewers BE. Impacts of bark beetle outbreaks from stands to watersheds. Public Lecture Sponsored by UW Ruckelhaus Institute. Saratoga, WY May 2013.

(Invited) Ewers BE. Hydraulic Limitations Help Explain the Behavior of Plants: from clocks to mortality to ghosts. Department of Biology, U. of New Mexico, February, 2013

(Invited) Ewers BE. Hydraulic Limitations Help Explain the Behavior of Plants: from clocks to mortality to ghosts. Department of Biology, Los Alamos National Labs, February, 2013

(Invited) Ewers BE. Impact of Fire and Insect Disturbance on Water Cycling in Ecosystems. Land Managers of the Laramie District of the Medicine Bow National Forest. February 2013

(Invited) Ewers BE. Surprising effects of bark beetle-induced mortality on snowpacks and water yield. Wyoming Weather Modification Technical Advisory Team Meeting, Cheyenne, WY January, 2013.

(Invited) Ewers BE. Impact of bark beetle outbreaks on forest water yield. Wyoming Association of Conservation Districts. Casper, WY, December, 2012.

P.D. Brooks; A.A. Harpold; J.A. Biederman; M.E. Litvak; P.D.Broxton; D. Gochis; N.P. Molotch; P.A. Troch; B.E. Ewers. Insects, firests, and climate change: implications for snow cover, water resources and ecosystem recovery in Western North America. American Geophysical Union Meeting, San Francisco, CA, Dec. 2012.

Ewers, BE, DS Mackay, C Guadagno, **SD Peckham**, E Pendall, B Borkhuu, **T Aston**,

JM Frank, WJ Massman, **DE Reed**, Y Yarkhunova, C Weinig. Nonstructural carbon dynamics are best predicted by the combination of photosynthesis and plant hydraulics during both bark beetle induced mortality and herbaceous plant response to drought. American Geophysical Union Meeting, San Francisco, CA, Dec. 2012.

King A, BE Ewers, R Sivanpillai, E Pendall. Testing remote sensing estimates of bark beetle induced mortality in lodgepole pine and Engelmann spruce with ground data. American Geophysical Union Meeting, San Francisco, CA, Dec. 2012.

Peckham, SD, BE Ewers, DS Mackay**, JM Frank**, WJ Massman, MG Ryan, H Scott, E Pendall. Modeling net ecosystem exchange of carbon dioxide in a beetle-attacked subalpine forest using a data-constrained ecosystem model. American Geophysical Union Meeting, San Francisco, CA, Dec. 2012.

Mackay, DS, BE Ewers, **DE Reed**, E Pendall, NG McDowell. Plant hydraulic controls over ecosystem responses to climate-enhanced disturbances. American Geophysical Union Meeting, San Francisco, CA, Dec. 2012.

(Invited) Ewers BE. Impact of bark beetle outbreaks on forest water yield. Wyoming Water Development Commission. Cheyenne, WY, November, 2012.

(Invited) Ewers BE. Impact of bark beetle outbreaks on forest water yield. Joint meeting of the Wyoming Water Development Commission and the Select Water Subcommittee of the Wyoming Legislature. Casper, WY, November, 2012.

(Invited) Ewers BE. Impact of bark beetle outbreaks on forest water yield. Wyoming Water Association Annual Meeting. Lander, WY, October, 2012.

Reed, DE, BE Ewers, E Pendall, RD Kelly, U Norton, **FN Whitehouse**. Mountain pine beetle epidemic changes ecosystem flux controls of lodgepole pine. Ecological Society of America Annual Meeting, Portland, OR, August 2012.

Brooks, PD, HR Barnard, J Biederman, B Borkhuu, SL Edburd, BE Ewers, D Gochis, E Gutmann, AA Harpold, JA Hicke, DJP Moore, E Pendall, **D Reed**, A Somor, PA Troch. Multi-scale observation of hydrologic partitioning following insect-induced tree mortality: Implications for ecosystem water and biogeochemical cycles. Ecological Society of America Annual Meeting, Portland, OR, August 2012.

Frank, JM, WJ Massman, BE Ewers. Linking bark beetle caused hydraulic failure to declining ecosystem fluxes in a high elevation Rock Mountain (Wyoming, USA) forest. Ecological Society of America Annual Meeting, Portland, OR, August 2012.

Ewers BE, DS Mackay, E Pendall, J**M Frank, DE Reed,** WJ Massman, **TL Aston**, **JL Angstmann, K Nathani, B** Mitra. Use of plant hydraulic theory to predict plant controls over mass and energy fluxes in response to changes in soils, elevation and mortality. Ecological Society of America Annual Meeting, Portland, OR, August 2012.

Barnard, HR, A Byers, A Harpold, BE Ewers, D Gochis, P Brooks. Examining the response of lodgepole transpiration to snow melt and summer rainfall in subalpine Colorado, USA. Ecological Society of America Annual Meeting, Portland, OR, August 2012.

Brown, NR, U Norton, E Pendall, BE Ewers, **B Borkhuu**. High levels of soil and litter nitrogen contents after bark beetle-induced lodgepole pine mortality. Ecological Society of America Annual Meeting, Portland, OR, August 2012.

Ewers BE et al. Use of plant hydraulic theory to predict plant controls over mass and energy fluxes in response to changes in species, soils and mortality. American Society of Plant Biology Annual Meeting, Austin, TX, July, 2012.

(Invited) Ewers BE. Simulation modeling of bark beetle effects on stand water budgets. Wyoming Weather Modification Technical Advisory Team Meeting. Saratoga, WY July 2012.

Leveraged Support to this Project.
NSF ESPSCOR. Water in the West. $20 million total grant, $500,000 to Ewers. A major justification for this grant was the lack of correlation between increased water in stands and streams after bark beetle mortality. The TREES model funded by this project will now be tested against other, less biologically sophisticated hydrology models. This grant establishes the Wyoming Center for Environmental Hydrology and Geophysics (WyCEHG).

NSF ETBC Hydrologic Science. ETBC: Collaborative Research: Quantifying the Effects of Large-Scale Vegetation Change on Coupled Water, Carbon, and Nutrient Cycles: Beetle Kill in Western Montane Forests. CoPI Elise Pendall. $219,261. This NSF funding provided partial funding for several of the data sets used to test TREES.

Ag Exp Station and McIntire Stennis. Quantifying the impact of a massive mountain pine beetle outbreak on carbon, water and nitrogen cycling and regeneration of southern Wyoming lodgepole pine forests. CoPIs Elise Pendall and Urszula Norton $60,000. This grant provided partial funding for several of the data sets used to test TREES.

Mapping annual surface area changes since 1984 of lakes and reservoirs in Wyoming that are not gauged using multi-temporal Landsat data

Basic Information

Title:	Mapping annual surface area changes since 1984 of lakes and reservoirs in Wyoming that are not gauged using multi-temporal Landsat data
Project Number:	2013WY84B
Start Date:	3/1/2013
End Date:	2/28/2015
Funding Source:	104B
Congressional District:	1
Research Category:	Climate and Hydrologic Processes
Focus Category:	Water Quantity, Models, Education
Descriptors:	
Principal Investigators:	Ramesh Sivanpillai

Publications

There are no publications.

Mapping annual surface area changes since 1984 of lakes and reservoirs in Wyoming that are not gauged using multi-temporal Landsat data.

Project Duration
03/01/2013 - 02/28/2014

Principal Investigator:
Ramesh Sivanpillai
Senior Research Scientist – Extended Term
Department of Botany & Wyoming Geographic Info Science Center (WyGISC)
University of Wyoming
sivan@uwyo.edu
Phone: 307-766-2721
Web: http://www.uwyo.edu/wygisc/people/sivanpillai_ramesh/index.html

Abstract:
Information on water stored in lakes and reservoirs are essential for their prudent management. However if these water bodies are not gauged, information about the amount of water entering and leaving the reservoir is unknown. Without this information it is difficult for planners and policy makers to devise appropriate management plans. In the absence of inflow/outflow data, remotely sensed data collected from satellites can be used for mapping how the surface area of these lakes have responded to seasonal, annual and long-term changes in precipitation and weather conditions. This research project aims to test the utility of Landsat data (collected and distributed at no-cost by USGS) to map surface area changes in selected Wyoming lakes and reservoirs that are not gauged. This research will test various image enhancements techniques and digitally classification algorithms for generating 30-year trend in surface area changes for each water body. Methods developed through this proposal will help us to map more water bodies in Wyoming using next generation of Landsat data (Landsat 8) which is scheduled for launch in Feb 2013. This proposal will also focus on undergraduate education and research through internship opportunities. Students will be required to present their research findings in local (Laramie, WY) and regional (Denver, CO) conferences.

Report:
A project report was not received by the submission deadline. A no-cost extension has been granted. A final report for this project is expected for inclusion in the FY14 report.

Micro-Patterned Membrane Surfaces with Switchable Hydrophobicity

Basic Information

Title:	Micro-Patterned Membrane Surfaces with Switchable Hydrophobicity
Project Number:	2013WY85B
Start Date:	3/1/2013
End Date:	2/28/2015
Funding Source:	104B
Congressional District:	1
Research Category:	Water Quality
Focus Category:	Treatment, Wastewater, Water Supply
Descriptors:	None
Principal Investigators:	Carl Frick, Jonathan Brant

Publications

There are no publications.

WRP Annual Report FY2013

Micro-Patterned Membrane Surfaces with Switchable Hydrophobicity

Submitted to: WWDC WRP Priority and Selection Committee, May 1, 2014
By: Chris Laursen for PIs Dr. Carl Frick and Dr. Jonathan Brant
(Year 1 of 2)

Abstract:

Interest in, and the use of, membrane distillation for desalination applications is growing in areas like Wyoming that are grappling with dwindling freshwater supplies and the large volumes of saline water that are generated from the development of our energy resources. Realizing the full potential of membrane distillation hinges on the development of new membrane materials that are tailored for the unique requirements of this process. The *overarching goal* of our proposed research is the synthesis, characterization, and testing of a new membrane surface coating whose properties can be changed in response to environmental stimuli. The *objective* is to create a micro-structured surface capable of switchable hydrophobicity for improving the performance of membrane distillation processes in order to make it viable for desalination applications. It is our *central premise* that a biologically inspired micro-patterned surface manufactured through conventional photolithography techniques using shape-memory polymers, can create a highly hydrophobic surface when erect, while demonstrating dramatically less hydrophobicity when in a relaxed state, as a result of the relationship between surface roughness and hydrophobicity. Such a surface would facilitate easier cleaning of the membrane by backwashing, while maximizing the separation efficiency and permeate flux rate through the membrane. Our *rationale* for undertaking this research is that new treatment strategies, like membrane distillation, are needed to effectively manage highly saline waters. We will accomplish the overall objective of this proposal by pursuing the following specific aims:

Specific Aim #1 – Synthesize membrane surface treatments from shape-memory polymers having tunable surface structure controlled hydrophobicity. Standard photopolymerization techniques will be used to fabricate micro-patterns, consisting of arrays of vertical micro-pillars, onto micro-porous substrates to form a membrane.

Specific Aim #2 – Assess and evaluate the efficacy of membrane surfaces with tunable surface structure and hydrophobicity. We will characterize the structure and hydrophobicity of the shape-memory polymer structures as a function of environmental parameters relevant to membrane distillation applications and evaluate any changes in polymer structure in terms of their impact on membrane performance.

1. Purpose:

The overarching goal of the current research is to create a structured surface coating to be cast onto water membrane surfaces out of a unique, tailored shape-memory polymer that can alter its material properties under environmental stimuli, to aid in the anti-fouling properties and assist in "self cleaning" during membrane backwashing. Through the use of a shape-memory polymer, a structured surface composed of an array of micro pillars will maintain their rigidity under normal operating conditions; then, when cleaning of the membrane surface is required, an elevated water temperature and backwashing will bring the pillars to a pliable state where the pillars will bend and move. Upon relief of back pressure and cross-flow shear (external forces), followed by cooling to normal operating temperatures, the pillars will return to their undeformed state.

It is our central premise that a biologically inspired micro-patterned surface manufactured through conventional photolithography techniques, as well as soft molding techniques using shape-memory polymers will assist in anti-fouling in two ways. First, through a change in hydrophobicity. It is hypothesized that we can create a highly hydrophobic surface when erect, while demonstrating dramatically less hydrophobicity when in a relaxed state, as a result of the relationship between surface roughness and hydrophobicity. Second, is through the mechanical alteration of the material properties within the structured surface. Through changing the material from a rigid state to a pliable state, it is hypothesized that build up of fouling materials will be destabilized and encouraged to break off and continue into the waste stream.

Our rationale for undertaking this research is that new treatment strategies, like membrane distillation, are needed to effectively manage highly saline waters. The ultimate goal of the Investigators is to leverage these results towards an SBIR proposal geared toward developing our switchable hydrophobic surfaces for commercial applications.

2 Problem:

Population growth, energy development, and agricultural interests are all competing for the limited freshwater supplies in Rocky Mountain region. As such, both industry and the public sector are using less pristine raw water sources such as brackish groundwater and oil and gas produced waters in an attempt to develop new water supplies [1]. Desalination is therefore receiving serious interest across the western US, for managing produced waters and augmentation of drinking water supplies [2,3]. Membrane fouling owing to high-energy requirements on the part of pressure driven membrane processes however remain significant challenges to processes like reverse osmosis (RO). An important need is the development of a membrane surface coating whose surface structure may be manipulated, i.e., a smart surface, to be rigid during process operation and flexible to facilitate backwashing the membrane during cleaning to optimize permeability recovery. The development of new materials whose surface properties may be controlled so as to provide greater flexibility in process operation is needed to realize the full potential of membrane distillation processes. In the absence of such advancements, the use of membrane distillation in desalination applications will be stagnated, particularly for produced waters, which have high total dissolved solids (salt) concentrations.

3 Research Objective and Methodology:

Research up to this point has followed a progression of four major steps, and is currently moving into the fifth stage. The "stages" progressed through (1) fundamental thermo-mechanical observations of nine acryl based macromolecules (five monofunctional and five multifunctional) in order to cherry pick specific properties expected to produce a good shape-memory effect. This transitioned into (2) systematic alteration of relative weight percents of a ternary polymer network consisting of three of the previous marcomolecules, tert-Butyl acrylate, 2-Hydroxyethyl methacrylate, and Poly(ethylene glycol) dimethacrylate ($M_n \sim 550$) to reach optimal shape-memory properties. Stage (3) fully characterized mechanical properties of the custom tailored system at various temperatures, and (4) established soft molding techniques creating structured, patterned surfaces. Current focus is transitioning from stage (4) to stage (5) where anti-fouling properties will be observed through adhesion analysis of colloidal debris using atomic force microscopy. In addition, observations of deposition and desorption of colloids in a cross-flow situation with the structured surfaces will be made and contact angle testing will be performed. This will investigate the robustness and effectiveness of the polymer system while offering incite into the optimal structured surface pattering.

4 Materials:

The following materials for the polymer network were procured from Sigma-Aldrich Corporation, St. Louis, MO. Macromolecules *tert-Butyl acrylate* (tBA), *2-Ethoxyethyl methacrylate* (2EEM), *Poly(propylene glycol) acrylate* (PPGA), *2-Carboxyethyl acrylate* (2CEA), *Di(ethylene glycol) dimethacrylate* (DEGDMA), *Poly(ethylene glycol) dimethacrylate* $M_n \sim 550$ (PEGDMA550), *Poly(ethylene glycol) dimethacrylate* $M_n \sim 750$ (PEGDMA750), release agent *Trichloro(1H,1H,2H,2H-perfluorooctyl)silane*, and photo-initiator *2,2-Dimethoxy- 2-phenyl-acetophenone* (DMPA).

Additional macromolecules, *2-Hydroxyethyl methacrylate* (2HEMA) and *Dipentaerythritol penta/hexaacrylate* (DPPHA) were obtained through Alpha Aesar, Ward Hill, MA, and Santa Cruz Biotechnology Incorporated, Santa Cruz, CA respectively.

Three different silicon systems were used in the creation of soft-molding and were purchased from Dow Corning Corporation, Midland, MI. *Slygard® 184 silicone elastomer*, *Silastic® 7-4860 silicone elastomer*, and *Xiameter® RTV-4251-S2* silicone mold making rubber.

5 Experimental Methods:

5.1 Polymer Synthesis

Fundamental studies of the basic macromolecules were prepared for photo-initiation by the addition of 0.5 wt.% DMPA. Monofunctional acrylates required an extremely light amount of crosslinking to fully polymerize done through the addition of 1 wt.% DEGDMA. Therefore, PPGA, 2EEM, 2CEA, tBA, and 2HEMA systems consisted of 98.5 wt.% there respective monofunctional macromolecule, 1 wt.% DEGDMA, and 0.5 wt.% DMPA. Similarly macromolecules consisted of 99.5 wt.% DEGDMA, PEGDMA550, PEGDMA750, or DPPHA mixed with 0.5 wt.% DMPA. Samples were mixed in 5g batches. After mixing the proper ratios, samples were subsequently hand shaken for

two minutes, and then ultrasonically shaken in a Branson 1510 ultrasonicator for five minutes to ensure complete dispersion of constituents.

The final ternary network that was investigated consisted of a linear building mixture of 9:1 by weight tBA to 2HEMA, which was subsequently mixed with a multifunctional (crosslinking) system, PEGDMA550, and the photoinitiator, DMPA such that final composition consisted of 94.5/5.0/0.5 wt.% linear building mixture, PEGDMA550, and DMPA. The final relative weight percentage of each constituent overall was 85.05/9.45/5.00/0.50 wt.% tBA, 2HEMA, DEGDMA, and DMPA. Materials were mixed together according to their respective relative weight percentages in a 100 g batch and dispersed using the method described above. The mixture was stored in a UV-resistant vial and placed in a refrigerator at 5°C. All test samples were procured from this batch, except for soaked tensile samples that were tested at room temperature; these came from an additional batch of the same composition.

Both Dynamic Mechanical Analysis (DMA) and tensile samples were cast in a similar method described in detail in their respective section below. To prepare the molds, first Rain-X release agent was applied to two pre-cleaned plain glass microscope slides. A thin layer of Dow Corning High Vacuum Grease was applied to the contact regions between the respective Teflon spacer and the glass, and the pieces were sandwiched and clamped together. The uncured mixture of interest was then be injected in between the slides. Photopolymerization was induced using a 365 nm wavelength UV lamp (UVP Blak-Ray B-100A/R lamp, intensity ~8mW/cm^2) for approximately 30 minutes. Subsequently the samples were placed into an furnace (Fisher Scientific Isotemp) at 90°C for 60 min to ensure complete polymerization. Samples were finalized for DMA or tensile testing by trimming and sanding samples edges.

5.2 Water Absorption

Samples were soaked at 30°C, and 90 RPM in ultra pure water obtained from a Millipore Direct-Q system on a shaking incubator (Benchmark Incu-Shaker Mini). Samples were periodically observed at predetermined intervals for water absorption through use of **Equation 1**.

$$\%Abs_{H_2O} = \left(\frac{M_{wet}}{M_{dry}} - 1\right)100$$

Where M_{wet} and M_{dry} are the dry and wet masses respectively. The dry mass was taken immediately before placing the sample in the ultra pure water. The procedure for taking the wet mass was to remove the sample, dab any water on the surface off with a Kimwipe, and mass it at the required time interval.

5.3 Dynamic Mechanical Analysis (DMA):

Dynamic Mechanical Analysis (DMA) was performed using a TA interments Q800 DMA affixed with tensile grips. Samples were prepared as described above with Teflon molds approximately 1 mm thick, and had cutouts for four 15 x 6 mm^2 samples. Immediately before placing into the DMA, sample's final dimensions were measured. In addition, if soaked samples were required, a wet mass was taken and because of the duration of the test and the relatively high temperature ranges, samples were coated in Dow Corning High Vacuum Grease during testing to prevent evaporation of absorbed water.

Tests was performed under a strain controlled temperature sweep between the temperatures of interest ramped at 1°C /min and a frequency of 1 Hz. Observed temperature ranges depended on the sample of interest, with a maximum range of -50°C to 200°C. Preload force, target strain, and force track was 0.1 N, 0.1%, and 150% respectively. In order to assure proper equilibrium between the sample and thermal chamber, the test sequence also included initially flooding the system with liquid nitrogen until 20% below the initial data acquisition temperature was reached. The sequence held isothermally for 5 minutes, and then began ramping at 1°C/min until the data acquisition starting temperature was met, where normal operation commenced.

5.4 Tensile Testing

Tensile testing was performed only on the final ternary polymer network consisting of 94.5 wt.% 9:1 tBA-co- 2HEMA, 5 wt.% PEGDMA550, and 0.5 wt.% DMPA. Samples were cast using the method described in the above Polymer Synthesis subsection, with a Teflon mold modeled after a ASTM D-638-5-IMP die, including an overall length of 2.50in. (63.5 mm), width of 0.375 in. (9.53 mm), gage width of 0.125 in. (3.18 mm), and a gage length of 0.50 in (12.7 mm) and were approximately 3.2 mm thick before sanding.

Samples were tested on a MTS 858 Mini Bionix II servo-hydraulic load frame affixed with a MTS 407 Controller, though data acquisition and control was applied through an in house LabView Program. Force was typically measured with a MTS 661.09B-21 100N force transducer and routed through the 407 Controller while displacement was measured via an MTS LX 500 Laser Extensometer using MTS retro reflective tape placed on the gage length of the sample. To control signal to noise ratio, samples tested at 90°C used a Transducer Techniques MLP-10 10 lb_f force transducer. The load frame was enclosed in a MTS 651 Environmental Chamber with both liquid nitrogen cooling and two electric heating elements coupled with a fan for diffused convective heating. Temperatures for testing ranged from 10 to 90°C. As with DMA testing, all samples were massed and measured immediately before testing if soaked. Samples however were not coated in vacuum grease, due to its adverse effects on the laser extensometer readings. Testing was completed at a strain rate of 0.1%/s and data acquisition of 2 Hz.

5.5 Soft-Molding

Materials to create the pillared molds included Delrin custom machined negatives of the structured surface, Silastic® 7-4860 silicone elastomer, and Xiameter® RTV-4251-S2 silicone mold making rubber. To create a final mold for the network, the Delrin negative was used to create a Silastic positive, subsequently followed by a Xiameter negative. The reasoning for the mold making process was to assist in de-lamination of the final structured surface. The acrylate network was found to adhere to many substitutes during polymerization.

The process can be better understood through observing **Figure 1**, where the six steps are shown from left to right. The first frame displays a model of the prepared Delrin mold. Represented in the next frame is Silastic - colored blue in the figure - which is supplied in extremely viscous two part base constituents that are mixed in equal parts to start the chemical polymerization. To achieve complete mixing of the base products, a paint mixer was affixed to a drill and stirred, cleaning the sides and mixer when necessary. The compound was then wiped into the molds covering the whole area. The molds were placed in a vacuum desiccator with non-stick foil and weight on top in order

to assist the degassing process for 3 to 5 days to allow all of the gas to escape and the Silastic to fill the pillars. Upon sufficient degassing, the curing was finalized in a 100°C oven for 2 hours. No special technique was required for de-molding of the Silastic from the Delrin.

As seen in frame three, once the Silastic positive was demolded, it was placed in a custom dish that maintained the footprint of the positive, and added deeper walls that would ultimately allow for pouring the acrylate system into the Xiameter negative. Because both the Silastic and the Xiameter are silicon based materials, a release agent was necessary between the positive and negative molds. Multiple drops of *Trichloro(1H,1H,2H,2H-perfluorooctyl)silane* were dropped in a dish next to the sample and vacuum dessicated to approximately 380 Torr, sealed, and left for one day in order to be vapor deposited onto the Silastic molds.

Immediately after vapor deposition of the release agent for 1 day, Xiameter was mixed in at 10:1 weight ratio of base to curing agent with a stainless stir rod and poured onto the Silastic mold and dish; represented by the green material in the fourth frame. The material was degassed and cured at 150°C for one hour. This method allowed for a good de-lamination between the Silastic positive and Xiameter negative.

With the welled Xiameter negative, the ternary acrylate network could finally be cast into the structured surface as is displayed in the fifth frame. Before casting, the polymer system was precured using a 254 nm wavelength crosslinking oven (Spectrolinker XL-1500 intensity $\sim$1.5mW/cm^2, Spectronics Corporation) for 15 minutes. The mixture was then poured in it the Xiameter mold, degassed for one minute, and photopolymerization was completed using a the 365 nm wavelength UV lamp for 15 minutes and placed in the oven at 90°C for 60 minutes, as described above in the Polymer Synthesis subsection. This process ultimately providing the structured Acrylate surface seen in frame six.

6 Results / Principal Findings:

6.1 Base Polymer Networks

Initially, nine acryl based macromolecule systems were investigated both for their thermo-mechanical behavior as well as water absorption in order to ultimately isolate an optimal combination of systems based on aqueous glass transition behavior, water absorption, and mechanical properties. For the proposed application it was determined that the polymer systems must exhibit good shape-memory properties targeted for an onset temperature of approximately 30-40°C under submerged conditions, appropriate high and low temperature mechanical properties including strain-to-failure, and the ability to be photopolymerized into a structured surface. Five of these initial systems were monofunctional (linear-builders), while the remaining four were multifunctional (crosslinking) molecules. To ensure good shape-memory effects, both linear builders, as well as a light amount of crosslinking are necessary. A small amount of crosslinking in the system is added for two reasons: it will allow for hard segments needed for the polymer to remember its initial shape, and to assist in a well-established rubbery regime. However, too much crosslinking and the material ductility will greatly decrease. Additionally, the amount of cross linking is expected to dramatically affect the amount of water absorption due to an alteration

in the amount of free volume in the polymer network. The nine macromolecules were chosen from a broad family based on ease of fabrication and nontoxicity.

Water absorption testes were run using ultra-pure water over a duration of 10 days; results can be seen in **Figure 2**. For linear builders, water absorption ranged from 53.8 ± 1.2% to 0.94 ± 0.47% represented by 2HEMA and tBA. Water absorption for pure crosslinkers ranged from 44.2 ± 2.7% to 3.9 ± 1.2% as PEGDMA750 and DEGDMA. The water absorption reached steady state for all synthesized polymers within approximately one day. It is worthy of note that 2CEA is not included in the part (a) of the figure as it dissolved in the water within the initial testing period of 1 hour.

Initial thermo-mechanical testing of soaked samples was performed using the DMA to observe each constituents dry glass transition temperature, storage modulus in the rubbery and glassy regime, and shape-memory properties seen in **Figure 3**. A material is expected to exhibit promising shape-memory effects if there is a large transition in the storage modulus over the transition region, altering the material from a stiff, rigid state to a soft, pliable state as temperature, combine this over a short temperature range and the result is a steep transition region such as the tBA curve of **Figure 3**.

6.2 Ternary Polymer Networks

Based on the observations in the last section, three polymer constituents were chosen to systematically vary including the linear builders tBA and 2HEMA, along with a small weight percentage of the crosslinker PEGDMA550. The choices of macromolecules were based on water absorption properties and promise of good shape-memory characteristics at the desired onset temperature around 30-45°C when soaked. As aforementioned, a light amount of crosslinking has historically shown better shape-memory effects. Because of this, the weight percentage of PEGDMA500, the crosslinker and DMAPA, the photoinitiator were held constant at 5% and 0.5% of the total respectively, while the relative percentage of tBA to 2HEMA were varied in six sample sets. Note that 2HEMA has a high water absorption at 53.8 ± 1.2%, while tBA was much lower 0.94 ± 0.47% in **Figure 2**. Therefore through the varying the relative percentages, an alteration in the amount of water absorption is expected. This is reflected in **Figure 4**. In the figure the relative percentage of the 94.5% linear building solution change from 100/0, 90/10, 75/25, 50/50, 25/75, 0/100, tBA to 2HEMA.

As the percentage of 2HEMA in the system increased there was an increase in the water content displayed in the curve fit. The target water absorption of approximately 4% of the materials original mass was a predetermined value.

Figure 5 (b) displays representative curves of storage moduli with samples in dry form. The glass moduli of the materials are relatively consistent ranging between 2 and 3 GPa, while the rubbery modulus of the materials range from approximately 1 to 10 MPa. General trends observed as the monofunctional builder mixture transitioned from a low percentage of 2HEMA to a low percentage of tBA is an increase in the glass transition temperature, and a gradual lengthening of the transition region.

Similarly **Figure 5 (a)** shows the results of DMA testing for soaked samples. However, as the amount of 2HEMA increases in the linear building mixture now, the glass transition of the material tends to decrease. This is indicative to the amount of water absorbed into the system, as compared to **Figure 4** seen before.

To clarify results, a trend of both the glass transition temperatures and the onset temperatures of soaked and dry samples are displayed in **Figure 6**. The glass transition temperature is defined here as the peak of the Tan delta curve, which has been omitted for clarity, and the onset temperature chosen as the intersect of two tangent lines to the glassy and transition regions. Note the target region for the onset of the shape-memory transition is displayed as the hashed gray region between 30°C and 45°C. The effect of the water absorption into the polymer system can readily be seen in the figure as the glass transition greatly decreases. From this figure one can also infer the relative duration of the transition region. The difference between the T_g and T_{on} of the 100% tBA over the 50/50% tBA-2HEMA is an indication of a steep transition region vs. a more gradual transition, and can be compared to **Figure 5**. A steep transition is favored.

6.3 Mechanical Properties of Final Network

Once the ternary network was customized for (1) glass transition temperature and (2) water absorption, a detailed inquiry was further made into the DMA and mechanical properties of the material.

A representative result from DMA testing of the final network can be seen below in **Figure 7 (a)**. Storage modulus is plotted on the left-hand axis, while the materials Tan delta is plotted on the right, both as a function of temperature. A five order of magnitude change in the materials storage modulus over the temperature range can be seen and is indicative of a transition of the material from its glassy region at lower temperatures to its rubbery region at the higher temperatures.

Additional test results found an onset temperature of 29.8±4.4°C and a glass transition temperature of 49.2±2.2°C, which are represented on the storage modulus curve in the figure. Note the modulus at five different temperatures that are used in tensile tests displayed in **Figure 7 (b)**. These points are tabulated in **Table 1** highlighting the orders of magnitude decrease in stiffness over the transition region.

The five temperature regions mentioned above were examined due to their location in the glassy-to-rubbery transition region. First well into the glassy region at 10°C, next at room temperature of ~26°C - close to the onset temperature, then at the glass transition temperature of 50°C, and rounded off at 70°C and 90°C which have transitioned fully into the rubbery region of the material.

As the material transitions from it glassy to rubbery regime, its mechanical properties are also expected to change. These transitions can be seen in the representative stress-strain curves for each of the five temperatures displayed in **Figure 7 (b)**. Results of strain to failure and ultimate tensile strength are additionally tabulated as a function of temperature in **Table 1**.

In **Figure 7 (b)** as well as **Table 1** note the large change in the materials mechanical behavior as temperature transitions from high to low both in ductility and ultimate strength, as well as overall

behavior. There is a fundamental change in characteristic behavior between the 50°C and 26°C, the glass and onset temperatures respectively.

7 Discussion / Significance:

Of the nine macromolecules investigated, two monofunctional units – 2HEMA and tBA – as well as one multifunctional unit – PEGDMA550 – were chosen to vary systematically. Within the monofunctional units, 2CEA dissolved completely and PPGA dissolved more slowly (loss in mass seen in **Figure 2**), and therefore are completely impractical. In addition, although the full transition of PPGA is not seen in the results of **Figure 3** and it might display good shape-memory properties, the material has this transition at temperatures well below that of interest. This left 2EEM and tBA, both similar in transition temperature and water absorption, as candidates. However, looking closer at tBA, it exhibits a starker glass transition and was moved forward with, abandoning 2EEM. 2HEMA was the natural choice to adjust the properties of tBA due to its high water absorption ability (~50 wt.%), and higher glass transition temperature.

In addition the choice of the crosslinker was important - even at the low quantities they were to be added - because the length of linear chains as well as functional nodes would have an effect on transition temperature, water absorption, and ductility. Both PEGDMA550 and DEGDMA, the more conservative crosslinkers were initially used. Note, PEGDMA550 and DEGDMA are very similar crosslinking constituents with the same functional groups on the chain ends and same repeating *Poly(ethylene glycol)* mer unit in the center, PEGDMA550 just has approximately double the amount of mer-units, meaning longer crosslinking chains. Initial mechanical testing of ternary networks including DEGDMA reflected this when compared to PEGDMA550, offering much lower ductility and was abandoned.

With the fundamental knowledge of the nine macromolecules, now simplified to three constituents of interest, the next stage systematically altered the relative ratio of tBA, 2HEMA, and PEGDMA550 observing the effects of water absorption to the expected shape-memory behavior. There was a large correspondence seen between the increase in water absorption as the relative percentage of 2HEMA increased in the system, highlighted in **Figure 4**. As mentioned, a target of 4 wt.% water absorption was targeted for the final system. Through observation of the figure, on a approximate mixture of 65/35 wt.% tBA:2HEMA would provide this, however it is important to also note the effect water has on the shape-memory behavior and transition temperature of the network.

Noting that an onset temperature between 30-45°C is required and observing **Figure 6**, a balance between the target water absorption, glass transition region, and onset temperature must be met between the two figures. That the target water absorption with a mixture of 65/35 wt.% tBA:2HEMA found from **Figure 4** will put the soaked onset temperature too low when observing **Figure 6**. It is also important to note in **Figure 6** that as the percentage of 2HEMA increases up to approximately 75/25 tBA:2HEMA, the length of the glass transition also increases, inferred though the increase in temperature difference between the soaked t_g and t_{on}, after which it begins decreasing again. Ultimately, it was concluded that in order to balance all three factors, a ternary network consisting of 94.5/5.0/0.5 wt.% 9:1 tBA to 2HEMA, PEGDMA550, and DMPA. Therefore total weight percentage of each constituent overall was 85.05/9.45/5.00/0.50 wt.% tBA,

2HEMA, DEGDMA, and DMPA. This would provide a onset temperature close to 30°C, a short transition region, and some water absorption at 1.34 ± 0.19 wt.%

Further inquiry into the mechanical properties of the chosen system over the transition region display large changes in modulus, strain to failure and ultimate tensile strength, as seen in **Table 1**. Additionally through observation of **Figure 7 (b)** one can seen a fundamental change in material behavior from low temperatures up to the onset temperature (~26°C) and then from the glass transition on. Materials in glassy regime display plastic behavior with significant ductility, while materials in the rubbery regime display hyper-elastic behavior [4]. This fundamental change in mechanical behavior is due to the increase in free volume space in the polymer, relaxing steric effects between polymer chains. The practical effect is a stiffer, stronger, yet less elastically ductile product in the glassy regime, while in the rubbery regime you have a very ductile and low stiffness material that can easily bend and fold under low loads.

Of particular interest from **Table 1** and **Figure 7** is the temperatures where maximum strength and ductility are reached. The material is found to be the strongest near its onset temperature at 26°C, and also shows relatively high strain to failure at this temperature as well. In its rubbery state, the material is found to reach its highest strain to failure near the glass transition temperature (50°C). A high strain to failure in this transition region is found to be the case in similar works by Yakacki et al. [5]. It is also interesting to note that at temperatures past the glass transition, the ductility of the material decreases as temperature is increased, yet the stress-strain behavior apparently follows the same path. Therefore, it is recommended that materials mechanical behaviors can be optimized by using it at or near the onset glass transition for use when a higher stiffness in the polymer system is required (i.e. normal filtration operation), and that the water temperature is brought to the glass transition temperature for operation in its ductile state.

8 Proposed Continuation of Research:

Future work will examine the effectiveness of the proposed polymer system as a structured surface, shifting to Specific Aim #2 described in the initial proposal. Although the mold making process is developed, it is yet unknown what the most effective surface pattering will be. Initially, soft molds will be created using cylindrical pillars on hexagonal arrays. Both the packing factor of the pillars as well as the pillar height to diameter ratios will be systematically varied, and then put in a cross-flow membrane setup, observing both anti-fouling properties as well as cleansing properties. It is expected that a critical balance must be reached between both of these for maximum effectiveness. For example, the farther apart the pillars are it is hypothesized that foulants will collect easier. However, if the pillars are too close together then they will have difficulty under the crossflow at elevated temperatures in the in the pliable cleaning mode. Similarly, it is hypothesized that too tall of pillars will break off under normal operations if the pillars are too tall, however if they are too short, it will not be possible to produce enough load to bend them in the cleaning state. The anti-fouling and “self cleansing” properties of the structured acylate system will be also be quantified through adhesion analysis of colloidal debris with atomic force microscopy, and through contact angle studies observing the wetting character of the unstructured (flat sheet) polymer and its structured counterparts.

Surface hydrophobicity will be measured in terms of the contact angle with water using the captive bubble technique [6]. An environmental chamber will be used to control the temperature of the contact angle liquid (water) and observe changes in surface hydrophobicity (increasing or decreasing contact angle with water) *in situ*. A minimum of five samples, with three air bubbles per sample, will be analyzed to establish repeatability between surface coatings and to account for surface heterogeneities. Samples of SMPs will be immersed in water for selected time periods (2, 10, 24, 48, and 168 hrs) and the contact angle measurements repeated in order to assess their durability following continued exposure to an aqueous environment. Other solution chemistry / composition variables that will be assessed in these experiments include: ionic strength, pH, and ionic composition. Solution chemistry variables will be established to approximate those in a brackish water (produced water) desalination process. Contact angle values will be interpreted with regards to changes in surface hydrophobicity as well as pore-liquid entry pressure, *LEP* which will be calculated according to **Equation 2** [7]:

$$P_{liquid} - P_{vapor} = \Delta P = \frac{-2B\gamma_L \cos\theta}{r_{\max}} < LEP$$

where B is a geometric factor (= 1 for circular pores); γ_L is the liquid surface tension; θ is the liquid–solid contact angle; and r_{max} is the largest pore radius. The LEP will be compared to the pressure drop, and range thereof, expected to occur in a membrane element as a function of flow rate and channel dimensions. Contact angle measurements will also allow us to make inferences regarding the SMP surface structures.

To be effective, it is necessary that the SMP pillar structures, in both relaxed and erect orientations, not overly constrict the pores in the microporous support as this would result in a loss of membrane permeability. We expect that in the relaxed orientation (i.e., during backwashing) some pore constriction will occur. We will use a temperature controlled stirred cell apparatus operated in dead end mode to quantify how changes in solution temperature, and thus the orientation of the SMP pillar structures, affects the hydraulic permeability of the microporous support (microfiltration membrane). The hydraulic permeability and LEP provides information on pore flooding under any given condition, which will be used to establish operating and cleaning (backwashing) parameters. Permeability results for coated microporous membrane substrates will be compared to that determined for the virgin substrate samples.

9 Project Publications:

9.1 Publications in Preparation

N/A at this point

9.2 Presentations

N/A at this point

10 Student Support and Training:

Graduate: Christopher M. Laursen, Anthony J. Hoyt

Undergraduate: Samuel R. Gates

11 References:

[1] T. Asano, F. L. Burton, H. Leverenz, R. Tsuchihashi, and G. Tchobanoglous, Water Reuse Issues, Technologies, and Applications. McGraw-Hill, 2007.

[2] J. Mallevialle, P. Odendaal, and M. Wiesner, The Emergence of Membranes in Water and Wastewater Treatment, in Water Treatment Membrane Processes. McGraw-Hill, 1996.

[3] S. J. Duranceau, "The future of membranes," Journal American Water Works Association, vol. 92, no. 2, pp. 70–71, 2000.

[4] R. W. Hertzberg, Deformation and fracture mechanics of engineering materials. Wiley, 5th ed., 2013.

[5] C. M. Yakacki, S. Willis, C. Luders, and K. Gall, "Deformation limits in shape-memory polymers," Advanced Engineering Materials, vol. 10, no. 1-2, pp. 112–119, 2008.

[6] J. A. Brant and A. E. Childress, "Assessing short-range membrane-colloid interactions using surface energetics," Journal of Membrane Science, vol. 203, no. 1-2, pp. 257–273, 2002.

[7] M. El-Bourawi, Z. Ding, R. Ma, and M. Khayet, "A framework for better understanding membrane distillation separation process," Journal of Membrane Science, vol. 285, no. 12, pp. 4 – 29, 2006.

12 Figures and Tables:

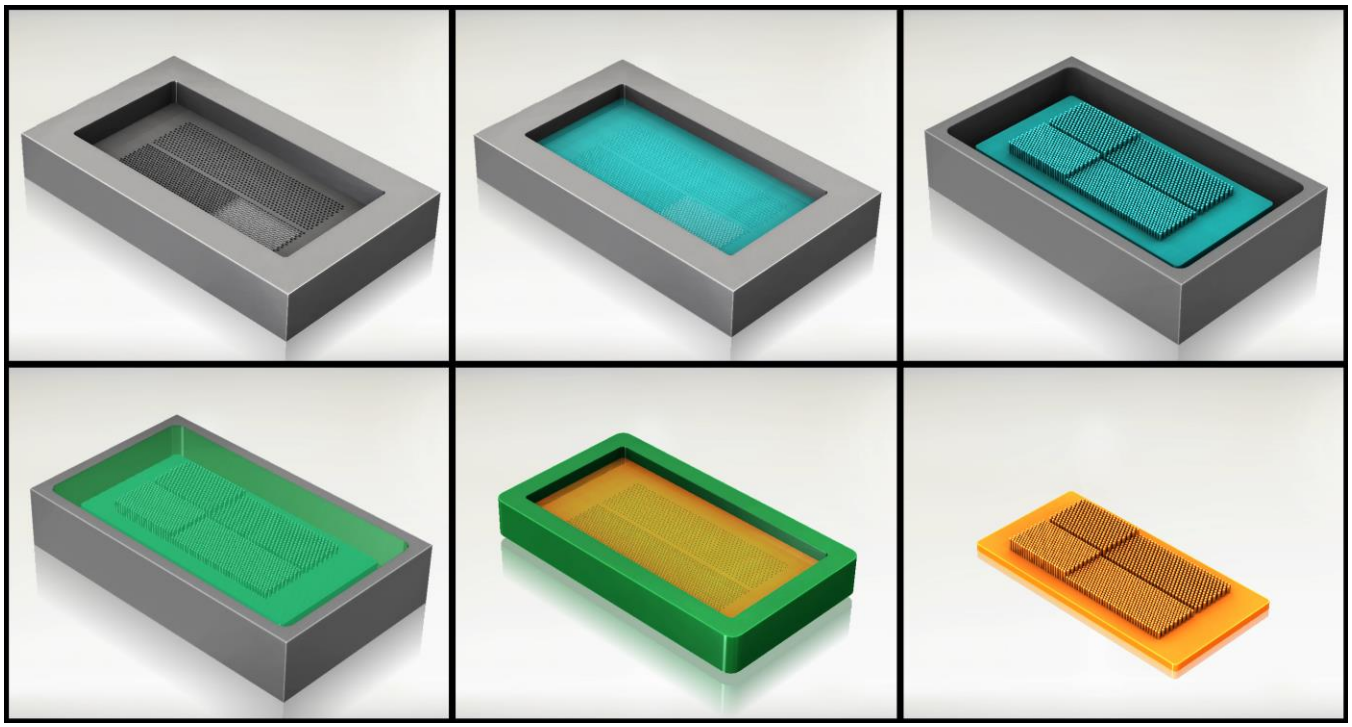

Figure 1: Molding process of acrylate structured surface.

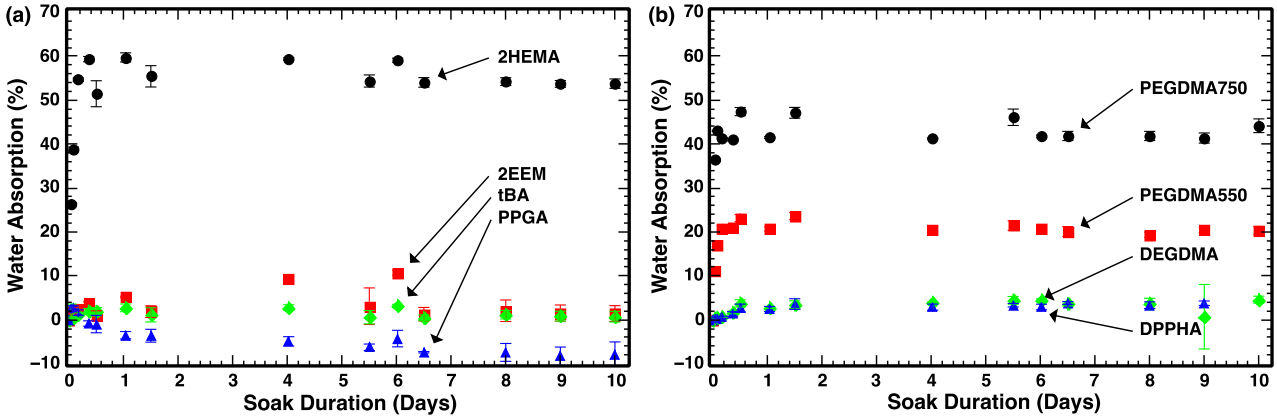

Figure 2: Water absorption for individual (a) monofunctional and (b) multifunctional acryl systems. Note 2CEA dissolved in water and therefore has not been included.

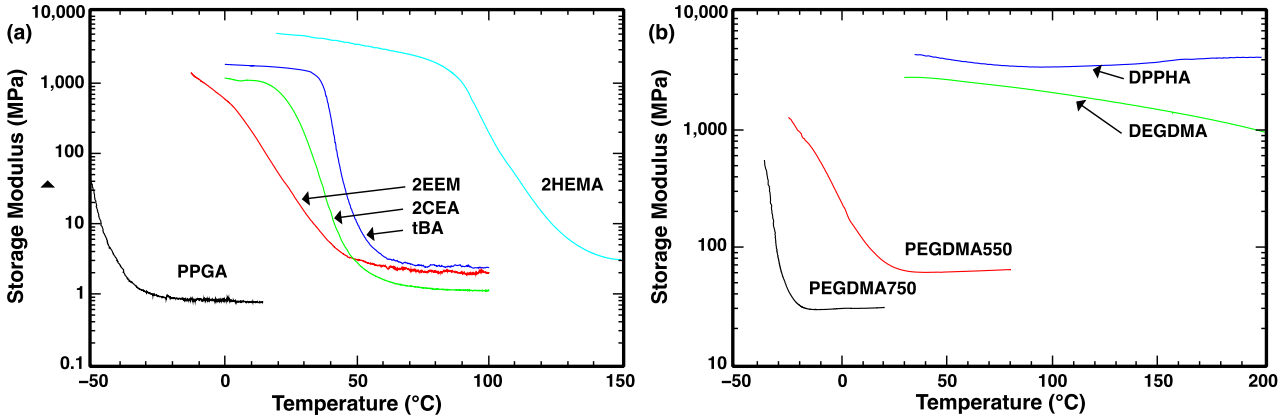

Figure 3: Representative curves of storage modulus transition as a function of temperature for individual (a) monofunctional and (b) multifunctional acryl systems.

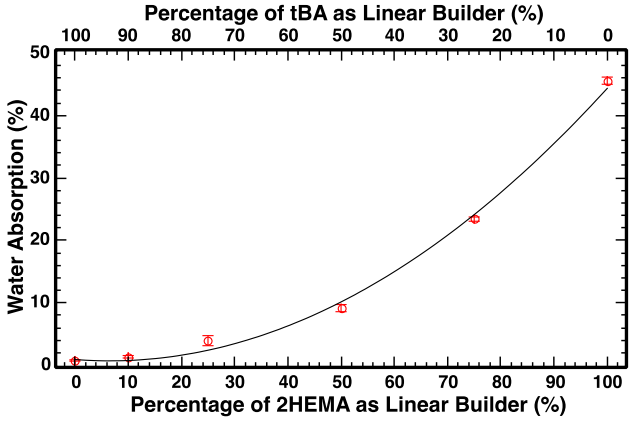

Figure 4: Water absorption as a function of varying the relative amounts of tBA and 2HEMA in a system with 5 wt.% PEGDMA550

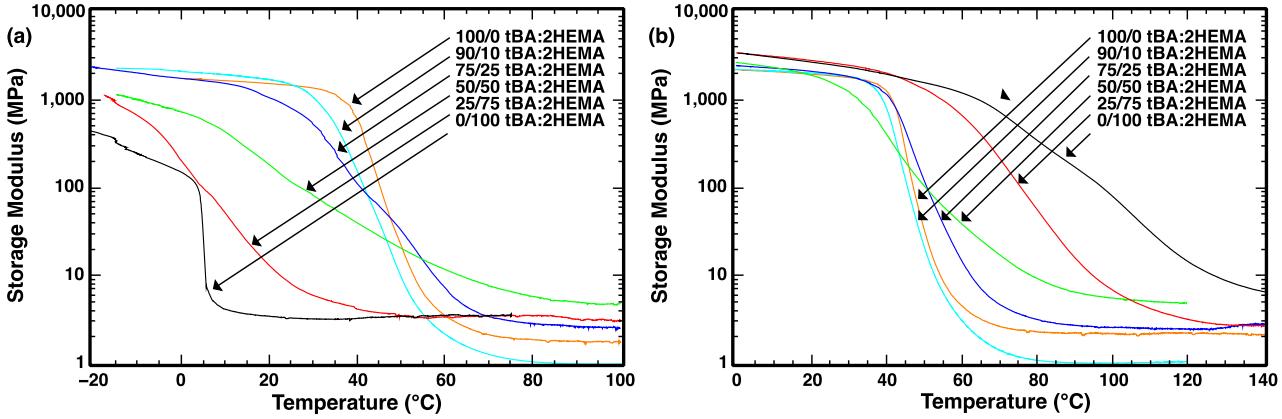

Figure 5: Representative (a) soaked and (b) dry DMA tests maintaining 5 wt.% PEGDMA550, while varying the relative wt. ratio of linear builders tBA and 2HEMA.

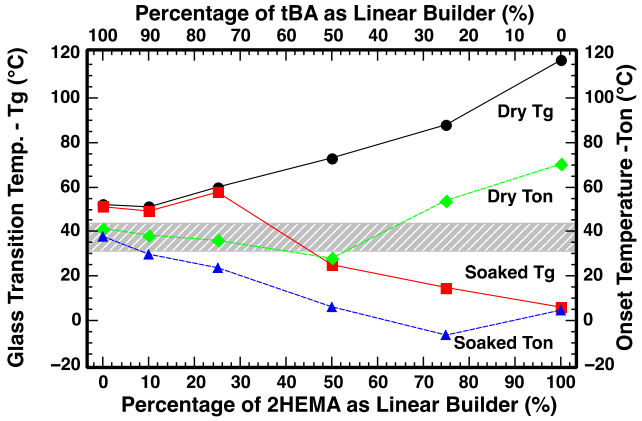

Figure 6: Effect on glass transition temperature and onset temperature as a function of varying the relative amounts of tBA and 2HEMA in a system with 5 wt.% PEGDMA550 for both dry and soaked samples.

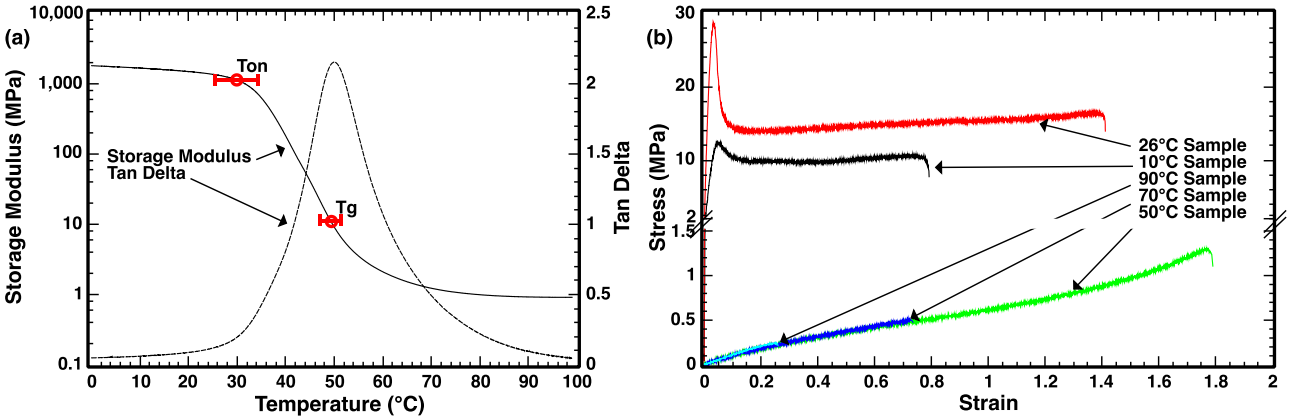

Figure 7: (a) Representative DMA curve of final ternary network along with the average Ton, Tg of the tests. (b) Tensile stress strain behavior as a function of temperatures tested over the glass transition region.

Table 1: Average sample storage moduli, ultimate tensile strength, and strain to failure at various temperatures.

	Storage Modulus (MPa)	Ultimate Tensile Strength (MPa)	Strain to Failure
10 °C	1405 ± 437	14.2 ± 2.8	0.60 ± 0.18
26 °C	916 ± 386	19.7 ± 6.9	1.33 ± 0.17
50 °C	7.13 ± 3.08	0.93 ± 0.47	1.34 ± 0.64
70 °C	1.13 ± 0.15	0.48 ± 0.06	0.87 ± 0.16
90 °C	0.81 ± 0.35	0.14 ± 0.09	0.17 ± 0.08

Use of Fe(VI) for the Improvement of Water Quality in Wyoming

Basic Information

Title:	Use of Fe(VI) for the Improvement of Water Quality in Wyoming
Project Number:	2013WY86B
Start Date:	3/1/2013
End Date:	2/29/2016
Funding Source:	104B
Congressional District:	1
Research Category:	Water Quality
Focus Category:	Water Quantity, Water Quality, Water Use
Descriptors:	None
Principal Investigators:	Maohong Fan, Lamia Goual

Publication

1. Tuwati, Abdulwahab M. Ali., New Technologies for Dealing with CO2 Emission and Carbonate Discharge Control Issues Associated with Energy Production, Ph.D. Dissertation, Department of Chemistry, University of Wyoming, December 2013, 100 pgs.

Use of Fe(VI) for Removal of Total Organic Carbons (TOC) and Heavy metals from Coproduced Water in Wyoming

Annual Report

(Year 1 of 3)

Andrew Thomas Jacobson, Abdulwahab M. Ali Tuwati, and Maohong Fan
Department of Chemical & Petroleum Engineering
University of Wyoming
Phone: (307) 766 5633 Email: mfan@uwyo.edu

ABSTRACT

The objective of the research is to develop a new, simple, and environmentally friendly method for the simultaneous removal of heavy metals and total organic carbon (TOC) in coproduced water (CW) from the energy production industry. Ferrate anions (FeO_4^{2-}) or Fe(VI) oxidation ability is very strong over the whole pH scale. Fe(VI) has been considered one of the future-generation water quality improvement agents. The oxidation of CWs TOC into CO_2 and H_2O can be done via Fe(VI). The result of the reduction of Fe(VI) is Fe(III) which is an excellent adsorbent for removal of heavy metals in CWs. Once the heavy metals and TOC have been removed from the CWs it is much easier to then remove the total dissolved solid (TDS) from the CWs. Water supply around the world is becoming insufficient for the growing populations and sources for additional water supplies must be established. Treated CWs can potentially be used to partly mitigate the tight water supply dilemmas in states such as Wyoming.

I. Description of Proposed Research

Wyoming is widely considered to be in a semi-arid hydro-climatic region. A vast majority of the time, rivers and streams throughout the state have little flow, granted during rare events, these rivers and streams can swell to very large levels. Wyoming has limited sustainable surface water available for use in general. Furthermore natural disasters such as droughts and tornadoes can suddenly scourge some regions of Wyoming by undermining agricultural and industrial productivity as well as the well-being and social fabric of communities. Point and nonpoint pollution is a manmade disaster that has been a long-standing concern that may further weaken Wyoming's capability to reach its water requirements. It is vital that Wyoming will not be threatened indefinitely due to a lack of water resources. In response to the water crisis, Wyoming statute Title 35, Chapter 11, Article 3 (35-11-309) declares "water is one of the Wyoming's most important natural resources, and the protection, development and management of Wyoming's water resources is essential for the long-term public health, safety, general welfare and economic security of Wyoming and its citizens." Wyoming mining and energy production companies have generated a great deal of water known as coproduced water (CW). These CWs regularly contain difficult to remove inorganic heavy metals and organic compounds whose disposal will not only cause serious environmental problems, but also waste the precious water resources that are desperately required in Wyoming. Consequently, treatment of CWs for use in Wyoming is a win-win approach.

CWs from various energy production industries [1] have been considered as important new water resources. Nonetheless some of the CWs need to be treated due to quality issues including heavy metals, total dissolved solids (TDS), and high total organic carbon (TOC) associated with fossil fuels [2-3], natural gas and coal. Removal of heavy metals and TOC can greatly help

facilitate TDS reduction and removal. Presently there are two separate steps and two different technologies to remove heavy metals and TOC. The first step is to remove the TOC. TOC can be degraded through biological processes that are environmentally friendly, but slow [4]. TOC can also be destroyed using UV photolytic [5] and electrochemical [6] methods, but they are expensive and difficult to control. Most recently a combination of the methods has been studied [7-10] to achieve high removal efficiencies of TOC with some progress being made, however these processes are complex. To overcome these downfalls of a multistep method efforts have been put into using a simple multifunctional technology for simultaneous removal of the organic compounds and heavy metals to improve the overall CW quality of Wyoming. Specifically, a proprietary green method to produce a multifunctional K_2FeO_4 (simply called Fe(VI) henceforth) and propose to use it for the simultaneous removal of total organic carbons (TOC) and heavy metals in numerous CWs preceding their further treatments for total dissolved solids (TDS) removal with other technologies such as reverse osmosis.

Success in this project will benefit water resource conservation, environmental quality protection, and agricultural and energy development. These benefits will be accomplished with the following results. Firstly, the optimal Fe(VI) quality for removal of TOC and heavy metals in CWs will be established. Second, the operation conditions for the proposed CW contaminant removal technology will be obtained from laboratory bench-scale data collection. A TOC analyzer will be used to find the concentrations of TOC before and after treatment to determine the effectiveness of Fe(VI) on removing TOC from the CWs. The concentrations of heavy metals will be measured before and after treatment with an inductively coupled plasma optical emissions spectrometer (ICP-OES) to determine the performance of Fe(VI) in removing the heavy metals. Lastly, to demonstrate the applicability of the proposed technology, a pilot-scale test set-up will be designed

and built based upon test results from the laboratory bench-scale setup. The results from the pilot-scale set-up are expected to reveal the operation conditions needed for use of the proposed technology in industry for future use. Studies in the use of Fe(VI) have not been done for its application in CW treatment, but it has for other water treatments. Success in the proposed project will advance the application of Fe(VI) in the energy industry as well as other industries working with organic compounds and heavy metals.

Ferrate anions (FeO_4^{2-}) or Fe(VI) oxidation ability is very strong over the whole pH scale. Fe(VI) has been considered one of the future-generation water quality improvement agents. The oxidation of CWs TOC into CO_2 and H_2O can be done via Fe(VI). The result of the reduction of Fe(VI) is Fe(III) which is an excellent adsorbent for removal of heavy metals in CWs.

II. Tasks

Task 1 includes building the laboratory setups seen in Figure 1 and Figure 2. The first step for treatment of CW will be to add 1 L of collected CW to the vessel followed by turning on and setting the stirrer to the desired speed. The temperature control unit will then be turned on to control the operating temperature (5, 10, 15, 20, or 25 ˚C) depending on the test. Next a chosen amount of Fe(VI) will be added once the CW reaches the desired temperature. The reaction will be conducted for a predetermined amount of time with samples being taken periodically to monitor TOC and heavy metal concentrations during the reaction.

Task 2 includes analyzing the samples from the as-received CWs as well as the CWs treated with Fe(VI) under varying conditions. A TOC analyzer will be used to measure the concentrations of TOC and an ICP-OES will be used to measure the concentrations of heavy metals. Other water quality parameters such as suspended solids (SS), total dissolved solids (TDS), electrical conductivity (EC), and pH values of CWs will also be monitored using corresponding instruments

available on UW campus. Also, the concentrations of Fe(VI) solution used to treat the CWs will be determined using UV spectroscopy.

Task 3 is the performance evaluation of Fe(VI) on the removal of TOC and heavy metals from CWs on the bench-scale set-up under different conditions. These tests will be used to investigate the TOC and heavy metal removing efficiencies of Fe(VI) under different CW conditions including TOC and heavy metal concentration levels, SS, pH, TDS, temperature, stirring speed and Fe(VI) dosage. The major organic compounds (major TOC contributors) in the CWs will be identified, as well as the kinetics associated with reactions between major organic compounds and Fe(VI).

Task 4 will be to test if the sludge resulting from treatment of CW with Fe(VI) is stable when landfilled. The TOC is expected to be completely decomposed into CO_2 and H_2O when the optimal treatment conditions and dosage of Fe(VI) are used. So, this task is designed to evaluate the stability of heavy metals in the sludge using EPA SW-846 Method 1311 (Toxicity Characteristic Leaching Procedure (TCLP)). The optimal CW treatment conditions for achieving the greatest heavy metal stabilities in sludge will be investigated.

Task 5 is to perform industrial/commercial-scale demonstration of the proposed CWs management technology based on the results achieved with bench-scale tests. The volume of the batch vessel will be scaled to up to 1,000-2,000 L. The on-site industrial/commercial-scale demonstrations will be done in one of oil or natural gas production companies. The specific location of the project will be determined by discussing with the associated landowner and oil/gas companies. Less than 0.5 acre of land will be used for pilot-scale and industrial/commercial-scale demonstrations of the proposed technology. The quality parameters (including TOC and heavy metal concentrations, pH, SS and TDS) of the as-received CW from the chosen company will be

characterized. The data obtained from bench-scale tests will be used as the references of the industrial/commercial-scale tests. Factorial tests will be done to assess the performance of Fe(VI) on CWs treatment at industrial/commercial-scale.

III. Methods and Progress:

Apparatus

Two setups are considered be used for this project.

1. Jar tester

A photo (Figure 1) shows the PB-700 jar tester that is being used for water sample mixing. It is equipped with six stainless steel 1" x 3" paddles which are spaced six inches apart and are adjustable to a maximum depth of nine inches. An electronic motor control system offers regulated variable speeds of all paddles simultaneously, from 1-300 rpm, with the exact speed clearly displayed on a digital readout. A fluorescent lamp illuminator is built into the jar tester base to provide soft, diffused lighting of samples being tested. This setup is used in the first part of this project and the final analysis of water samples are analyzed via Total Organic Carbon (TOC) analyzer.

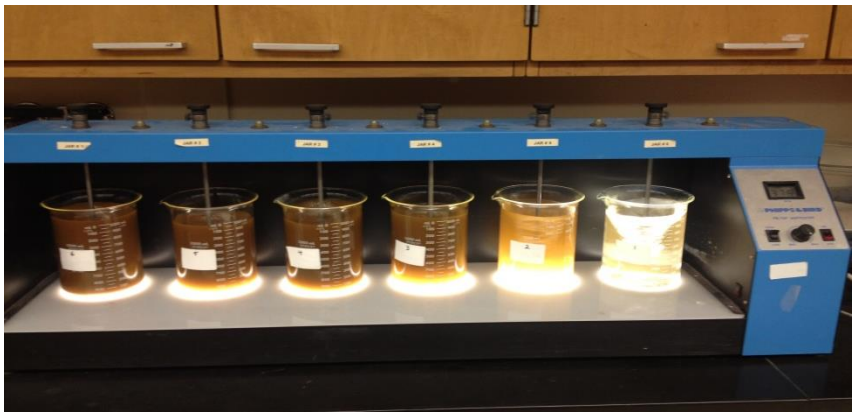

Figure 1. *Photo of the jar tester setup'*

2. Glass reactor

A comparative laboratory scale set-up that will be used to remove TOC and heavy metals from CWs with Fe(VI) is schematically illustrated in Figure 2. Each of the experiments will be executed in a 1 L stirred glass vessel (5). The glass vessel will have five inlets through its lid. In the center inlet of the glass lid a Teflon shaft with a propeller will be inserted (6). The next inlet will be used to introduce CWs and Fe(VI) into the vessel (4). A thermometer will be inserted into another one of the five inlets (7) to monitor the temperature that will be controlled by a separate temperature control unit (3). The fourth inlet will be used to introduce nitrogen when needed to increase the efficiency of mixing in the vessel, which will be controlled by a rotameter (2). A condenser (8) will be connected to the last inlet to condense any vapor released from the reaction mixture and return it to the vessel. The condenser regulating unit (9) will be used to control the condenser temperature. A sampling port will be fitted at the bottom of the vessel as can be seen in Figure 2.

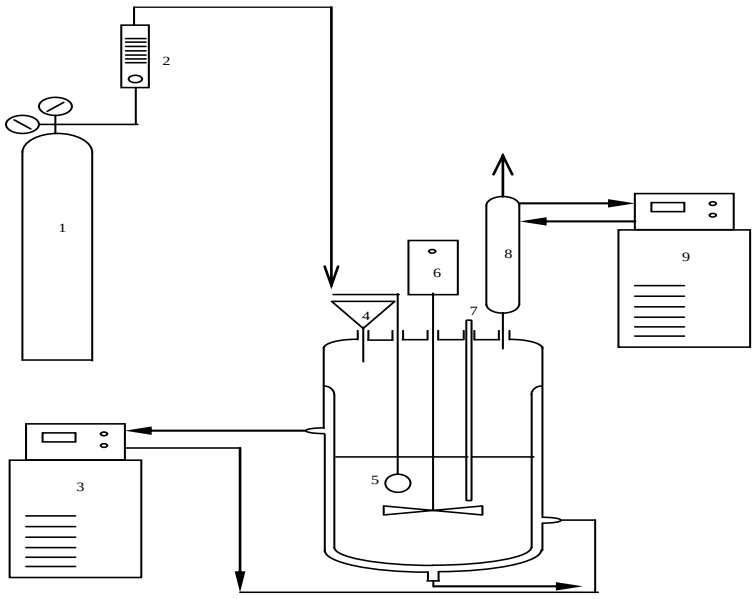

Figure 2. *Experimental setup for removal of TOC and heavy metals from CWs with Fe(VI) [(1) nitrogen tank (2) rotameter (3) temperature control unit (4) funnel (5) vessel (6) stirrer motor (7) thermometer (8) condenser (9) condenser regulating unit]*

2. Progress

In accordance to task 1 the first set-up as seen in Figure 1 is currently running and being used for experiments. The experiments include varying temperature, pH, sorbent concentrations, TOC concentrations, and stirring rates. These parameters will help find the optimal use of Fe(VI) in removing TOC. The reactor set-up in Figure 2 is currently being built to complete task 1. Experiments will be run in this set-up to compare with the jar testers. Much effort has been put into task 5 to find a company willing to allow a pilot-scale setup to be built next to a CW source, as well as in finding a company to provide water for research. The latter of these two endeavors has been only recently successful. Soon CW samples will be provided for research, in the meantime simulated water has been used with common TOCs from Wyoming CWs [11] being spiked into clean water. Analysis of completed experiments with the TOC analyzer has been done in agreement with task 2. The data is currently being analyzed and will be included in the next report. Heavy metals have not been included in the experiment as of yet, but an ICP-OES has been established for use to complete the analysis of heavy metal concentrations when needed. The completion of this project has been assumed by Abdulwahab M. Ali Tuwati, a post doc with a PhD in chemistry, and Andrew Thomas Jacobson, a Masters candidate in chemical engineering at the University of Wyoming. The ideas behind the project have also been introduced to students through the GK-12 Environmental and Energy Nanotechnology NSF Fellowship through Andrew Jacobson. As a fellow, travel has been done to Chugwater, WY to introduce science topics including this ongoing research. Students from around Wyoming have also been given lab tours explaining the ideas behind the setups of this research and what the goal of this research is.

IV. Future Work

Future work includes completing all of the tasks explained previous. The setup of the glass reactor in Figure 2 will be completed and experiments will start to be run with it. Upcoming experiments will also include the addition of heavy metals to the simulated water. Water samples will be obtained from gas companies to be analyzed as well as tested to be compared with the simulated waters. Work on finding a company to partner with and allow a pilot-scale setup will also be accomplished. Data analysis is currently under way and will be included in the next report for the removal of TOC as well as heavy metals. The characteristics of the sorbent Fe (VI) are also in the process of being tested via analytical methods including thermogravimetric analysis (TGA), scanning electron microscopy (SEM) and transmission electron microscopy (TEM). Results from these tests will be included in the upcoming report. Kinetic theory of reactions between major components in TOC and Fe(VI) will also be evaluated Tests on the decomposition of the sludge created form the removal of TOC and heavy metals for its stability when landfilled will be done.

V. References

1. Alapi, T., Gajda-Schrantz, K., Ilisz, I., Mogyorosi, K., Sipos, P., Dombi, A., Journal of Advanced Oxidation Technologies (2008), 11(3), 519-528.
2. Dallbauman, L., Sirivedhin, T., Separation Science Technology (2005) 40, 185-200.
3. Li, H., Cao, H., Li, Y., Zhang, Y., Liu, H., Environmental Engineering Science (2010), 27(4), 313-322.
4. Samiha, H., Ali, O., Nizar, B., Mohamed, D., Journal of hazardous materials (2009), 163(1), 251-258.
5. Liu, L., Zhao, G., Pang, Y., Lei, Y., Gao, J., Liu, M., Industrial & Engineering Chemistry Research (2010), 49(12), 5496-5503
6. Diwani, G. E., Rafie, S. E., Hawash, S., International Journal of Environmental Science and Technology (2009), 6(4), 619-628.
7. Gonzalez, O., Esplugas, M., Sandfrs, C., Esplugas, S., Water Science and Technology (2008), 58(9), 1707-1713.
8. Badawy, M. I., Gohary, F. El., Ghaly, M. Y., Ali, M. E. M. Journal of Hazardous Materials (2009), 169(1-3), 673-679.
9. Mearns, A. J., Reish, D. J., Oshida, P. S., Ginn, T., Effects of Water Environment Research (2010), 82(10), 2001-2046.
10. Santos, H. F., Cury, J. C., Carmo, F. L., Rosado, A. S., Peixoto, R. S. PLoS One (2010), 5(8).
11. William H. Orem, et al. "Organic compounds in produced waters from coalbed natural gas wells in the Powder River Basin, Wyoming, USA." Applied Geochemistry 22 (2007) 2240-2256

Rumen Microbial Changes Associated With High Sulfur A Basis for Developing Treatments for Ruminant Livestock in High Sulfur Water Regions

Basic Information

Title:	Rumen Microbial Changes Associated With High Sulfur A Basis for Developing Treatments for Ruminant Livestock in High Sulfur Water Regions
Project Number:	2013WY87B
Start Date:	3/1/2013
End Date:	2/28/2015
Funding Source:	104B
Congressional District:	1
Research Category:	Biological Sciences
Focus Category:	Agriculture, Treatment, Water Quality
Descriptors:	None
Principal Investigators:	Kristi Cammack, Kathy Austin, Gavin Conant, William Lamberson, Ken C Olson, Cody L Wright

Publications

There are no publications.

Rumen Microbial Changes Associated With High Sulfur – A Basis for Developing Treatments for Ruminant Livestock in High Sulfur Water Regions

Annual Report
(Year 1 of 2)

UPDATE: 05/01/2014

Principal Investigators**:**

Kristi M. Cammack, Ph.D., Assistant Professor, Animal Science, University of Wyoming
kcammack@uwyo.edu; 307-766-6530

Kathy J. Austin, M.S., Research Scientist, Animal Science, University of Wyoming
kathyaus@uwyo.edu; 307-766-5180

Cody L. Wright, Ph.D., Professor, Animal Science, South Dakota State University
cody.wright@sdstate.edu; 605-688-5448

Ken Olson, Ph.D., Associate Professor, Animal Science, South Dakota State University
Kenneth.Olson@sdstate.edu; 605-394-2236

Gavin Conant, Ph.D., Assistant Professor, Animal Sciences, University of Missouri
conantg@missouri.edu; 573-882-2931

William Lamberson, Ph.D., Professor, Animal Sciences, University of Missouri
Lambersonw@missouri.edu; 573-882-8234

Abstract: Reliable drinking water sources that meet minimum quality standards are essential for successful livestock production. Recent surveys have shown that many water sources, especially throughout the semi-arid rangelands of the U.S., are not of sufficient quality to support optimum herd/flock health and performance, in particular because of high concentrations of sulfur (S) and S-compounds present in the water. High S concentrations in water sources can arise from several factors. First, water sources can be naturally high in S. Second, drought conditions can cause S to be concentrated within the water source. Third, conventional oil and gas production can also increase S content within the water source. Combinations of these conditions can further exacerbate S levels in the water. Many of these water sources are used for livestock production systems, especially throughout the western states. However, high-S water is associated with poor performance and health in ruminant livestock, and is a primary cause of polioencephalomalacia (PEM), a disease state that can cause 25% morbidity and 25-50% mortality in affected populations. Unfortunately, producers are typically limited in available water resources and cannot avoid high S water situations; there are also no practical means of treating high S water. Although no effective treatments are currently available for animals suffering from the effects of high dietary S, it has been noted that animals vary in their response to elevated levels of S. While some animals consuming high S water exhibit reduced performance and/or poor health, others appear unaffected. We hypothesize that differences in rumen microbial populations, which are responsible for the breakdown of S and S-compounds, are associated with the variation in animal response to high S. Therefore, in this study we aim to 1) determine how rumen microbial populations change in response to high S water, and 2) determine if the extent of those changes are associated with tolerance to high S. A better understanding of the rumen microbial response to high S will lead to development of treatments for affected animals.

Title: Rumen Microbial Changes Associated With High Sulfur – A Basis for Developing Treatments for Ruminant Livestock in High Sulfur Water Regions

Statement of Critical Regional or State Water Problem: *Need for Project.* Ruminant livestock consuming water high is sulfur (S) and S-compounds (e.g., sulfate) are prone to poor performance and health. High S can also cause polioencephalamalcia (PEM), a disease state in that can cause 25% morbidity and 25-50% mortality in affected population. Ruminants are especially susceptible to S toxicity because of S metabolism in the rumen by sulfate-reducing bacteria (SRB). High S triggers metabolism by SRB to sulfide, which ultimately increases hydrogen sulfide (H_2S) production in the rumen. It is this increase in H_2S production that is thought to be causal to the poor performance and health (including PEM) of ruminant animals.

Unfortunately, many livestock water sources, especially throughout the semi-arid rangelands of the U.S. and Wyoming, are high in S and S-compounds because of underlying soil conditions or man-made contaminants (e.g., conventional gas and oil water), and are exacerbated by evaporation concentrating S during persistent drought conditions. Unfortunately, producers are typically limited in available water resources, and there are no practical means of treating high S water, especially in range conditions, nor animals suffering the effects of high S water.

The literature is replete with studies aimed at identifying treatments for animals affected by high S. Why, then, have no effective, consistent treatments been discovered yet? Most studies have identified potential treatments *in vitro*, or in laboratory studies using rumen bacterial cultures. However, once these treatments were tested *in vivo*, or in the live animal, limited effects on animal health or performance were typically observed. It is apparent from these studies that *in vivo* and *in vitro* conditions respond differently to high S, indicating the need for a whole-animal approach. A better understanding of how rumen microbial populations (e.g., bacteria) *in vivo* change in response to high S is a critical first step to whole animal studies aimed at targeted treatment development.

Who Would Benefit and Why. Many water sources high in S are still used for livestock production due to lack of alternative available sources, especially in range production settings. Additionally, in many of these areas it is neither feasible nor practical to haul in water low in S. Therefore, identification of an effective treatment for either 1) high S water sources or 2) animals suffering from high S would benefit livestock producers by 1) preventing the health and performance problems associated with livestock consuming high S water, and 2) allowing them to use available water resources despite high S concentrations.

Statement of Results or Benefits: *Information to be Gained and How Information will be Used.* Past studies of changes in rumen microbial population in response to high S have utilized technologies either limited to determining the presence/absence of microbial species, or have utilized *in vitro* culture methods capable of altering bacterial metabolism so that *in vivo* conditions are not truly reflected. We will use DNA sequencing techniques to better identify and quantify changes in rumen microbial populations in response to high S water. We hypothesize that this information is critical for future development of treatments to counteract high S. It has also been well documented in the literature that animals vary in response to high S, with some individuals being highly tolerant, and others lowly tolerant. Through this project we will not only determine general changes to rumen microbial populations in response to high S, but also if the magnitude of those changes differs between animals more tolerant and less tolerant to high S. This

information could not only be used for treatment development, but also for management strategies. If animals could be identified as more tolerant or less tolerant to high S, producers in high S water regions could manage those animals differently.

The results of this research will provide valuable insights into the response by rumen microbes, a necessary next-step in the development of effective treatments for animals affected by high S water. In the short-term, we will also work with the office of the Wyoming State Veterinarian to determine ways to provide information to our targeted audience: livestock producers. *In the long-term, we expect the results of this research to direct future efforts aimed at treatment development to enable livestock producers to better utilize available water resources high in S.*

Nature, Scope, and Objective of the Project: The basic nature of the proposed research is to determine changes in rumen microbial populations in response to high S water. Our objective is to use DNA sequencing to quantify and characterize rumen microbial populations in sheep (our model ruminant) consuming high S water; this approach will allow us to more accurately determine important rumen microbial changes in response to high S. We hypothesize that differences in rumen microbial populations, which are responsible for the breakdown of S and S-compounds, are associated with the variation in animal response to high S. Therefore, in this study our objectives are to 1) determine how rumen microbial populations change in response to high S water, and 2) determine if the extent of those changes are associated with tolerance to high S.

Timeline of Research Activities: ***Year 1*** – Completed animal trial, serum mineral analyses, production data analyses, and DNA extractions and preparations. ***Year 2*** – DNA sequencing (conducted at the DNA Core Laboratory in Columbia, Missouri) has been completed. Bioinformatic analyses are currently underway to identify specific rumen microbes that change in response to high S water, and importantly identify if such changes infer a "tolerance" to high S. Ruminal volatile fatty acids (VFAs) can also indicate shifts in rumen function; therefore, VFA analysis of d 0, 7, and 28 samples was conducted as an add-on to this project. M.S. student Cara Clarkson has completed her initial thesis chapters (literature review and performance results), and is on-schedule to complete her final thesis chapter (rumen microbial results) this summer/fall.

Methods, Procedures, and Facilities: This study used Hampshire wether lambs (n = 40; 6 months of age) maintained at the UW Stock Farm. Lambs were administered a high S water treatment (~3,000 mg/L) over a 28 d trial period; they were individually penned to enable collection of individual feed and water intake. A 28 d trial period was chosen as signs of S toxicity would be more easily observed with the collection of individual feed and water intake; a common sign of S toxicity is decreased feed and water intake. Individual water and feed intake were estimated, along with average daily gain and feed efficiency measures. Blood and rumen fluid samples were collected on d 0 (baseline), d 7, and d 28.

Blood samples were analyzed for S, Cu, and Mo content, and no differences between individual animals were detected. Lambs were selected as highly tolerant (n = 4) and lowly tolerant (n = 4) to high dietary S based on individual water and feed intake, average daily gain and feed efficiency measures, and daily behavioral responses (recorded on a scale of 1 to 5). DNA was extracted from d 0, d 7, and d 28 samples from these selected lambs (n = 24 samples in total), and samples were sent to the University of Missouri's DNA Core Facility for DNA sequencing. Sequence analysis of the d 7 samples will allow us to determine microbial species/classes

important to the early response to high S, and d 28 samples a more stabilized (or perhaps adapted) response to high S. Identification of microbes most important to the response to high S will be important in identifying potential treatments, or even prevention strategies, for high S situations. Finally, VFA analysis of d 0, 7, and 28 rumen samples indicated that initial (d 0) concentrations of propionate were greater in tolerant lambs. Propionate is an end-product of starch and sugar fermentation, and considered a more efficient energy source for fermentation. The greater initial concentrations of propionate in tolerant animals may have given rise to greater ability to metabolize high levels of S.

DNA Sequence Analyses. Taxa (i.e. organism) abundance will be estimated from sequence data using a custom analysis pipeline that will match the sequencing data to a database of known genes to provide taxa identifications. Both the diversity and abundance of the taxa will be used to characterize the rumen microbial populations. Co-PIs Conant and Lamberson have developed a pipeline method that analyzes the taxa counts for each sampling time (d -1, d 7, and d 28). This approach will statistically distinguish the "intolerant" and "tolerant" lambs and will identify key microbial taxa responsible for these differences. Comparison of taxa profiles will allow us to identify changes in rumen microbial populations associated with high dietary S. We will also track population changes due to a more immediate response (d 7) and a more chronic response (d 28) to high S. These analyses should be completed this summer.

Related Research: *High S Water.* The current NRC recommendation for dietary sulfur is < 0.3% dry matter (DM), with the maximum tolerable concentration estimated at 0.4% DM. Sulfur content in water, however, is typically reported in parts per million (ppm), and the most common form of S in water is SO_4^2. Polioencephalmalacia is associated with water SO_4^{2-} concentrations of ≥ 2,000 mg/L, which when combined with a typical 0.2% DM S feedstuff results in 0.53% DM total dietary S. Therefore, when S or SO_4^{2-} content of water is included in the estimation of dietary S, the total dietary S is often much higher than anticipated.

Survey and field data have consistently shown surface and subsurface water can be high in SO_4^{2-}, particularly throughout the western regions of the U.S. The Water Quality for Wyoming Livestock & Wildlife review reported that of > 450 forage and water collection sites located throughout the U.S., 11.5% exceeded the dietary S concentrations considered safe for livestock. Of those sites, 37% were located in the western U.S., including Wyoming. Drought further exacerbates the high SO_4^{2-} problem, as SO_4^{2-} is concentrated in the water due to greater evaporation and reduced moisture recharge. Finally, conventional oil and gas production can also increase S content within the water source.

Effects on Livestock: Several experimental and field studies have reported reductions in performance of animals exposed to high S drinking water sources. Declines in average daily gain in cattle consuming high SO_4^{2-}water have been reported in both grazing and confined environments. In addition, decreases in feed consumption and overall body weight gain are consistently reported. Polioencephalomalacia (PEM), a prevalent central nervous system disease in cattle and sheep, can also be caused by high S. Clinical signs of PEM include head pressing, blindness, incoordination, and recumbency accompanied by seizures, with young ruminants more commonly affected.

Biological Mechanisms: In ruminants, production of toxic metabolites from S occurs in the rumen. Two classes of bacteria, assimilatory and dissimilatory, are present in the rumen capable of reducing SO_4^{2-}. Sulfide is produced by assimilatory S-reducing bacteria (SRB) and is

used immediately for incorporation into metabolic processes. The assimilatory SRB also reduce SO_4^{2-} to create amino acids. Dissimilatory SRB use SO_4^{2-} in respiration pathways and for energy to fuel growth and metabolism. However, in the respiratory pathways excess S^{2-} and H_2S are produced. It is the dissimilatory class of SRB that cause the overproduction of toxic S products leading to cell damage, secondary infections, and the development of sPEM. These bacteria can also produce high amounts of S^{2-}, causing H_2S levels to increase rapidly.

Summary of Progress. To-date, the animal trial has been completed, and associated blood and rumen fluid samples have been collected. Blood samples have been analyzed by the M.S. student for this project (Cara Clarkson) at the Wyoming State Veterinary Laboratory. Additionally, Cara has completed VFA analysis for this project. DNA was extracted from rumen fluid samples collected from highly tolerant (n = 4) and lowly tolerant (n = 4) lambs on d 0 (baseline), d 7 (immediate response), and d 28 (more chronic response). These DNA samples were sent to the University of Missouri for DNA sequencing, which was completed this spring.

Analysis of sequence data will be the primary responsibility of co-PIs Conant and Lamberson, using in-house software developed for this type of data. Following microbial identification and quantification, M.S. student Cara Clarkson will determine which microbial species are associated with 1) the overall response to high S; 2) an animal's ability to tolerate (or not tolerate) high levels of S in drinking water; and 3) a more immediate (d 7) versus a more chronic (d 28) response to high S. Finally, she will summarize all information, and complete and defend her thesis to meet her M.S. requirements.

Training. Graduate student training is a priority in the Department of Animal Science. Research endeavors are overseen by faculty and staff, but carried out by graduate and undergraduate students. This project is the thesis project of a M.S. student (advised by PI Cammack) in Animal Science, Ms. Cara Clarkson. The student is currently being trained in the areas of animal production, toxicity, genomics, data analysis, and water quality. The student has been, and will continue to be, responsible for carrying out all aspects of this research project, including both the animal and laboratory components. Together with the PIs, the student will prepare manuscripts and bulletins for submission as her project nears completion. This research has also provided a training opportunity for undergraduates employed by PI Cammack. In particular, one undergraduate student served as an intern for this project; she presented her internship experience and research results at the University of Wyoming Undergraduate Research Day.

In addition, two other graduate students in the PIs graduate program have become involved in this project. One is a M.S. student, also working in the rumen microbial field but more focused on feed efficiency. Cara and this student will compare rumen microbial results to determine which microbial species are affected by high S that lead to decreases in feed efficiency. The other is a Ph.D. student who is currently working on this project's microbial sequence data analysis. This student is conducting the bioinformatic analyses while training Cara on methods used. This has become a great teaching/learning experience for both students involved. The Ph.D. will continue to use the high S sequence data set in the fall to perform novel analysis techniques and infer metabolic pathways to better describe and interpret sequence results. As such, this project has evolved to being a major part of > 1 graduate student programs.

Publications. M.S. student Cara Clarkson has had one abstract and proceedings paper accepted for oral presentation at the 2014 Western Section of the Society of Animal Science Meeting this summer. Her paper is entitled "Effect of high sulfate water on behavior, feed efficiency, blood mineral metabolites, and VFA production in lambs." She will present her paper in the Graduate Student Competition section of that meeting. Cara has attended other meetings recently and has had the opportunity to discuss her project and her methods with other experts in the genetics field. Finally, Cara is schedule to complete her thesis shortly (summer/fall 2014), which is expected to lead to the publication of two peer-reviewed manuscripts.

Information Transfer Program Introduction

Information dissemination efforts include reports and presentations by the University of Wyoming Office of Water Programs (OWP) Director to State and Federal entities and the private sector. The OWP Director reports annually to the Wyoming Water Development Commission and to the Select Water Committee (of the Wyoming Legislature). Presentations were given throughout the state concerning the research program and project results. The OWP Director serves as the University of Wyoming Advisor to the Wyoming Water Development Commission and attends their monthly meetings. This provides a means for coordinating between University researchers and Agency personnel. The OWP Director also serves as an advisor to the Wyoming Water Association (www.wyomingwater.org) and regularly attends meetings of the Wyoming State Water Forum.

Publications and other information dissemination efforts were reported by the PIs of the projects funded under this program. The project PIs report to the Institute Advisory Committee on an annual basis. Presentations discussing final results are made by PIs of projects which were completed during the year at the July committee meeting. Presentations discussing interim results are made by PIs of continuing projects at the fall/winter committee meeting. PIs are encouraged to publish in peer reviewed journals as well as participate in state-wide water related meetings and conferences. Publications are listed in the individual research reports.

FY13 OWP Director information dissemination activities and those reported by research project PIs are listed, by project, in the following paragraphs.

OWP DIRECTOR FY13 INFORMATION DISSEMINATION ACTIVITIES, SERVICE AND PRESENTATIONS: (1) Wyoming Water Forum, Presentation on Water Research Program update, Cheyenne, WY., March 5, 2013, (2) Wyoming Water Development Commission/Select Water Committee Meeting, Cheyenne, WY., March 7-8, 2013, (3) Weather Modification Association -- Annual Conference, San Antonio, TX., April 9-11, 2013, (4) Wyoming Weather Modification pilot program Technical Advisory Team meeting, San Antonio, TX., April 11, 2013, (5) Wyoming Water Forum, Presentation on Water Research Program update, Cheyenne, WY., May 7, 2013, (6) Wyoming Water Development Commission water project consultant selection approval, Cheyenne, WY., May 10, 2013, (7) Wyoming Water Development Commission/Select Water Committee joint workshop, Presentation on the UW Office of Water Programs and Water Research Program, Cheyenne, WY., June 5-7, 2013, (8) Universities Council on Water Resources/National Institutes for Water Resources joint conference, Lake Tahoe, CA., June 11-13, 2013, (9) Wyoming Water Development Office development of new Water Research Program support process, Cheyenne, WY., July 9, 2013, (10) Wyoming Water Association Board meeting (Advisor), Evanston, WY., July 10, 2013, (11) Wyoming Water Association Summer Water Tour, (Advisor), Evanston, WY., July 11-12, 2013, (12) UW Water Research Program, WRP Priority and Selection Committee meeting to select research priorities and review final project reports, Cheyenne, WY., July 25, 2013, (13) Wyoming Weather Modification pilot program Technical Advisory Team meeting, Lander, WY., July 30-31, 2013, (14) Wyoming Water Development Commission/Select Water Committee joint meeting/summer tour, Baggs, WY., August 21-23, 2013, (15) Wyoming Water Forum, Presentation on Water Research Program final project reports, Cheyenne, WY., September 3, 2013, (16) University of Wyoming-Water Interest Group, UW, Laramie, WY., September 18, 2013, (17) Wyoming Water Forum, Presentation on Water Research Program update, Cheyenne, WY., October 1, 2013, (18) Wyoming Center for Environmental Hydrology and Geophysics-Water Interest Group Conference, UW, Laramie, WY., October 7, 2013, (19) Wyoming Water Association Board meeting (Advisor), Sheridan, WY., October 21, 2013, (20) Co-Sponsor Wyoming Water Association Annual Meeting & Educational Seminar, University of Wyoming Water Research Initiatives, Sheridan, WY., October 22-24, 2013, (21) Wyoming Water Development Commission/Select Water Committee joint workshop, Presentation on the UW Office of Water Programs and Water Research Program-preliminary funding recommendation, Casper, WY., November 6-8, 2013, (22) Wyoming Water

Research Program Meeting, WRP Advisory Committee review and ranking of water research projects, Cheyenne, WY., November 26, 2013, (23) Wyoming Governor s Water Strategy Meeting, Cheyenne, WY., December 2, 2013, (24) Wyoming Water Forum, Presentation on Water Research Program Update, Cheyenne, WY., December 3, 2013, (25) Wyoming Stock Growers Annual Conference, Casper, WY., December 3, 2013, (26) Wyoming Water Development Commission Meetings/Workshop, Presentation on recommendation for FY2014 WRP Annual funding, Cheyenne, WY., January 8-9, 2014, (27) Wyoming Legislative Select Water Committee, Presentation on WRP projects and recommendation for FY2013 WRP Annual funding, State Capital, Cheyenne, WY., January 10, 2014, (28) Wyoming Weather Modification pilot program Technical Advisory Team meeting, Cheyenne, WY., January 22, 2014, (29) Wyoming Water Forum, Presentation on Water Research Program update, Cheyenne, WY., February 4, 2014, (30) The National Institutes for Water Resources (NIWR) annual meetings, Washington, DC., February 10-12, 2014, (31) Wyoming State Legislature House Agriculture Committee, Wyoming Water Development Commission (Advisor), Omnibus Water Plan, State Capital Bld., Cheyenne, WY., February 13, 2014, (32) Wyoming Water Association Board Meeting, Legislative Review, (Advisor), Cheyenne, WY., February 26, 2014, (33) Wyoming State Legislature Senate Agriculture Committee, Wyoming Water Development Commission (Advisor), Omnibus Water Plan, State Capital Bld., Cheyenne, WY., February 27, 2014.

Project 2012WY80B, INTEGRATED ACCELERATED PRECIPITATION SOFTENING (APS) MICROFILTRATION (MF) ASSEMBLY AND PROCESS DEVELOPMENT TO MAXIMIZE WATER RECOVERY DURING ENERGY PRODUCTION AND CO2 SEQUESTRATION, information transfer activities: (1) Hegarty, Jennifer, 2013. Characteristics of CBM Produced Waters, Accelerated Precipitation Softening, and RO Membrane Fouling in the Presence/Absence of the Accelerated Softening Pretreatment, Poster Presentation at the North American Membrane Society Conference, Boise, ID.

Project 2012WY81B, MULTI-FREQUENCY RADAR AND PRECIPITATION PROBE ANALYSIS OF THE IMPACT OF GLACIOGENIC CLOUD SEEDING ON SNOW, information transfer activities: (1) Binod Pokharel presented an ASCII overview oral paper at the 45th Annual Meeting of the American Weather Modification Association, in San Antonio TX, 10-12 April 2013, (2) Bart Geerts presented an ASCII research update at the Wyoming Weather Modification Pilot Project (WWMPP) Technical Advisory Team meetings in July 2013, (3) Binod gave an updated at the WWMPP TAT meeting in Cheyenne in January 2014, (4) Bart Geerts gave a seminar Glaciogenic seeding of orographic clouds revisited to the Dept. of Atmospheric and Environmental Sci., University at Albany, May 6, 2013, (5) Bart Geerts gave am invited talk ASCII overview, key findings, and lessons learned at a planning meeting to prepare for a new, larger NSF proposal following up on ASCII atNCAR, Boulder CO, June 4, 2013, (6) Bart Geerts gave an invited presentation Impact of glaciogenic cloud seeding on mountain snowfall: an old question revisited at the National Institutes for Water Resources (NIWR) annual meeting, South Tahoe CA, June 13, 2013, (7) Bart Geerts presented Cocorahs webinar on glaciogenic cloud seeding , total full-time attendees of 87, available at http://youtu.be/Br8W0sf3bdM, Nov 6, 2013, (8) the project was part of the Weather Channel s Hacking the Planet series in early April 2013. The episode in which the project was featured can be viewed at http://youtu.be/rVl_pjEOi9w (this is one of several episodes in the Hacking the Planet series). Note that this is an unlisted and unlinked video, i.e. it is not public the only way to access it is through this link. The reason, of course, is copyright issues.

Project 2012WY82B, DECADAL SCALE ESTIMATES OF FOREST WATER YIELD AFTER BARK BEETLE EPIDEMICS IN SOUTHERN WYOMING, information transfer activities: (1) (Invited) Ewers BE, 2014. Hydraulic Limitations Help Explain the Behavior of Plants: from clocks to mortality to ghosts. Department of Biology, University of Northern Colorado. January, (2) Massman, WJ, Frank, JM, Swiatek, E, Zimmerman, H, Ewers, BE., 2013. Which are more accurate, orthogonal or non-orthogonal sonic anemometers?, American Geophysical Union Meeting, San Francisco, CA. Dec, (3) Bowling, DR, Ewers, BE, et al., 2013. Land-atmosphere carbon cycle research in the southern Rocky Mountains. American Geophysical Union Meeting, San Francisco, CA. Dec, (4) Kipnis, E, Chapple, WD, Traver, E, Frank, JM, Ewers, BE,

Miller, SN, Williams, DG., 2013. Spatial variability of snow water isotopes in montane southeastern Wyoming. American Geophysical Union Meeting, San Francisco, CA. Dec, (5) Brooks PD, Harpold, AA, Biederman JA, Gochis DJ, Litvak, ME, Ewers, BE, Broxton, PD, Reed, DE., 2013. Non-linear feedbacks between forest mortality and climate change: implications for snow cover, water resources, and ecosystem recovery in western North America. American Geophysical Union Meeting, San Francisco, CA. Dec, (6) Ewers BE, et al, 2013. Bark beetle impacts on ecosystem processes are over quickly and muted spatially. American Geophysical Union Meeting, San Francisco, CA. Dec, (7) Mackay, DS, Ewers, BE, Peckham, SD, Savoy, P, Reed, DE, Frank, JM., 2013. Towards scaling interannual ecohydrological responses of conifer forests to bark beetle infestations from individuals to landscapes. American Geophysical Union Meeting, San Francisco, CA. Dec, (8) Biederman, Ewers, BE, Reed, D, et al., 2013. Compensatory vapor loss and biogeochemical attenuation along flowpaths mute the water resources impacts of insect-induced forest mortality. American Geophysical Union Meeting, San Francisco, CA. Dec, (9) Peckham, SD, Ewers, BE, Mackay, DS, Pendall, E, Frank, JM, Massman, WJ., 2013. Simulating stand-level water and carbon fluxes in beetle-attacked conifer forests in the Western US. American Geophysical Union Meeting, San Francisco, CA. Dec, (10) (Invited) Ewers BE. Quantifying how bark beetles impact forest hydrology. Presentation to American Association for the Advancement of Science External Advisory Committee to UW EPSCOR, (11) (Invited) Ewers BE., 2013. Causes and consequence of bark beetle-induce mortality on water, carbon, and nitrogen cycling. Ecological Society of America Annual Meeting. Minneapolis Minnesota. August, (12) Peckham, SD, BE Ewers, DS Mackay, E Pendall, HN Scott, JM Frank, MG Ryan and WJ Massman, 2013. Bayesian analysis of a carbon cycle model: Implications for parameter estimation, model selection, and simulation of beetle-caused forest mortality. Ecological Society of America Annual Meeting. Minneapolis Minnesota. August, (13) Mackay, DS, BE Ewers, SD Peckham, PR Savoy, D Reed, JM Frank, NG McDowell, 2013. Plant hydraulic controls over the susceptibility of trees to mortality following climate-enhance disturbances. Ecological Society of America Annual Meeting. Minneapolis Minnesota. August, (14) (Invited) Ewers BE, 2013. Impacts of bark beetle outbreaks from stands to watersheds. Public Lecture Sponsored by UW Ruckelhaus Institute. Laramie, WY May, (15) (Invited) Ewers BE., 2013. Impacts of bark beetle outbreaks from stands to watersheds. Public Lecture Sponsored by UW Ruckelhaus Institute. Steamboat Springs, CO May, (16) (Invited) Ewers BE., 2013. Impacts of bark beetle outbreaks from stands to watersheds. Public Lecture Sponsored by UW Ruckelhaus Institute. Saratoga, WY May.

USGS Summer Intern Program

None.

Student Support					
Category	**Section 104 Base Grant**	**Section 104 NCGP Award**	**NIWR-USGS Internship**	**Supplemental Awards**	**Total**
Undergraduate	4	0	0	0	4
Masters	10	0	0	0	10
Ph.D.	14	0	0	0	14
Post-Doc.	1	0	0	0	1
Total	29	0	0	0	29

Notable Awards and Achievements

2012WY81B Multi-frequency Radar and Precipitation Probe Analysis of the Impact of Glaciogenic Cloud Seeding on Snow - Award - Pokharel, Binod was the recipient of the 2013 Weather Modification Association Student Award, which pays $1000 plus all travel expenses to the WMA annual meeting, where the recipient gave the presentation ASCII overview Impact of Glaciogenic Seeding on Clouds over the Medicine Range in Wyoming at the 45th Annual Meeting of the American Weather Modification Association, San Antonio TX, April 10-12.

2010WY57B Development of a Contaminant Leaching Model for Aquifer Storage and Recovery Technology Award - Sharrad, M. and M. Fan, 2010. Research Paper Award, Title of poster Removal of Se with FeOOH, Presented at 6th International Conference on Sustainable Water Environment, 7/29-7/31, 2010, Delaware, USA.

Publications from Prior Years

1. 2006WY33B ("Precipitation Measurement and Growth Mechanisms in Orographic Wyoming Snowstorms") - Dissertations - Wettlaufer, A., 2013. A Fully Compensated Algorithm for the Hotplate Precipitation Sensor, MS Thesis, Dept. of Atmospheric Science, University of Wyoming, 107 pp.
2. 2010WY57B ("Development of a Contaminant Leaching Model for Aquifer Storage and Recovery Technology") - Dissertations - Sharrad, Mustafa Omar, 2012. Removal of Heavy Metals and Carbonate as well as Bicarbonate from Water and Wastewater, Ph. D. Dissertation, Department of Chemical & Petroleum Engineering, University of Wyoming, May 2012, 205 pp.
3. 2010WY57B ("Development of a Contaminant Leaching Model for Aquifer Storage and Recovery Technology") - Dissertations - Bentley, Mark, A., Mercury Adsorption and Desorption Kinetics, M.S., Chemical & Petroleum Engineering, May, 2012, 132 pp.
4. 2010WY57B ("Development of a Contaminant Leaching Model for Aquifer Storage and Recovery Technology") - Articles in Refereed Scientific Journals - Tuwati, A., Fan, M., and Bentley, M., 2011. Reaction Kinetic Model for a Recent Co-produced Water Treatment Technology, Journal of Environmental Science, Vol. 23, No. 3, pp. 360-365.